Summer November 2014

UNDERSTANDING STRUCTURE-PROPERTY RELATIONSHIPS AT THE NANO-BIO INTERFACE FOR DELIVERY APPLICATIONS

Krishnendu Saha

UNDERSTANDING STRUCTURE-PROPERTY RELATIONSHIPS AT THE NANO-BIO INTERFACE FOR DELIVERY APPLICATIONS

A Dissertation Presented

by

KRISHNENDU SAHA

Submitted to the Graduate School of the

University of Massachusetts Amherst in partial fulfillment

of the requirements for the degree of

DOCTOR OF PHILOSOPHY

September 2014

Chemistry

UNDERSTANDING STRUCTURE-PROPERTY RELATIONSHIPS AT THE NANO-BIO INTERFACE FOR DELIVERY APPLICATIONS

A Dissertation Presented

by

KRISHNENDU SAHA

Approved as to style and content by:

Vincent M. Rotello, Chair

James Chambers, Member

Nathan Schnarr, Member

D Joseph Jerry, Member

Craig T. Martin, Department Head

Department of Chemistry

DEDICATION

To my father who could not see this day

ACKNOWLEDGEMENTS

I would like to express my heart-felt sense of gratitude to my advisor Prof. Vincent M. Rotello for his inspiring guidance, constant encouragement, and tremendous patience towards me. He made extremely valuable suggestions in every aspect of my thesis work including the designing of critical experiments and help in analyzing the data. Most importantly, he always encouraged and inspired me to come up with my own ideas and gave me absolute freedom to test my hypothesis. He also guided and taught me how to look for the 'big picture' of a project and critically think why it is important to work on. I will be always indebted to him for his constant effort to improve my scientific writing skills. His excitement and passion towards science have truly inspired me to be productive and enriched my scientific mind. I consider myself really fortunate to be a part of his scientific family.

I am also grateful to my thesis committee members Prof. D. Joseph Jerry, Prof. James Chambers, and Prof. Nathan Schnarr for their valuable advice and constructive comments towards this thesis work.

I really owe a lot to the present and past members of Rotello group. I really enjoyed the friendly and collaborative environment of the group that drives everyone towards to a common goal: to do better science. I am particularly thankful to Dr. Sung Tae Kim for teaching me every aspect of animal studies, sharing his vast knowledge in pharmaceutical sciences, and his kind help whenever I had problems. I am also thankful to Dr. Apiwat Chompoosor and Dr. Avinash Bajaj for sharing their experience, introducing me to the research, and teaching me important aspects of fundamental biology and mammalian cell culture. I also like to acknowledge my long-term collaborators in the lab, Daniel, Tsukasa, and Bo who made tremendous contribution towards this work. I am also thankful to my amazing friends in and outside the lab, Xiaoning, Vikas, Rubul, Moumita, Ziwen, NLe, Gulen, Yi-Cheun, Rui, Cola, Takashi, Ridhha, Akash, Brad, Brian,

Youngdo, Yuqing, and Kedar. I like to thank Carol and jms for their kind help in administrative work.

Finally, I convey my sincere gratitude to my parents and my family for their unconditional love, blessings, and inspiration that helped me to chase my dream. Last but not the least, I am and always will be indebted to Xiaoning, my fiancée and my best friend, who hold me together throughout my tough times, took care of me in my ill health, and helped me in every aspect of my life. Her constant love and encouragement made my journey easier and made this thesis possible.

ABSTRACT

UNDERSTANDING STRUCTURE-PROPERTY RELATIONSHIPS AT THE NANO-BIO INTERFACE FOR DELIVERY APPLICATIONS

SEPTEMBER 2014

KRISHNENDU SAHA, B.Sc., JADAVPUR UNIVERSITY

M.Sc., INDIAN INSTITUTE OF TECHNOLOGY MADRAS

Ph.D., UNIVERSITY OF MASSACHUSETTS AMHERST

Directed by: Professor Vincent M. Rotello

The surface chemistry of the nanomaterials creates an effective interface between two entirely different worlds: nanotechnology and biology. Understanding the interaction between nanomaterial surface chemistry and biological entities can be useful for a wide variety of biomedical applications as well as can provide crucial information for nanotoxicology. In my research, I have used gold nanoparticles as a model platform to synthesize a family of nanoparticles with atomic level control of their surface properties and probe their interaction with biological systems. First part of my research focused on the understanding the uptake mechanisms, toxicity, and hemolytic properties of cationic nanoparticles, an excellent gene delivery vectors, and provide design parameters to avoid toxic consequences. In the second part of my research, a new class of surface engineered antifouling nanomaterials were fabricated that can eschew plasma protein binding, providing opportunity to interrogate nano-biological behavior without any complications arising from the protein binding to nanomaterial surface. Since the surface chemistry of nanoparticles dictates the interaction between nanomaterials and biological entities, the findings in this thesis can be generalized to nanomaterials with a wide of variety of core materials of unique physical properties.

TABLE OF CONTENTS

LIST OF TABLES

LIST OF FIGURES

CHAPTER 1

NANOPARTICLES IN BIOLOGY

1.1. An Overview of Nanobiotechnology

The advent of nanotechnology in last two-three decades has opened up a new avenue of research areas. The great strength of nanotechnology relies on its strictly interdisciplinary nature; creation of new materials, understanding their properties, and apply them to solve important questions in materials science and biology. In particular, nanoparticles (size regime 1 to 100 nm) have numerous advantages in understanding biological systems as well as regulating numerous biological processes.[1,2,3] These 'tiny' materials essentially commensurate the size of various bio-macromolecules including protein and DNA and provide effective surface area/receptors for multivalent interaction.[4] The high surface-to-volume ratio, tunable functionality and a wide variety of available core materials (metal/semiconductor) featuring magnetic and optoelectronic properties has led to develop nanoparticles for a variety of biological applications including macromolecular surface recognition,[5,6] sensing,[7,8,9], imaging,[10,11,12] and drug/gene delivery [13,14,15,16,17,18] for cancer therapy and tissue engineering applications.[19,20]

Nanoparticles represent a synthetic intermediate between small molecule and macroscopic materials. They provide unique physicochemical properties compared to the bulk materials that make them attractive scaffolds for biomedical applications. In addition, the various size and shape-dependent synthesis of nanoparticles aided the study of their unique physical properties.[21,22] These novel physical properties of nanoparticles generally come from their high surface area compared to the bulk materials; as a typical example- bulk gold have a bright yellow color, however, gold nanoparticles can be dark brown to purple to red based on the core size. In addition to the physical properties arising from the metal/semiconductor core, a wide variety of small molecule ligands can be appended to the nanoparticle surface that can act as a protective

layer to improve nanoparticle stability in physiological condition as well as it can be further engineered to give the nanoparticles tunable surface property. For example, thiol-functionalized ligands have a great affinity to the gold core and have been used to functionalize gold nanoparticles of various sizes.[23] In addition, this thiol monolayer has further been engineered for sensing and delivery applications. Table 1.1 listed some well known core materials and corresponding surface ligands with their applications in various areas of nanobiotechnology.

Table 1.1 Characteristics, ligands and representative applications for various metal and semiconductor materials (reproduced from reference 2).

Core material	Characteristics	Ligand(s)	Applications
Au	Optical absorption, fluorescence and fluorescence quenching, stability	Thiol, disulfide, phosphine, amine	Biomolecular recognition, delivery, sensing
Ag	Surface-enhanced fluorescence	Thiol	Sensing
Pt	Catalytic property	Thiol, phosphine, amine, isocyanide	Bio-catalyst, sensing
CdSe	Luminescence, photo-stability	Thiol, phosphine, pyridine	Imaging, sensing
Fe_2O_3	Magnetic property	Diol, dopamine derivative, amine	MR imaging and biomolecule purification
SiO_2	biocompatibility	Alkoxysilane	Biocompatible by surface coating

1.2. Nanoparticles as Delivery Vehicles

Current pharmaceutical industry is based on the production of small molecule drugs that target mutated proteins, enzymes, ion channels, receptors, etc. to achieve a therapeutic effect for a particular disease. However, traditional pharmaceutical agents have several drawbacks including poor solubility, decomposition of drugs *in vivo*, poor pharmacokinetics (e.g. rapid renal clearance of drugs), and bioavailability.[24],[25] Drug delivery systems (DDSs) can overcome these issues,

providing better targeting efficacy and minimize side effects. Some important features of DDSs include improved targeting efficiency to the disease site by decorating DDSs surface with ligands specifically targeted to the disease cell surface receptors, sustained release of drugs thus maintaining effective concentrations of therapeutics with fewer dosing, and remote-controlled release of drugs from the DDS using external stimuli.[26],[27] Overall, DDSs provide the potential to enhance the drug safety while lowering unwanted side effects and improve patient compliance.[28]

The design and synthesis of nanoscale materials with unique properties provide an opportunity to target complex diseases and address the complicated issues that was not well understood. Nanoparticle-based therapeutic systems are important synthetic modalities that showed tremendous potential as DDSs to target a number of deadly diseases including cancer. A number of nanotechnology-based cancer therapeutic products are already in the market and under clinical trials. Nanoparticle-based cancer therapeutics has shown improved efficacy compared to traditional medicine owing to the facts such as higher tumor site specificity, efficient cellular uptake, and increased payload delivery.[29],[30],[31] Several physical and structural attributes of the nanoparticles provide these potential therapeutic efficiencies. First, smaller size (~10-100 nm) of the nanocarriers helps them to accumulate near tumor sites exploiting the enhanced permeability and retention (EPR) effect.[32],[33] Second, tunable surface properties allow efficient functionalization and increased circulation properties for desired therapeutic action. Third, high surface to volume ratio enables them to carry high payloads of single or multiple types of drug molecules to achieve simultaneous therapeutic outcome. For example, Zubarev et al. have demonstrated that a nanoparticle with 2 nm core diameter can load nearly 70 molecules of paclitaxel, a highly potent cancer drug.[34] These nanocarries can increase the local concentration of drugs to the tumor site exploiting EPR effect and can be released using internal (pH) or external (light) triggers with proper surface engineering. Moreover, the multivalent interaction of the targeting ligands on the nanoparticle surface can interact preferentially with cancer cell-surface receptors minimizing potential side effects of administrated drug molecules.[35] The two

popular approaches in cancer nanomedicine to combat solid tumors are 1) passive targeting, and 2) active targeting.[36] Passive targeting strategies mostly rely on the EPR effect of tumor surrounding leaky blood vessels while active targeting exploits the tethering of the targeting ligands directed to a particular receptor over-expressed by target tumor cells. Numerous nanoparticle-based systems has currently been explored for cancer research including liposomes, polymeric nanoparticles, micelles, gold nanoparticles, etc. while few already got clinical approval from US Food and Drug Administration (FDA).[37],[38]

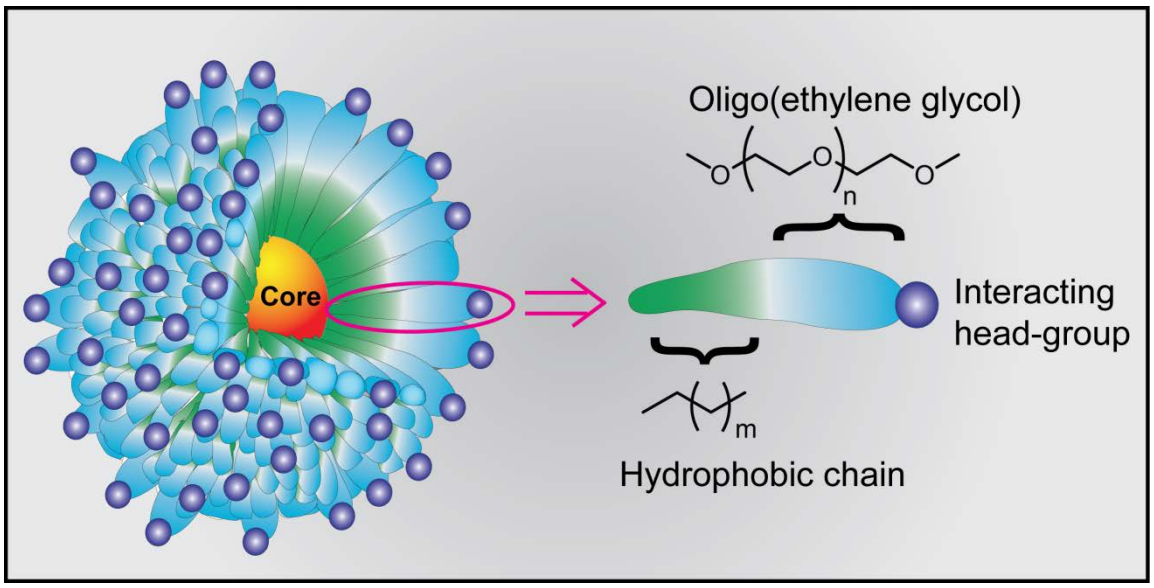

Figure 1.1. Monolayer protected gold nanoparticles used in this thesis work that feature a gold core, a hydrophobic organic monolayer to confer stability, an oligo(ethylene glycol) spacer to improve biocompatibility and solubility and a functional head group to probe the interaction of synthesized nanomaterials at the biological interface.

Gold nanoparticles (AuNPs) provide attractive features that have been exploited as excellent DDSs both *in vitro* and *in vivo*. First, the gold core is essentially inert and non-toxic.[39],[40] Second, AuNPs can be synthesized with a wide variety of size and shapes in a straightforward manner with highly monodisperse fashion. This provides effectively tunable surface area/ligand coverage for drug loading and/or multivalent interaction with DNA/siRNA for intracellular delivery. Finally and perhaps the most importantly, the surface of AuNPs can be decorated with a

wide range of functionality including small molecule ligands, antibodies, peptides, etc. that can interact with the cancer cells. Due to these above mentioned attributes, AuNPs were used by several groups as drug/gene delivery carriers. In this thesis, surface engineered AuNPs were used to probe the effect of surface properties on the biological systems. Therefore a brief introduction to the synthesis and surface functionalization of monolayer protected AuNPs (Figure 1.1) and its relevant biological applications will be discussed in this chapter.

1.3. Monolayer Protected Gold Nanoparticles (AuNPs)

AuNPs have been widely used in biomedical applications due to their non-toxic core, straightforward synthesis, and tunable surface functionalization.[41] The first synthesis of colloidal gold can be dated back to Michael Faraday's work in 1857,[42] however, significant boost in the synthesis of AuNPs was achieved after Turkevich developed a classic approach to synthesize 20 nm AuNPs by reducing gold salt using sodium citrate.[43] This is one of the most popular approaches to date to synthesize AuNPs in water with tunable size by simply varying the ratio of the gold salt to the sodium citrate.[44] Although relatively easy, AuNPs synthesized in this method lack proper chemical functional groups that compromise their stability in the physiological condition, compromising their utility in biological applications. A significant breakthrough in the synthesis of highly stable AuNPs was achieved when Brust and Schriffin synthesized dodecanethiol monolayer protected AuNPs in organic solvent with diameter 1.5-5 nm. In this method, sodium borohydride ($NaBH_4$) was used as a reducing agent and surfactant tetraoctylammonium bromide (TOAB) was used to transfer hydrogen tetrachloroaurate ($HAuCl_4$) from aqueous phase to the organic phase.[45] The size of AuNPs produced in this method can be readily controlled by varying the gold-to-thiol ratio, reduction rate, reaction temperature, time, etc.[46],[47],[48] These AuNPs are highly stable due to the synergic effect of strong thiol-gold interactions and van der Waals attractions between the monolayer ligands. In addition, AuNPs

synthesized in this way can be thoroughly dried and re-dispersed without any aggregation, attesting to their superior stability over other AuNPs.

A wide variety of ligands/capping agents including amino acids,[49] amines,[50,51,52] polymers[53,54,55] have been used to yield AuNPs of different core sizes and dispersities. These stabilizing agents also provide the necessary barrier to avoid particle coalescence. Table 1.2 listed some of the most common approaches used to synthesize monolayer protected gold nanoparticles.[56]

Table 1.2 Synthetic methods and capping agents for AuNPs of diverse core size (Reproduced from Ref 56).

re size	Synthetic methods	Capping agents	References
1-2 nm	Reduction of AuCl(PPh3) with diborane or sodium borohydride	Phosphine	57,58
1.5-5 nm	Biphasic reduction of $HAuCl_4$ by sodium borohydride in the presence of thiol capping agents	Alkanethiol	45,47,48
5-8 nm	Reduction of $HAuCl_4$ by sodium borohydride in the presence of TOAB	Quaternary ammonium salt (TOAB)	59
8-20 nm	Reduction of $HAuCl_4$ by oleyl amine in water under heating	Oleyl amine	50,60
10-40 nm	Reduction of $HAuCl_4$ with sodium citrate in water	citrate	43,44,61

The AuNPs produced by those capping agents listed on Table 1.2, however, are mostly soluble in organic solvent (except citrate) and most importantly lack chemical functionalities, thereby restricting their applications in biology. To solve this issue, Murray et al. developed a simple but efficient approach called place exchange (Figure 1.2) that can introduce chemical functional group on AuNP surface and provide water solubility.[62] In this approach, the initially

thiol-stabilizing monolayer was exchanged with another thiol-anchoring ligand when the later is present in excess.[63] Most importantly, using the place exchange reaction mixed monolayer AuNPs featuring two or more functional groups can also be tethered to the AuNP surface for synergistic applications. The reaction time and the feed ratio of the functional ligands further control the loading efficiency onto AuNPs surface. Using this place exchange reaction, several groups have developed water soluble AuNPs[64] that have been used for a wide variety of biological applications including sensing[65] and drug/gene delivery.[66]

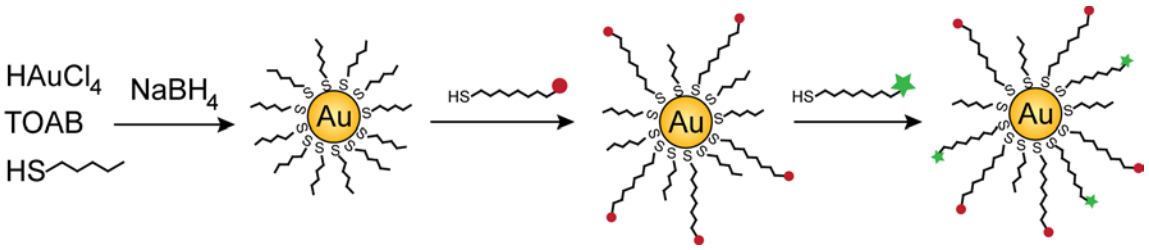

Figure 1.2. AuNP synthesis and surface functionalization via place exchange reaction. This strategy allowes to decorate AuNP monolayer with two or more of functional ligands for simultaneous applications.

1.4. Cellular Interaction of Gold Nanoparticles

The key requirement of any DDSs is to overcome the cellular barrier and intracellular delivery of therapeutics. Therefore, having high intracellular uptake is an essential requirement of any delivery vehicles to successfully release the cargo inside the cells. Several critical factors dictate nanoparticle entry into the cells and a systematic understanding these factors can lead to develop delivery vehicles with improved therapeutic efficacy and low cytotoxicity. Nanoparticle size is a key determinant of particle uptake inside the cells. For example, Chan et al. have demonstrated that cellular uptake of AuNPs is strictly dependent on their size; 50 nm AuNPs showed the highest uptake compared to other sizes of AuNPs tested (14-100 nm).[67] This particular size preference in uptake was also observed for other type of nanoparticles and was

thought to happen due to the enhanced receptor-mediated endocytosis of 50 nm nanoparticles over other sizes.[68] In a follow-up study, Chan et al. fabricated AuNP-coated with Herceptin and tested for ErbB2 receptor-mediated internalization in breast cells. Likewise, the most efficient cellular uptake was observed with the 20~50 nm particles and programmed cell death (apoptosis) was enhanced by particles with 40–50 nm range.[69]

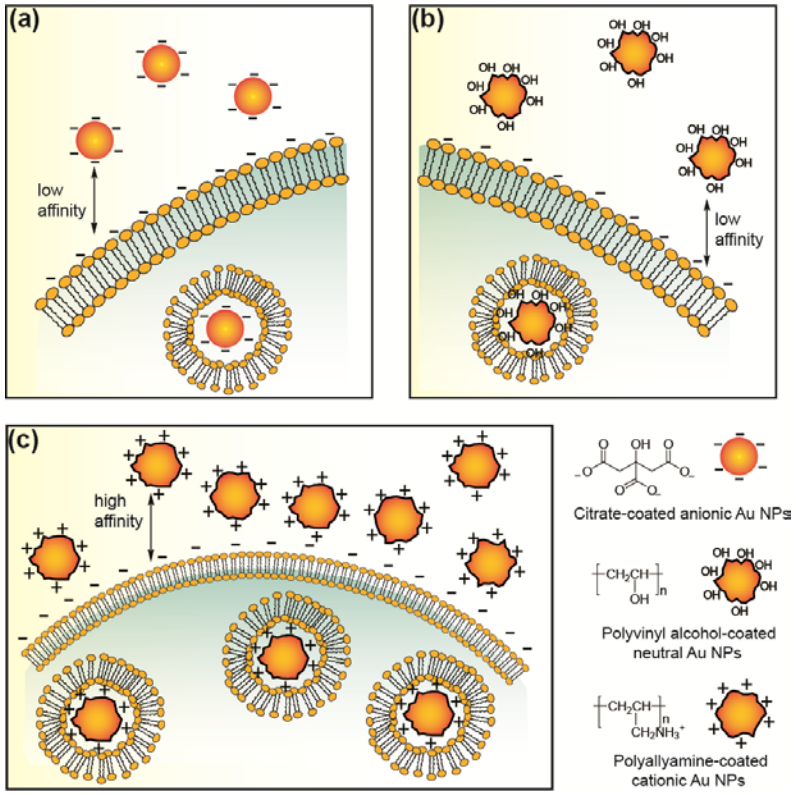

Figure 1.3. Schematic representation of the interaction between gold NPs bearing different surface charge and SK-BR-3 breast cancer cells. (a) Citrate-coated (negative), (b) polyvinylalcohol-coated (neutral), and (c) poly(allyamine hydrochloride)–coated (positive) NPs (Adapted from Ref 3)

Surface property of AuNPs perhaps plays the most important role in determining nanoparticle interaction with cells. For example, Xia *et al.* examined the role of surface charge on the internalization of gold NPs (Figure 1.3).[70] In their findings, positively charged NPs were adsorbed more efficiently on the negatively charged cell surface and consequently showed greater internalization than that of neutral and negatively charged NPs. However, efficient intracellular

uptake of negatively charged NPs is also known, presumably through pinocytosis or membrane diffusion.[71] Moreover, negatively charged quantum dots were shown to penetrate mouse skin, with higher degree of penetration observed upon exposure to UV light.[72] Likewise, DNA functionalized anionic gold NPs were shown to penetrate in epidermis layer of mouse skin with no apparent inflammation or toxicity.[73]

Two-dimensional cell culture models present a vastly different environment than tissues, complicating translation into *in vivo* systems. Rotello and Forbes *et al.* have demonstrated the role of NP surface charge for the delivery of covalently attached therapeutic drugs using a three-dimensional cell culture model. Significantly, cationic particles showed delivery of drugs on the proliferating peripheral cells due to their higher uptake; however, anionic particles had higher diffusion rates, delivering drug- and fluorophore-tagged NPs more rapidly to the center of the spheroid model (Figure 1.4).[74]

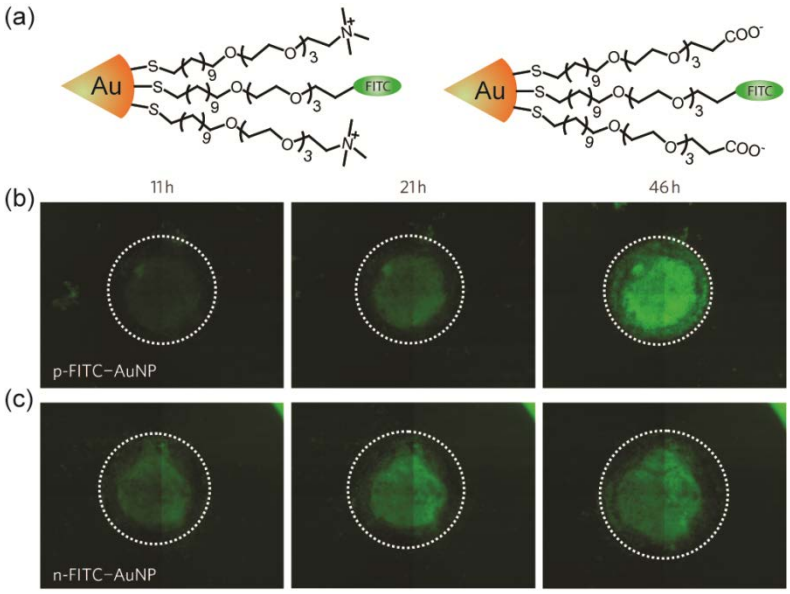

Figure 1.4. (a) Structure of mixed monolayer-protected cationic and anionic gold NPs loaded with thioalkylated fluorescein isothiocyanate (FITC). Green fluorescence images of tumor cylindroids treated with (b) cationic and (c) anionic particles. Adapted from Ref 3 and 74)

In addition to surface charge, NP hydrophobicity also plays an important role in the cellular uptake process. In one study, Mailänder *et al.* have demonstrated that increasing surface hydrophobicity of polymeric NPs increases intracellular uptake in a variety of cell lines.[75] Rotello *et al.* have demonstrated a linear correlation of surface hydrophobicity and intracellular uptake of gold NPs (2 nm core), arising from a stronger interaction of hydrophobic NPs with serum albumin.[76] However, in the absence of serum, no apparent trend between surface hydrophobicity and cellular uptake was found, demonstrating the importance of serum protein adsorption on the NP internalization process.

Due to its high cellular uptake cationic AuNPs have successfully used in intracellular DNA delivery applications. In early work, Klibanov and Thomas used polyethyleneimine (PEI) functionalized AuNPs and to deliver plasmid DNA into mammalian cells.[77] The most potent conjugates were 12 times more efficient at plasmid DNA delivery than their unmodified PEI counterparts. In an analogus example, Rotello et al. developed quaternary ammonium-functionalized AuNPs as the effective intracellular delivery vehicles for plasmid DNA.[78] These studies demonstrated that a number of parameters were important for successful transfection, including the AuNP surface charge coverage and hydrophobicity. Therefore cationic AuNPs provide a promising platform for gene delivery applications due to their high intracellular uptake and tunable transfection efficiency based on their surface functionality.

1.4.1. Toxicity of Cationic Gold Nanoparticles

The significant higher uptake of cationic AuNPs, however, comes with a potential cons. During the uptake process, cationic AuNPs can strongly interact with cell membrane leading to membrane rupture/cell lysis that can initiate apoptosis and/or necrosis pathway. In early studies on NP toxicity, Rotello *et al*. demonstrated that a cationic mixed monolayer protected cluster (NP1) showed higher cytotoxicity than its anionic analogue (NP2), demonstrating the key role of

surface charge on NP cytotoxicity (Figure 1.5a).[79] Likewise, MMPC1 disrupted anionic phosphatidylcholine/phosphatidylserine vesicles more efficiently than MMPC2 due to the strong electrostatic interactions with the negatively charged lipid bilayer (Figure 1.5b). Similarly, alkylamine functionalized nanoparticles with 2 nm gold cores were shown to disrupt supported lipid bilayers (SLB).[80]

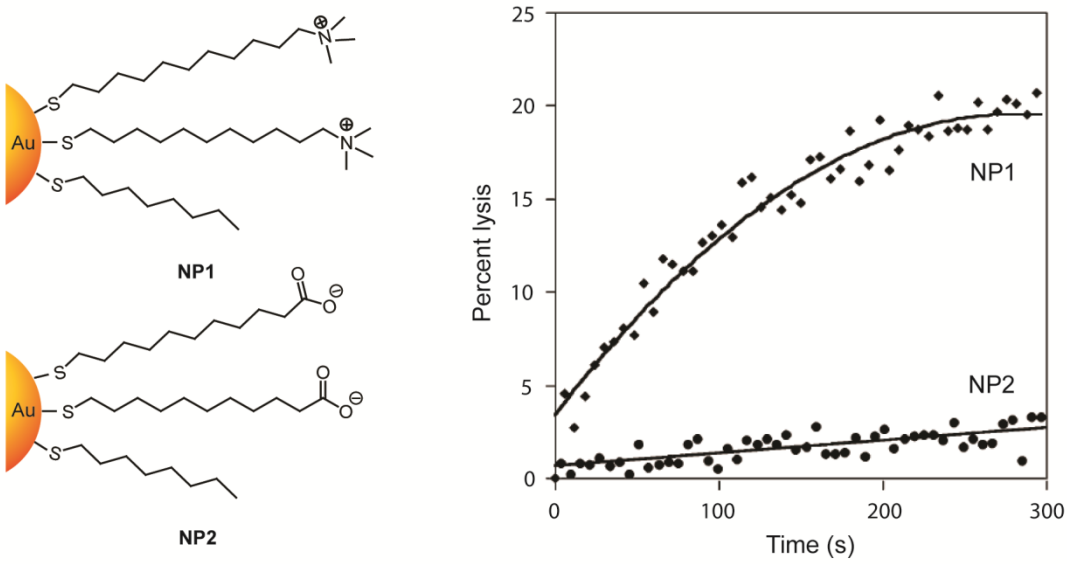

Figure 1.5. Effect of functionalized AuNPs on the disruption of lipid bilayers. (a) Surface functionalized NP1 and NP2 and (b) Comparison of cationic NP1 and anionic NP2 (220 nM) in disrupting vesicles with an overall negative charge (SOPC/SOPC, L-R-stearoyloleoyl-phosphatidylcholine/L-R-stearoyl-oleoyl-phospha-tidylserine). (Adapted from Ref 79 and 81).

Mukherjee and Rotello *et al*. further investigated the role of NP surface charge on the cell membrane potential. Four AuNPs with varying surface charges (e.g. cationic, anionic, zwitterionic, and neutral) were incubated with cells (Figure 1.6a).[82] Positively charged AuNPs depolarized the membrane potential in a dose dependent manner across different cell types compared to other NPs (Figure 1.6b). Furthermore, cationic AuNPs rapidly increased the intracellular Ca^{2+} concentration, $[Ca^{2+}]_i$ by stimulating plasma membrane Ca^{2+} influx as well as Ca^{2+} release from the endoplasmic reticulum, with the concomitant inhibition of proliferation of human bronchial epithelial cells (BEC) and human airway smooth muscle cells (ASM) (Figure

1.6c).[83] Taken together, positively charged AuNPs lead to perturbation of the cell membrane by structural reconstruction and phase transition of the lipid bilayer. Furthermore, they induce cytotoxicity and/or cell death due to intracellular signaling by changing the membrane potential and increasing $[Ca^{2+}]_i$.

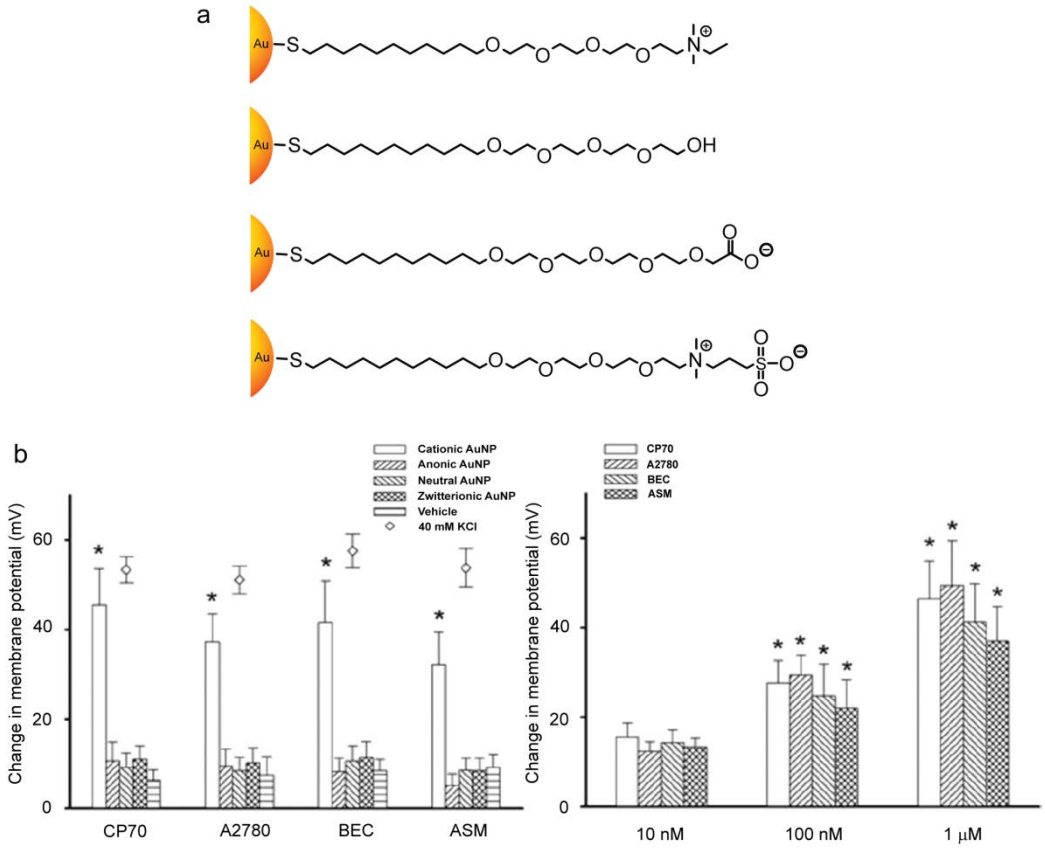

Figure 1.6. Effect of gold NPs with different surface charges on cellular membrane potential. (a) Cationic, anionic, neutral, and zwitterionic NPs. (b) Membrane potential changes following the exposure to NPs for ovarian cancer cells (CP70 and A2780), human bronchial epithelial cells (BEC), and human airway smooth muscle cells (ASM) using cell permeable fluorescent membrane potential indicator RH414 and real-time fluorescence microscopy. In addition, the extent of membrane potential change was analyzed in a cationic NP concentration dependent manner. (*$p < 0.05$) (c) Scheme of NP effects on cell and TEM of cationic NP interactions with plasma membrane. Adapted from Ref 82.

Surface functionalized nanoparticles can cause immune responses[84] and/or immunotoxicity through several mechanisms.[85] In addition to surface charge, Rotello *et al*. have demonstrated that surface hydrophobicity of AuNPs dictates the immune response of splenocytes

(Figure 1.6).[86] AuNPs (NP1-8) with different hydrophobicities (Figure 1.7a) showed a direct, quantitative correlation between hydrophobicity and immune activation related to the gene expression of cytokines (e.g. interferon (IFN)-γ, tumor necrosis factor (TNF)-α, interleukin (IL)-2, 6, and 10). In particular, increasing the hydrophobicity of the NP surface elicited the increased the expression of TNF-α, a pro-inflammatory cytokine (Figure 1.7b), and the expression of IL-10, an anti-inflammatory cytokine (Figure 1.7c).

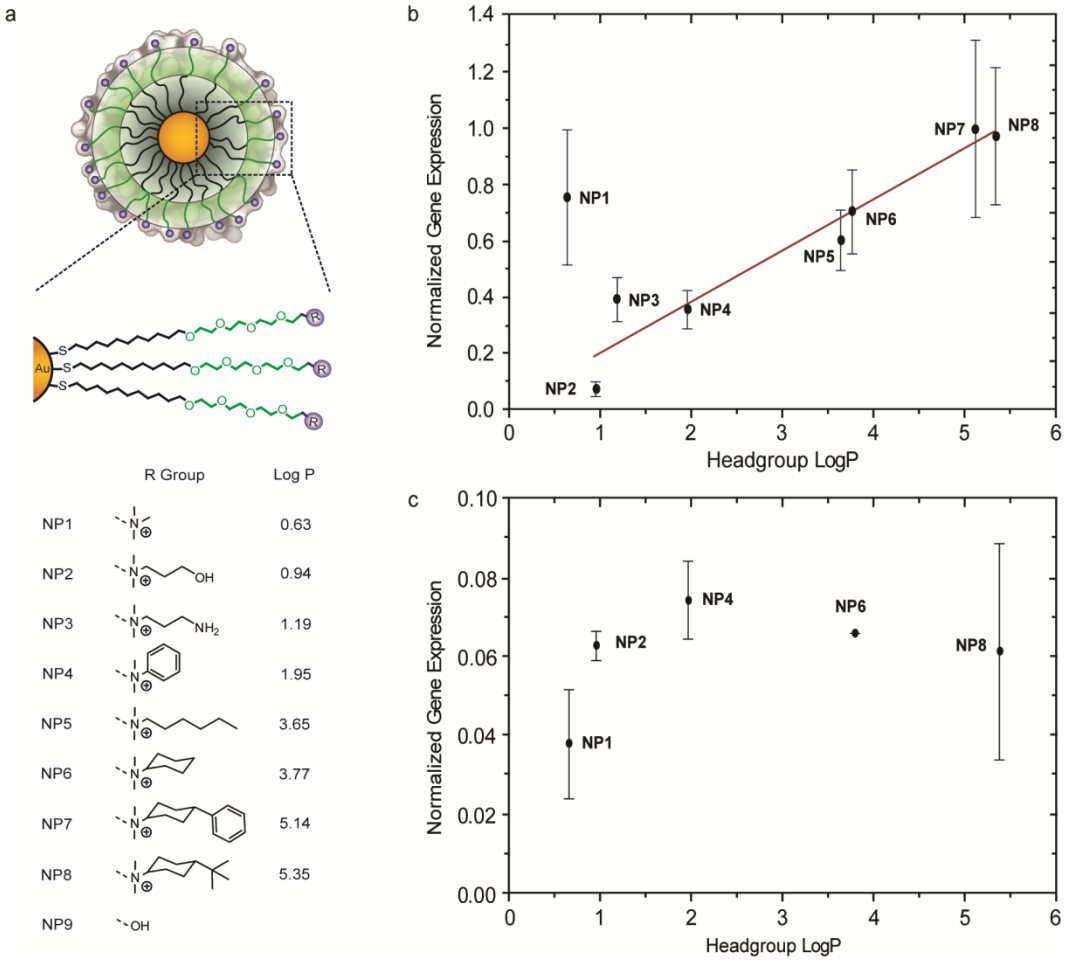

Figure 1.7. Effect of AuNP surface hydrophobicity on gene expression related to immune response. (a) Surface functionalized AuNPs controlling the surface hydrophobicity and cytokine gene expression of (b) TNF- α *in vitro* and (c) IL-10 *in vivo* as a function of NP headgroup LogP. LogP represents the relative hydrophobic indices of the head group. Adapted from Ref 86.

1.5. Dissertation Overview

Understanding the interaction of surface functionalized nanomaterials with biosystems can help in design materials with improved therapeutic efficacy and minimize unwanted side effects. In my research, I have employed a structure-activity based approach to probe, optimize, and develop new nanomaterials that can mitigate the common issues (toxicity, opsonization, poor biodistribution) of delivery systems for both *in vitro* and *in vivo* applications. I have used gold nanoparticles as a model platform to synthesize a family of nanoparticles with atomic level control of their surface properties and probe their interaction with biological systems (Figure 1.8). In the following chapters, I will give a detail description about the design and synthesis of these nanostructures and their use in recognition of proteins and cell surface for delivery applications.

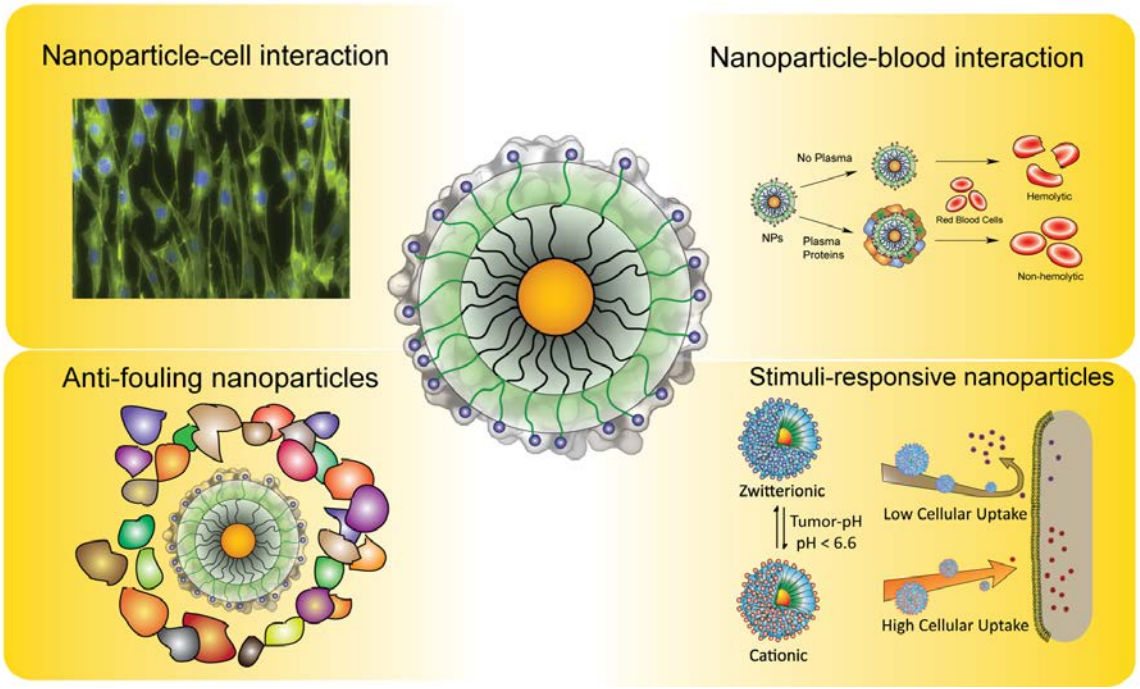

Figure 1.8. Dissertation overview. Schematic illustration of the biological applications of functionalized gold nanoparticles (AuNPs) described in this thesis.

Development of new nanomaterials for biomedical applications requires thorough knowledge of its interaction with mammalian cells. In particular, how nanoparticles enter into the

cells and access cytosol is of utmost importance in the nanobiotechnology. Nanoparticles are taken up in the cells through a variety of mechanisms including phagocytosis, pinocytosis, and passive diffusion. Understanding the pathway involved in nanoparticle transport in the cells can aid in develop delivery vehicles targeting particular pathway in malignant cells over normal cells. Cationic nanoparticles are frequently used as transfection vectors for nucleic acids. Therefore, probing their mechanisms of entry in both malignant and non-malignant cells can help in design nanoparticles for selective delivery and minimal toxicity. In chapter 2, we have demonstrated that surface chemistry of cationic nanoparticles dictate their endocytic mechanisms in mammalian cells and mostly rely on dynamin, scavenger receptors, and caveolae/lipid raft-mediated pathways. Significantly, the existence of differential uptake pathways for the same NP in cancer and normal cells were observed that provides an opportunity to design nanocarriers of specific therapeutic action and reduced cytotoxicity.

Toxicity of nanocarriers is a serious issue for any kind of delivery systems. Cationic nanoparticles are promising delivery vehicles and have been shown to possess differential transfection efficiency depending on their surface hydrophobicity. In Chapter 3, we have demonstrated that the mechanism of cytotoxicity of hydrophobic cationic nanoparticles. Hydrophobic nanoparticles showed higher cytotoxicity compared to the hydrophilic counterpart and concomitant reactive oxygen species generation in cancer cells. The genotoxicity is also observed for both hydrophilic and hydrophobic nanoparticles. This systematic study provides an understanding of nanoparticle interaction with mammalian cells that can be potentially harmful despite their high transfection capability.

Any therapeutic nanocarriers are bound to come in contact with blood upon systemic administration. Blood cells and proteins are the first major entities nanoparticles interact in the body. Therefore, understanding the key parameter of nanoparticle surface properties that is not harmful for the red blood cells can mitigate severe life threatening consequences. In Chapter 4, we have demonstrated that hemolytic properties of nanoparticles linearly increase with the

surface hydrophobicity. However, the presence of plasma proteins (mimicking *in vivo* systems) masks the nanoparticle surface and rescues red blood cells from hemolytic activities. This parametric study also depicts a limit of nanoparticle surface hydrophobicity that can be safely used as injectable materials for *in vivo* applications.

Evasion of mononuclear phagocytic system upon systemic administration is another critical aspect of designing delivery vehicles. Nanoparticles can bind serum proteins (opsonins) on its surface that can help macrophages to recognize and subsequent clearance from the circulation. Serum proteins, in general, mask the nanoparticle chemical identity and give them a unique biological identity depending on the surface functionality. In Chapter 5, we have demonstrated the interplay of protein adsorption and macrophage recognition of nanoparticle surface functionality. Using proteomics approach, detailed information of protein layer bound to surface engineered nanoparticles was investigated and found that nanoparticles bound to a variety of serum proteins including lipoproteins, immunoglobulins, acute phase proteins, coagulation proteins, etc that might dictate their fate in vivo. Importantly, the protein layer of each nanoparticle is unique depending on their surface functional groups. Hydrophobic nanoparticles demonstrated lower uptake in macrophage compared to hydrophilic nanoparticles and provide a design parameter to develop nanoparticles for *in vivo* applications.

Binding of proteins at the surface of nanoparticles in the presence of biological fluids mask the surface properties of the particle and complicates the relationship between chemical functionality and biological effects. Unlike cationic nanoparticles, neutral particles do not bind proteins on their surface due to their strong interaction with water. In Chapter 6, we have designed a series of zwitterionic nanoparticles of variable hydrophobicity that do not adsorb proteins at moderate levels of serum protein and do not form hard coronas at physiological serum concentrations. These particles provide platforms to evaluate nanobiological behavior such as cell uptake and hemolysis dictated directly by chemical motifs at the nanoparticle surface. These

nanoparticles are also expected to be long circulating in blood, making them highly useful for studying nano-bio interaction *in vivo*.

Stilumi-responsive nanoparticle provides a great platform to selectively enhanced uptake or release of therapeutics in response to internal triggers (pH, enzyme, etc.). Tumor microenvironment is known to be acidic (6-6.8) that makes it a highly promising stimulus for selective uptake of nanomaterials in tumor cells over normal cells. In chapter 7, we have developed a zwitterionic gold nanoparticle featuring a newly engineered pH-responsive alkoxyphenyl acylsulfonamide group. Due to its ligand structure, this nanoparticle is neutral at pH 7.4, eshew protein adsorption thereby evade immune system recognition and can become positively charged at tumor pH (< 6.5). The particle uptake and cytotoxicity increases dramatically over this pH range, while having high blood compatibility at blood pH. This smart design of nanomaterials can improve the blood half life of nanoparticles while gaining selective access to the tumor microenvironment.

1.6. References

1. Wang, E. C.; Wang, A. Z. *Integr. Biol.* **2014**, *6*, 9.

2. De, M.; Ghosh, P. S.; Rotello, V. M. *Adv. Mater.* **2008**, *20*, 4225.

3. Tonga, G. Y.; Saha, K.; Rotello, V. M. *Adv. Mater.* **2014**, *26*, 359.

4. Saha, K.; Bajaj, A.; Duncan, B.; Rotello, V. M. *Small* **2011**, *7*, 1903.

5. You, C. C.; Chompoosor, A.; Rotello, V. M. *Nano Today* **2007**, *2*, 34.

6. You, C. C.; Verma, A.; Rotello, V. M. *Soft Matter* **2006**, *2*, 190.

7. Agasti, S. S.; Rana, S.; Park, M. H.; Kim, C. K.; You, C. C.; Rotello, V. M. *Adv. Drug Delivery Rev.* **2010**, *62*, 316.

8. Asefa, T.; Duncan, C. T.; Sharma, K. K. *Analyst* **2009**, *134*, 1980.

9. Saha, K.; Agasti, S. S.; Kim, C.; Li, X. N.; Rotello, V. M. *Chem. Rev.* **2012**, *112*, 2739.

10. Shin, S. J.; Beech, J. R.; Kelly, K. A. *Integr. Biol.* **2013**, *5*, 29.

11. Rosen, J. E.; Chan, L.; Shieh, D. B.; Gu, F. X. *Nanomedicine*, **2012**, *8*, 275.

12. Gindy, M. E.; Prud'homme, R. K. *Expert Opin. Drug Deliv.* **2009**, *6*, 865.

13. Kanasty, R.; Dorkin, J. R.; Vegas, A.; Anderson, D. *Nat. Mater.* **2013**, *12*, 967.

14. Brannon-Peppas, L.; Blanchette, J. O. *Adv. Drug Delivery Rev.* **2012**, *64*, 206.

15. Davis, M. E.; Chen, Z.; Shin, D. M. *Nat. Rev. Drug Discov.* **2008**, *7*, 771.

16. Doane, T.; Burda, C. *Adv. Drug Delivery Rev.* **2013**, *65*, 607.

17. Al-Jamal, W. T.; Kostarelos, K. *Acc. Chem. Res.* **2011**, *44*, 1094.

18. Mura, S.; Nicolas, J.; Couvreur, P. *Nat. Mater.* **2013**, *12*, 991.

19. Langer, R.; Tirrell, D. A. *Nature* **2004**, *428*, 487.

20. Goenka, S.; Sant, V.; Sant, S. *J. Control. Release* **2014**, *173*, 75.

21. Link, S.; El-Sayed, M. A. *J. Phys. Chem. B* **1999**, *103*, 4212.

22. Chen, M.; Liu, J. P.; Sun, S. H. *J. Am. Chem. Soc.* **2004**, *126*, 8394.

23. Mout, R.; Moyano, D. F.; Rana, S.; Rotello, V. M. *Chem. Soc. Rev.* **2012**, *41*, 2539.

24. Allen, T. M.; Cullis, P. R. *Science* **2004**, *303*, 1818-1822.

25. Discher, D. E.; Eisenberg, A. *Science* **2002**, *297*, 967.

26. Mura, S.; Nicolas, J.; Couvreur, P. *Nat. Mater.* **2013**, *12*, 991.

27. Hubbell, J. A.; Langer, R. *Nat. Mater.* **2013**, *12*, 963.

28. Kopecek, J. *Adv. Drug Delivery Rev.* **2013**, *65*, 49.

29. Peer, D.; Karp, J. M.; Hong, S.; FaroKHzad, O. C.; Margalit, R.; Langer, R. *Nat. Nanotechnol.* **2007**, *2*, 751.

30. Petros, R. A.; DeSimone, J. M. *Nat. Rev. Drug Discov.* **2010**, *9*, 615.

31. Cho, K. J.; Wang, X.; Nie, S. M.; Chen, Z.; Shin, D. M. *Clin. Cancer Res.* **2008**, *14*, 1310.

32. Greish, K. *J. Drug Target.* **2007**, *15*, 457.

33. Iyer, A. K.; Khaled, G.; Fang, J.; Maeda, H. *Drug Discovery Today* **2006**, *11*, 812.

34. Gibson, J. D.; Khanal, B. P.; Zubarev, E. R. *J. Am. Chem. Soc.* **2007**, *129*, 11653.

35. Hong, S.; Leroueil, P. R.; Majoros, I. J.; Orr, B. G.; Baker, J. R.; Holl, M. M. B. *Chem. Biol.* **2007**, *14*, 107.

36. Danhier, F.; Feron, O.; Preat, V. *J. Control. Release* **2010**, *148*, 135.

37. Allen, T. M.; Cullis, P. R. *Adv. Drug Delivery Rev.* **2013**, *65*, 36.

38. Chauhan, V. P.; Jain, R. K. *Nat. Mater.* **2013**, *12*, 958.

39. Shukla, R.; Bansal, V.; Chaudhary, M.; Basu, A.; Bhonde, R. R.; Sastry, M. *Langmuir* **2005**, *21*, 10644.

40. Connor, E. E.; Mwamuka, J.; Gole, A.; Murphy, C. J.; Wyatt, M. D. *Small* **2005**, *1*, 325.

41. Dykman, L.; Khlebtsov, N. *Chem. Soc. Rev.* **2012**, *41*, 2256.

42. Faraday, M. *Philos. Trans. R. Soc. London,* **1857**, *147*, 145.

43. Turkevich, J.; Stevenson, P. C.; Hillier, J. *Discuss. Faraday Soc.* **1951**, 55.

44. Frens, G. *Nature: Phys. Sci.* **1973**, *241*, 20.

45. Brust, M.; Walker, M.; Bethell, D.; Schiffrin, D. J.; Whyman, R. *J. Chem. Soc., Chem. Commun.* **1994**, 801-802.

46. Chen, S. W.; Templeton, A. C.; Murray, R. W. *Langmuir* **2000**, *16*, 3543.

47. Leff, D. V.; Ohara, P. C.; Heath, J. R.; Gelbart, W. M. *J. Phys. Chem.* **1995**, *99*, 7036.

48. Hostetler, M. J.; Wingate, J. E.; Zhong, C. J.; Harris, J. E.; Vachet, R. W.; Clark, M. R.; Londono, J. D.; Green, S. J.; Stokes, J. J.; Wignall, G. D.; Glish, G. L.; Porter, M. D.; Evans, N. D.; Murray, R. W. *Langmuir* **1998**, *14*, 17.

49. Bhargava, S. K.; Booth, J. M.; Agrawal, S.; Coloe, P.; Kar, G. *Langmuir* **2005**, *21*, 5949.

50. Aslam, M.; Fu, L.; Su, M.; Vijayamohanan, K.; Dravid, V. P. *J. Mater. Chem.* **2004**, *14*, 1795.

51. Leff, D. V.; Brandt, L.; Heath, J. R. *Langmuir* **1996**, *12*, 4723.

52. Newman, J. D. S.; Blanchard, G. J. *Langmuir* **2006**, *22*, 5882.

53. Shan, J.; Nuopponen, M.; Jiang, H.; Kauppinen, E.; Tenhu, H. *Macromolecules* **2003**, *36*, 4526.

54. Duan, H. W.; Nie, S. M. *J. Am. Chem. Soc.* **2007**, *129*, 2412.

55. Zhu, M. Q.; Wang, L. Q.; Exarhos, G. J.; Li, A. D. Q. *J. Am. Chem. Soc.* **2004**, *126*, 2656.

56. Wang, B.; Anslyn, E.V. *Chemosensors-Principles, Strategies, and Applications*, New York, NY: John Wiley & Sons, Inc., 2011. pp.175.

57. Schmid, G. *Chem. Rev.* **1992**, *92*, 1709.

58. Weare, W. W.; Reed, S. M.; Warner, M. G.; Hutchison, J. E. *J. Am. Chem. Soc.* **2000**, *122*, 12890.

59. Fink, J.; Kiely, C. J.; Bethell, D.; Schiffrin, D. J. *Chem. Mater.* **1998**, *10*, 922.

60. Hiramatsu, H.; Osterloh, F. E. *Chem. Mater.* **2004**, *16*, 2509.

61. Grabar, K. C.; Freeman, R. G.; Hommer, M. B.; Natan, M. J. *Anal. Chem.* **1995**, *67*, 735.

62. Templeton, A. C.; Wuelfing, M. P.; Murray, R. W. *Acc. Chem. Res.* **2000**, *33*, 27.

63. Hong, R.; Fernandez, J. M.; Nakade, H.; Arvizo, R.; Emrick, T.; Rotello, V. M. *Chem. Commun.* **2006**, 2347.

64. Kanaras, A. G.; Kamounah, F. S.; Schaumburg, K.; Kiely, C. J.; Brust, M. *Chem. Commun.* **2002**, 2294.

65. You, C. C.; Miranda, O. R.; Gider, B.; Ghosh, P. S.; Kim, I. B.; Erdogan, B.; Krovi, S. A.; Bunz, U. H. F.; Rotello, V. M. *Nat. Nanotechnol.* **2007**, *2*, 318.

66. Ding, Y.; Jiang, Z. W.; Saha, K.; Kim, C. S.; Kim, S. T.; Landis, R. F.; Rotello, V. M. *Mol. Ther.* **2014**, *22*, 1075.

67. Chithrani, B. D.; Ghazani, A. A.; Chan, W. C. W. *Nano Lett.* **2006**, *6*, 662.

68. Osaki, F.; Kanamori, T.; Sando, S.; Sera, T.; Aoyama, Y. *J. Am. Chem. Soc.* **2004**, *126*, 6520.

69. Jiang, W.; Kim, B. Y. S.; Rutka, J. T.; Chan, W. C. W. *Nat. Nanotechnol.* **2008**, *3*, 145.

70. E. C. Cho, J. W. Xie, P. A. Wurm, Y. N. Xia, *Nano Lett.* **2009**, *9*, 1080-1084.

71. a) X. Y. Shi, T. P. Thomas, L. A. Myc, A. Kotlyar, J. R. Baker, *Phys. Chem. Chem. Phys.* **2007**, *9*, 5712; b) P. C. Patel, D. A. Giljohann, W. L. Daniel, D. Zheng, A. E. Prigodich, C. A. Mirkin, *Bioconjugate Chem.* **2010**, *21*, 2250.

72. L. J. Mortensen, G. Oberdorster, A. P. Pentland, L. A. DeLouise, *Nano Lett.* **2008**, *8*, 2779.

73. D. Zheng, D. A. Giljohann, D. L. Chen, M. D. Massich, X. Q. Wang, H. Iordanov, C. A. Mirkin, A. S. Paller, *Proc. Natl. Acad. Sci. U.S.A.* **2012**, *109*, 11975.

74. B. Kim, G. Han, B. J. Toley, C. K. Kim, V. M. Rotello, N. S. Forbes, *Nat. Nanotechnol.* **2010**, *5*, 465.

75. S. Lorenz, C. P. Hauser, B. Autenrieth, C. K. Weiss, K. Landfester, V. Mailander, *Macromol. Biosci.* **2010**, *10*, 1034.

76. Z. J. Zhu, T. Posati, D. F. Moyano, R. Tang, B. Yan, R. W. Vachet, V. M. Rotello, *Small* **2012**, *8*, 2659.

77. Thomas, M.; Klibanov, A. M. *Proc. Natl. Acad. Sci. U.S.A.* **2003**, *100*, 9138.

78. Sandhu, K. K.; McIntosh, C. M.; Simard, J. M.; Smith, S. W.; Rotello, V. M. *Bioconjugate Chem.* **2002**, *13*, 3.

79. Goodman, C. M.; McCusker, C. D.; Yilmaz, T.; Rotello, V. M. *Bioconjugate Chem.* **2004**, *15*, 897.

80. Leroueil, P. R.; Berry, S. A.; Duthie, K.; Han, G.; Rotello, V. M.; McNerny, D. Q.; Baker, J. R.; Orr, B. G.; Holl, M. M. B. *Nano Lett.* **2008**, *8*, 420.

81. Kim, S. T.; Saha, K.; Kim, C.; Rotello, V. M. *Acc. Chem. Res.* **2013**, *46*, 681.

82. Arvizo, R. R.; Miranda, O. R.; Thompson, M. A.; Pabelick, C. M.; Bhattacharya, R.; Robertson, J. D.; Rotello, V. M.; Prakash, Y. S.; Mukherjee, P. *Nano Lett.* **2010**, *10*, 2543.

83. Monteith, G. R.; McAndrew, D.; Faddy, H. M.; Roberts-Thomson, S. J. *Nat. Rev. Cancer* **2007**, *7*, 519.

84. Zolnik, B. S.; Gonzalez-Fernandez, A.; Sadrieh, N.; Dobrovolskaia, M. A. *Endocrinology* **2010**, *151*, 458.

85. Chang, C. *J. Autoimmun.* **2010**, *34*, J234.

86. Moyano, D. F.; Goldsmith, M.; Solfiell, D. J.; Landesman-Milo, D.; Miranda, O. R.; Peer, D.; Rotello, V. M. *J. Am. Chem. Soc*. **2012**, *134*, 3965.

CHAPTER 2

SURFACE FUNCTIONALITY OF NANOPARTICLES DETERMINES CELLULAR UPTAKE MECHANISMS IN MAMMALIAN CELLS

2.1. Introduction

Nanoparticles (NPs) are key tools for biology and medicine, offering new strategies for biomedical applications including drug delivery[1] and gene therapy.[2] However, development of NPs with improved therapeutic efficacy requires a thorough knowledge of their interactions with cells to enhance delivery efficiency.[3] In particular, the endocytic mechanisms by which NPs are transported into the cell control uptake and can potentially provide delivery strategies featuring enhanced targeting and minimal cytotoxicity.[4]

NPs can be uptaken by cells via two major mechanisms: phagocytosis and pinocytosis.[5] Phagocytosis occurs for particles larger than 0.5 μm in a limited number of mammalian cell types such as macrophages and monocytes. Pinocytosis is a far more general process that can be further classified into two subcategories: macropinocytosis and micropinocytosis. Macropinocytosis involves non-selective uptake of solute macromolecules of more than 0.2 μm diameter,[6] whereas micropinocytosis (clathrin-mediated, caveolae/lipid raft-mediated, and clathrin/caveolae-independent) occurs for smaller particles in all cell types (Scheme 1a).[7] Given the size regime of NPs commonly used for therapeutic purposes (10-200 nm), NPs are expected to enter cells predominantly via micropinocytosis.

Recent investigations have revealed that size,[8] shape,[9] and surface charge[10] of NPs govern entry and subsequent cytosolic access of NPs into living cells.[11] For example, cationic NPs have better cell membrane penetration efficiency than anionic NPs and are shown to enter mammalian cells via a different pinocytic mechanism.[12] Likewise, particles with diameters of <200 nm were uptaken via clathrin-coated pits, whereas caveolae-mediated internalization

became predominant with increasing particle size.[13] In addition to size and charge, NP surface functionality also plays an important role in terms of cellular uptake[14] and eliciting cellular responses.[15] Recently, Maysinger and coworkers have demonstrated that quantum dots bearing non-specific ligands on the surface were predominantly taken up by a lipid raft-mediated endocytosis in human kidney and liver cells.[16] However, it is not clear how changes on the NP surface (e.g., hydrophobicity and aromaticity) affect cellular internalization processes.

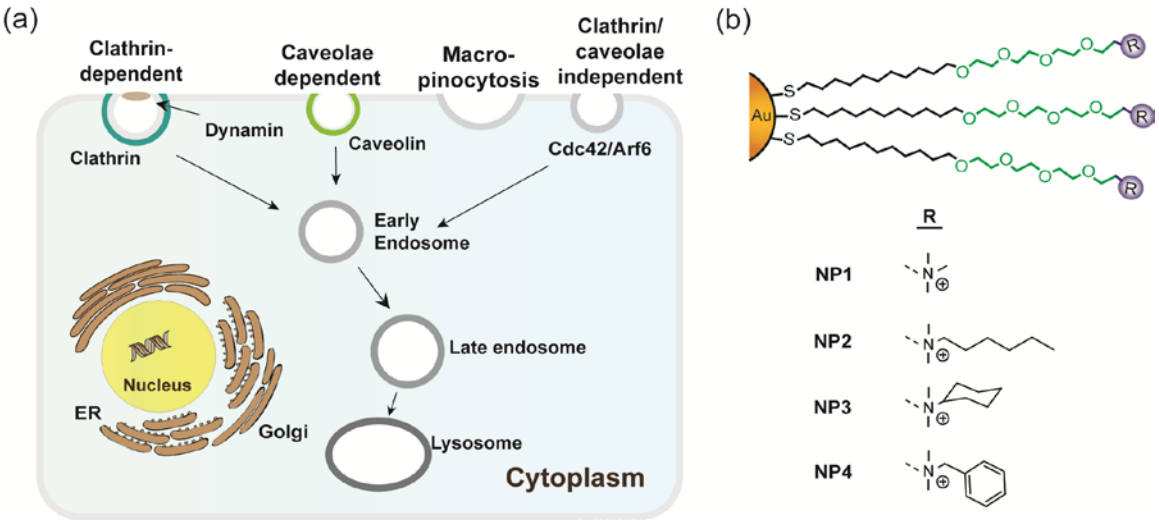

Figure 2.1. (a) Schematic representation of major pinocytic pathways of NPs in mammalian cells. (b) The gold NPs used in the present study.

Herein, we report a mechanistic study of cellular uptake pathways of four cationic gold NPs (~2 nm core) featuring cationic head groups differing in structure and hydrophobicity (Figure 2.1). Experiments were performed in the presence of different endocytic inhibitors using healthy and cancerous cells to determine the specific entry route of the gold NP in human cells. The results indicate that the mode of cellular uptake is strongly dependent on the subtle changes of the NP surface monolayer. Importantly, these gold NPs possess different uptake mechanisms in normal and cancer cells, providing a potential strategy for selective delivery of drugs to tumor tissues.

2.2. Results and Discussion

To probe the effect of NP surface functionality on the uptake mechanisms, we synthesized four structurally related gold NPs (NP1-NP4) that feature cationic ligands with diverse headgroups presented on a non-interacting scaffold (Figure 2.1b). All particles were synthesized from a single batch of pentanethiol-capped gold NPs (~2 nm core) via place exchange reactions[17] and showed substantial peak broadening in ^{1}H NMR spectra with no sign of free ligands after the reaction. As expected, all of the particles have similar hydrodynamic diameters and positive zeta potentials. We studied NP uptake in two human cell lines: HeLa (a cervical carcinoma cell line) and MCF10A (a non-tumorigenic mammary epithelial cell line), providing a platform to examine the uptake mechanisms of gold NPs in both malignant (HeLa) and non-malignant cells (MCF10A).

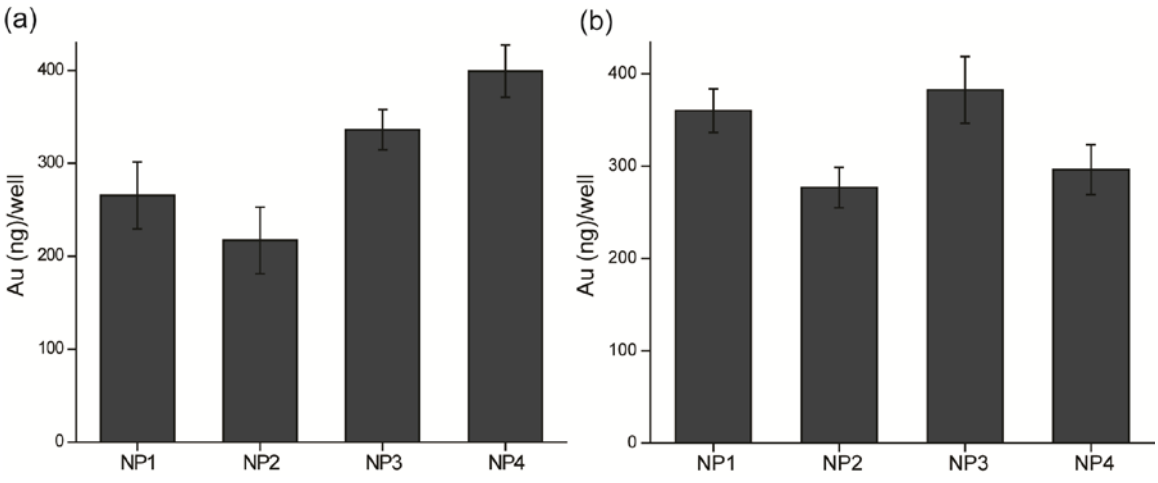

Figure 2.2. ICP-MS measurements of intracellular uptake of NP1-NP4 in (a) HeLa and (b) MCF10A cells after 1 h of NP incubation in serum free media. Error bars represent standard deviation.

NP uptake in cells was quantified using inductively coupled plasma mass spectrometry (ICP-MS).[18] After 1 h incubation of HeLa and MCF10A cells with NP1-NP4 (100 nM each) in serum free media, the cells were analyzed for intracellular gold content. The uptake amount

increases from NP1 to NP4 in HeLa cells (Figure 2.2a) while remained similar in the case of MCF10A cells (Figure 2.2b). No significant cytotoxicity was observed for any of the NPs (100 nM each) in either cell type (Figure 2.3).

Next, we investigated the effect of endocytic inhibitors on the cellular uptake mechanisms for the NPs. For all experiments, HeLa or MCF10A cells were pretreated with an inhibitor for 1 h followed by 1 h of incubation with the NPs in the presence of the inhibitor. Experiments were performed in serum free condition to exclude the effect of protein adsorption on NP surfaces that can potentially alter the endocytic pathways.[19] We focused first on the three major pinocytic pathways of cellular entry: macropinocytosis, clathrin-dependent, and caveolae/lipid raft-dependent micropinocytosis. No uptake inhibition was observed in either cell type for NP1-NP4 using wortmannin (WMN) (Figure 2.3a), an inhibitor that blocks the action of phosphoinositide 3-kinase, a key regulator in macropinocytosis.[20] This determination was further confirmed using sodium azide (NaN_3)/2-deoxyglucose (DOG), a system that depletes cellular ATP levels required for macropinocytosis (Figure 2.6). [21]

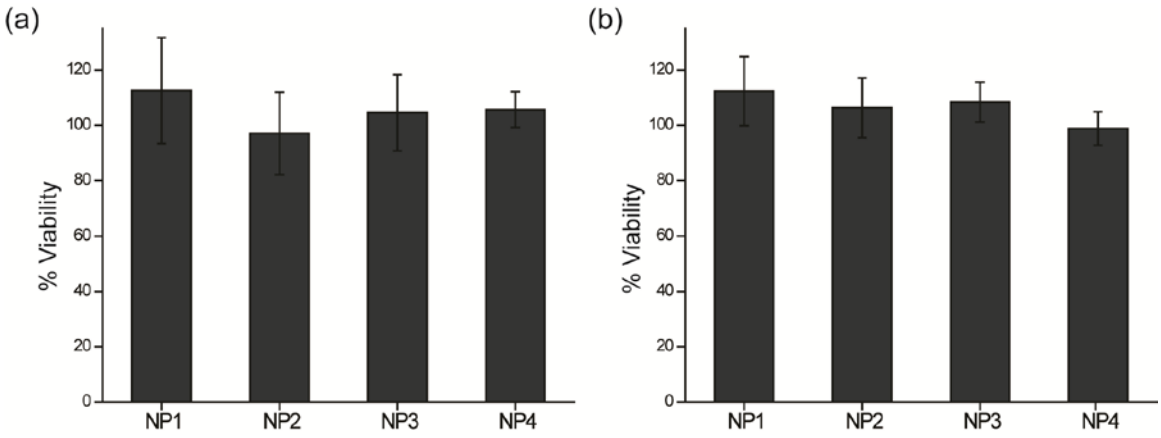

Figure 2.3. Cytotoxicity of NP1-NP4 (100 nM each) in (a) HeLa and (b) MCF10A cells after 1 hour, determined by alamar blue assay.

Membrane invagination during micropinocytosis requires microtubule and actin filament reorganization,[22] a process observed in NP uptake.[23] To evaluate the effect of cytoskeletal

rearrangement on NP uptake, we used two inhibitors: cytochalasin D (CytD)[24] and nocodazole[25] that disrupt F-actin polymerization and microtubule formation, respectively. In the case of CytD treated cells, the uptake of the NPs remained unaffected in both cell types except for NP3 that showed ~20 % inhibition in HeLa cells relative to the control (Figure 2.4b). Likewise, treatment with nocodazole did not show any significant inhibition for any of the particles in either HeLa or MCF10A cells (Figure 2.6), demonstrating cytoskeletal rearrangement is not critical for uptake of monolayer-protected NPs in either cell type.

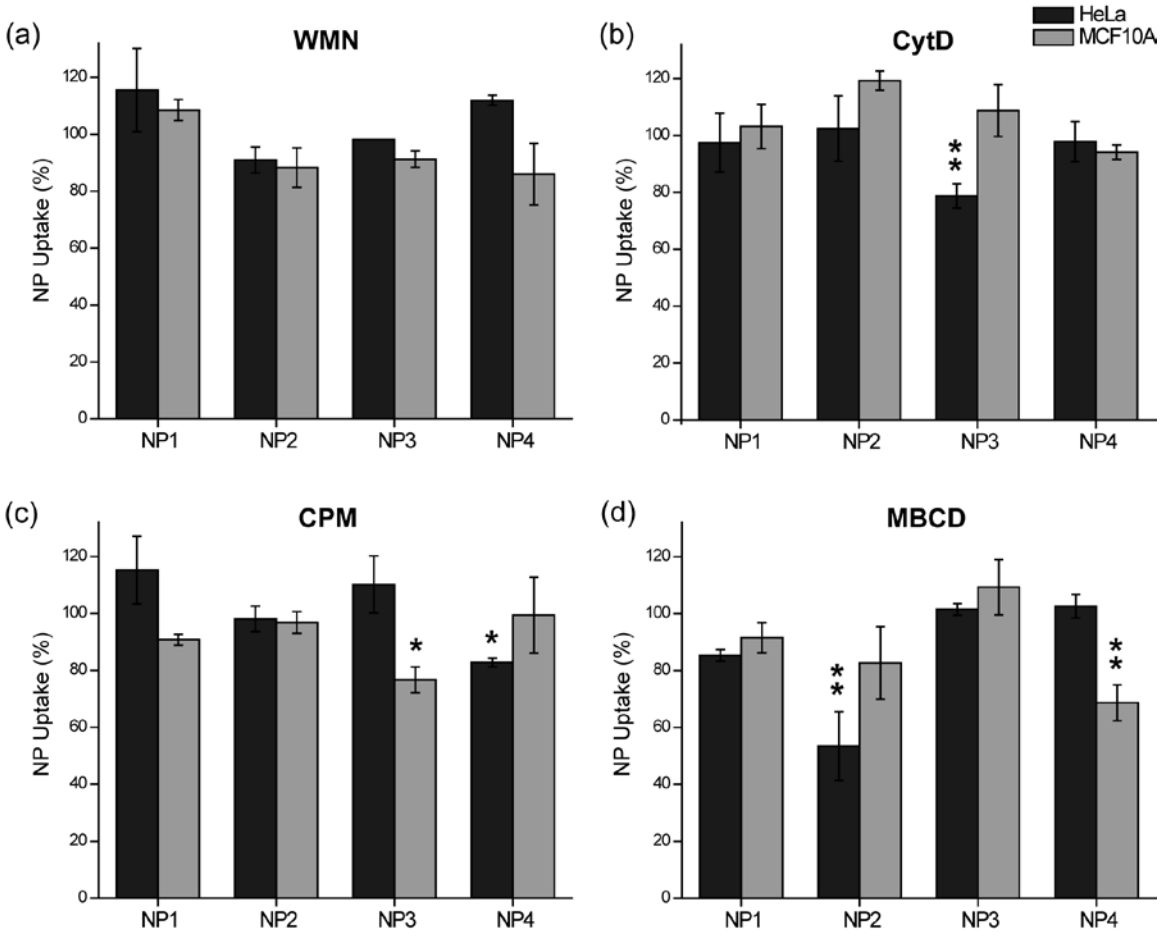

Figure 2.4. Uptake % of NP1-NP4 (compared to the positive controls) in the presence of different endocytic inhibitors in HeLa and MCF10A cells, (a) wortmannin (WMN), (b) cytochalasin D (CytD), (c) chlorpromazine (CPM), (d) methyl-β-cyclodextrin (MBCD). Error bars represent standard deviation. *$p<0.05$, **$p<0.01$ compared to the control.

Previous reports have demonstrated that cationic NPs (diameters ~90 nm) can enter HeLa cells via clathrin-dependent pathways.[26] However, we did not observe any strong inhibition in either HeLa or MCF10A cells using chlorpromazine (CPM),[27] an inhibitor of clathrin-mediated endocytosis (Figure 2.4c). In contrast, strong uptake inhibition (~50 %) was observed for NP2 in the cells pretreated with the cholesterol-depletion agent methyl-β-cyclodextrin (MBCD),[28] demonstrating the possible involvement of caveolae/lipid raft-mediated endocytosis for NP2 in HeLa cells (Figure 2.4d). In MCF10A cells, however, only NP4 showed significant uptake inhibition using MBCD. Therefore, subtle changes in the NP monolayer can switch the endocytic pathways in malignant and non-malignant cells, offering the potential for selective targeting strategies.[29] The other particles studied did not show any significant reduction of cellular uptake in the presence of any of the above inhibitors, indicating that the broader classes of endocytosis including macropinocytosis and clathrin-dependent endocytosis are not the major routes of entry of these monolayer-protected gold NPs into HeLa and MCF10A cells.

Recently, the dynamin-dependent endocytosis pathway has been extensively studied as a possible clathrin-independent transport mechanism into the cell.[30] We observed a significant inhibition of NP2 uptake (~60 %) in HeLa cells using dynasore (Figure 2.5a), an endocytic inhibitor that interferes with the dynamin-dependent pathways by blocking dynamin-GTPase.[31] Therefore, NP2 uptake is governed by both caveolae/lipid raft (Figure 2.4d) and dynamin-dependent pathways, a distinctly different feature from the other NPs studied. Surprisingly, in the case of MCF10A cells, uptake of all NPs was strongly inhibited by dynasore (Figure 2.5a) with NP2 being the most strongly inhibited (~80 %). Therefore, the dynamin-dependent pathway plays a key role in NP1-NP4 endocytosis in MCF10A cells, a striking difference from HeLa cells where only NP2 showed significant inhibition.

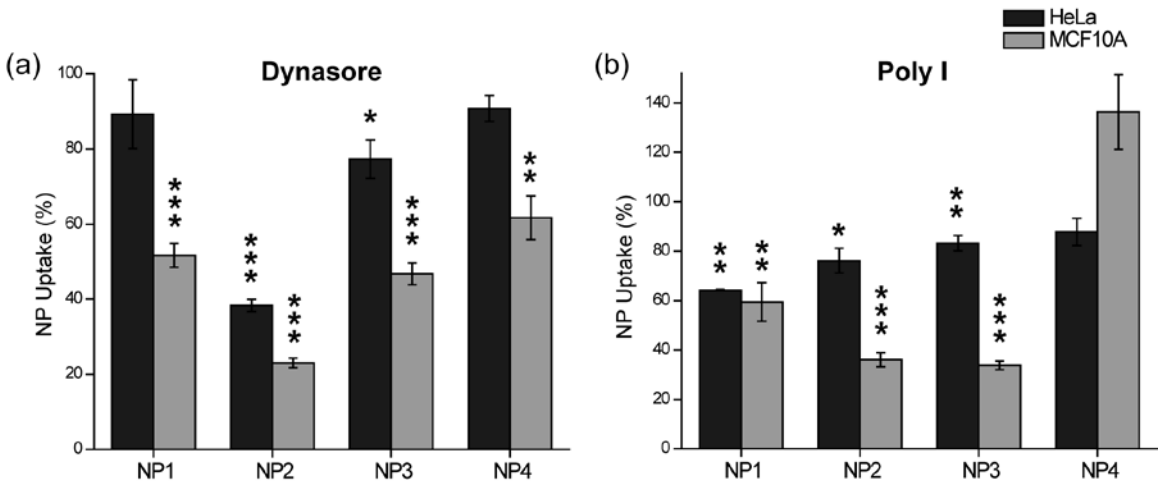

Figure 2.5. Uptake % of NP1-NP4 (compared to the positive controls) in HeLa and MCF10A cells in the presence of (a) dynasore and (b) poly I. Error bars represent standard deviation. *p<0.05,**p<0.01, ***p<0.001 compared to the control.

To investigate whether a more specific endocytic pathway is involved for the other NPs, we studied the involvement of scavenger receptors and membrane-bound G-protein coupled receptor (GPCR)[32]-mediated uptake pathways in both of the cell types. Scavenger receptors bind to a variety of ligands including low density lipoproteins and polysaccharides[33] and have been shown to be involved in gold NP uptake.[34] Poly I, a well-known inhibitor of scavenger receptors,[35] inhibited NP1 and NP3 uptake in both HeLa and MCF10A cells (Figure 2.5b), confirming the involvement of scavenger receptors for NP uptake in different mammalian cells. Significant uptake inhibition was observed for NP2 in MCF10A cells in the presence of poly I, however, this effect was not pronounced in HeLa cells. Conversely, $G\alpha_i$-protein (sub-family of GPCR) inhibitor pertussis toxin (PTX)[36] and phospholipase C inhibitor U-73122[37] did not show any reduction in uptake for any of the particles (Figure 2.6), demonstrating that GPCRs play no role in NP1-NP4 uptake in HeLa and MCF10A cells.

Table 2.1. Summary of uptake inhibition of NPs in presence of endocytic inhibitors

Inhibitor	Function	NP1		NP2		NP3		NP4	
		HeLa	MCF10A	HeLa	MCF10A	HeLa	MCF10A	HeLa	MCF10A
CytD	Inhibits F-actin polymerization	-	-	-	-	++	-	-	-
MBCD	Cholesterol depletion /caveolae	-	-	++	-	-	-	-	++
Nocodazole	Disruption of microtubules	-	-	-	-	-	-	-	-
NaN_3/DOG	ATP depletion	-	-	-	-	-	-	-	+
WMN	Inhibits phosphoinositide 3-kinase	-	-	-	-	-	-	-	-
PTX	Inhibits Gαi protein	-	-	-	-	-	-	-	-
U-73122	Inhibits phospholipase C (GPCR)	-	-	-	-	-	-	-	-
Poly I	Scavenger receptor inhibitor	++	++	+	+++	++	+++	-	-
CPM	Inhibits Rho GTPase (Clathrin)	-	-	-	-	-	+	+	-
Dynasore	Inhibits Dynamin-GTPase	-	+++	+++	+++	+	+++	-	++

+$p<0.05$, ++$p<0.01$, +++$p<0.001$ through unpaired t-test between control and inhibitor-treated groups

- no significant inhibition

Taken together, the broader classes of endocytic pathways including macropinocytosis and clathrin-mediated endocytosis were not the predominant uptake mechanisms for NP1-NP4 in both malignant and non-malignant cells. However, highly regulated uptake was observed via caveolae and dynamin-dependent micropinocytosis as well as through specific membrane-bound receptors in both of the cell types. For example, NP1 and NP3 showed scavenger receptor-mediated uptake while NP2 showed both caveolae and dynamin-dependent uptake in HeLa cells, demonstrating multifaceted internalization mechanisms of NPs into cells.[38] NP4 did not show strong uptake inhibition in HeLa cells for any of the classes of inhibitors tested, demonstrating the role of clathrin-independent/dynamin-independent mechanisms in mammalian cells.[30] In

MCF10A cells, both dynamin and scavenger receptor-mediated uptake was predominant for all of the particles except NP4 that also showed caveolae/lipid raft-mediated uptake (**Table 2.1**).

2.3. Conclusions

We have demonstrated that the mechanisms of small (~10 nm hydrodynamic diameter) cationic gold NP uptake in both malignant and non-malignant cells are strongly dependent on the gold NP monolayer structures and mostly rely on dynamin, scavenger receptors, and caveolae/lipid raft-mediated pathways. Significantly, the existence of differential uptake pathways for the same NP in cancer and normal cells provides an opportunity to design nanocarriers of specific therapeutic action and reduced cytotoxicity. Taken together, these studies indicate the importance of NP surface monolayer structures in endocytic pathways and signify the role of particle design in nanomedicine.

2.4. Experimental Section

Synthesis of NP1-NP4: 1-Pentanethiol capped gold nanoparticles (d=~2 nm) were synthesized according to Brust-Schiffrin method.[39] A place exchange reaction[40] was performed by dissolving corresponding thiol ligands and pentanethiol capped gold nanoparticles in dichloromethane (DCM) and stirring for 3 days in room temperature under argon atmosphere. The solvent was removed under reduced pressure and the resulting precipitate was dissolved in distilled water and dialyzed for 2 days (membrane molecular cut-off =10000) to remove excess ligands, acetic acid and other salts present in the nanoparticle solution. After dialysis, the particle was lyophilized to yield a solid brownish product. The particles are then redispersed in deionized water. ^{1}H NMR-spectra in D_2O showed substantial broadening of the proton peaks with no sign of free ligands.

Cell culture: HeLa cells were grown in low glucose Dulbecco's Modified Eagle's Medium (GIBCO, Catalog# 10567) supplemented with 10% fetal bovine serum (Thermo Scientific, SH3007103) and 1% antibiotics (Cellgro, 30-004-CI). The cells were maintained in the above media and subcultured once every four days. MCF10A cells were grown in mammary epithelium growth medium (Lonza, CC-3051A) supplemented with bovine pituitary extract (Lonza, CC-4009). Media were replaced every two days and cells were subcultured every seven days.

NP uptake and inhibition studies: HeLa or MCF10A cells were seeded in a 48 well plate at a density of ~2×10^4 cells/well 24 h prior to the experiment. On the following day, cells were washed one time with phosphate buffered saline (PBS) and incubated with following endocytic inhibitors in serum free media for 1 h at 37 ˚C: cytochalasin D (10 μg/mL), methyl-β-cyclodextrin (5 mg/mL), nocodazole (10 μg/mL), 3 mg/mL NaN_3/50 mM 2-deoxyglucose, wortmannin (100 ng/mL), pertussis toxin (100 ng/mL), U-73122 (4 μg/mL), polyinosinic acid (10 μg/mL), chlorpromazine (10 μg/mL) and dynasore (80 μM). The concentrations of the inhibitors were used as described in previous reports.[41] After 1 h, media were replaced with fresh media containing the inhibitors with NPs (100 nM) and further incubated for 1 h at 37 ˚C. Untreated cells and cells treated with only NPs (no inhibitor) were used as negative and positive controls, respectively. After incubation, cells were washed three times with PBS and lysis buffer was added to each well. All lysed cell samples were then further processed for ICP-MS analysis (*vide infra*) to determine the intracellular amount of gold. All inhibitors were purchased from Sigma except for dynasore, chlorpromazine, and pertusis toxin that were obtained from Fisher Scientific. Particle uptake (%) was calculated based on the following equation:

NP uptake (%) = (NP uptake in presence of inhibitors/NP uptake in absence of inhibitors) × 100

Sample preparation for ICP-MS and ICP-MS instrumentation: After cellular uptake, the lysed cells were digested with 0.5 mL of fresh *aqua regia (highly corrosive and must be used with extreme caution!)* for 10 minutes. The digested samples were diluted to 10 mL with de-ionized water. A series of gold standard solutions (20, 10, 5, 2, 1, 0.5, 0.2, and 0 ppb) were prepared before each experiment. Each gold standard solution also contained 5% *aqua regia*. The gold standard solutions and cellular uptake sample solutions were measured on an Elan 6100 ICP mass spectrometer (PerkinElmer SCIEX, Waltham, MA). The instrument was operated with 1550 W RF power and the nebulizer Ar flow rate was optimized at 0.96 L/min.

Cytotoxicity of NPs in HeLa and MCF10A cells: The cell viability was determined by alamar blue assay according to manufacturer protocol (Invitrogen Biosource, USA). HeLa or MCF10A cells (~15000 cells/well) were seeded in a 96-well plate 24 hours prior to the experiment. On the following day, the old media was aspirated and the cells were washed with phosphate buffered saline (PBS) for one time. NP1-NP4 (100 nM each) were then incubated with the cells in serum free medium for 1 hour at 37 ˚C. After the incubation period, the cells were washed three times with PBS and 220 µL of 10 % alamar blue solution in serum containing media was added to each well and cells were further incubated at 37 ˚C for 4 hours. After 4 hours, 200 µL of solution from each well were taken out and loaded in a 96- well black microplate. Red fluorescence, resulting from the reduction of the alamar blue solution by viable cells was monitored (Ex: 560 nm, Em: 590 nm) on a SpectroMax M2 microplate reader (Molecular Device). Viability (%) of NP-treated cells was calculated taking untreated cells as 100 % viable. Each experiment was done in triplicate.

2.5. Supplementary Information

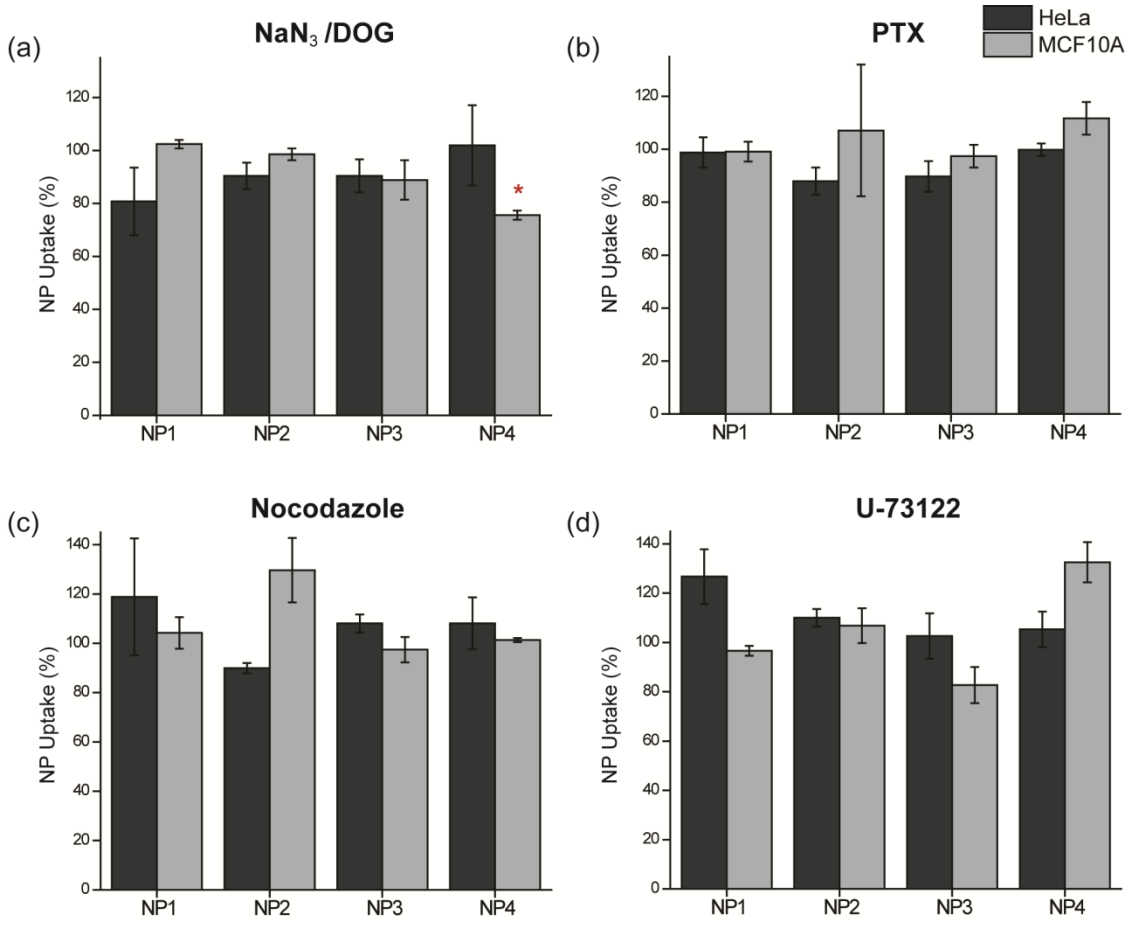

Figure 2.6. % Uptake of **NP1-NP4** (compared to positive controls) in both HeLa and MCF10A cells in the presence of endocytic inhibitors (a) NaN3/2-deoxyglucose, (b) pertussis toxin (PTX), (c) Nocodazole, (d) U-73122. *p<0.05 compared to control.

2.6. References

1. (a) Duncan, B.; Kim, C.; Rotello, V. M. *J. Control. Release* **2010**, *148*, 122. (b) Davis, M. E.; Chen, Z.; Shin, D. M. *Nat. Rev. Drug Discov.* **2008**, *7*, 771.

2. (a) Peer, D.; Lieberman, J. *Gene Ther.* **2011**, *18*, 1127. (b) Davis, M. E.; Zuckerman, J. E.; Choi, C. H. J.; Seligson, D.; Tolcher, A.; Alabi, C. A.; Yen, Y.; Heidel, J. D.; Ribas, A. *Nature* **2010**, *464*, 1067.

3. (a) Bareford, L. A.; Swaan, P. W. *Adv. Drug Delivery Rev.* **2007**, *59*, 748. (b) Zaki, N. M.; Tirelli, N. *Expert Opin. Drug Deliv.* **2010**, *7*, 895.

4. Sahay, G.; Alakhova, D. Y.; Kabanov, A. V. *J. Control. Release* **2010**, *145*, 182.

5. Conner, S. D.; Schmid, S. L. *Nature* **2003**, *422*, 37.

6. Swanson, J. A.; Watts, C. *Trends Cell. Biol.* **1995**, *5*, 424.

7. Kumari, S.; Swetha, M. G.; Mayor, S. *Cell Res.* **2010**, *20*, 256.

8. (a) Chithrani, B. D.; Ghazani, A. A.; Chan, W. C. W. *Nano Lett.* **2006**, *6*, 662. (b) Walkey, C. D.; Olsen, J. B.; Guo, H.; Emili, A.; Chan, W. C. W. *J. Am. Chem. Soc.* **2012**, *134*, 2139.

9. Chithrani, B. D.; Chan, W. C. W. *Nano Lett.* **2007**, *7*, 1542.

10. Cho, E. C.; Xie, J. W.; Wurm, P. A.; Xia, Y. N. *Nano Lett.* **2009**, *9*, 1080.

11. Cho, E. C.; Au, L.; Zhang, Q.; Xio, Y. *Small* **2010**, *6*, 517.

12. Dausend, J.; Musyanovych, A.; Dass, M.; Walther, P.; Schrezenmeier, H.; Landfester, K.; Mailander, V. *Macromol. Biosci.* **2008**, *8*, 1135.

13. Rejman, J.; Oberle, V.; Zuhorn, I. S.; Hoekstra, D. *Biochem. J.* **2004**, *377*, 159.

14. (a) Yang, H.; Fung, S. Y.; Liu, M. Y. *Angew. Chem. Int. Ed.* **2011**, *50*, 9643. (b) Oh, E.; Delehanty, J. B.; Sapsford, K. E.; Susumu, K.; Goswami, R.; Blanco-Canosa, J. B.; Dawson, P.

E.; Granek, J.; Shoff, M.; Zhang, Q.; Goering, P. L.; Huston, A.; Medintz, I. L. *Acs Nano* **2011**, *5*, 6434.

15. (a) Chompoosor, A.; Saha, K.; Ghosh, P. S.; Macarthy, D. J.; Miranda, O. R.; Zhu, Z. J.; Arcaro, K. F.; Rotello, V. M. *Small* **2010**, *6*, 2246. (b) Verma, A.; Stellacci, F. *Small* **2010**, *6*, 12. (c) Saha, K.; Bajaj, A.; Duncan, B.; Rotello, V. M. *Small* **2011**, *7*, 1903.

16. Al-Hajaj, N. A.; Moquin, A.; Neibert, K. D.; Soliman, G. M.; Winnik, F. M.; Maysinger, D. *Acs Nano* **2011**, *5*, 4909.

17. Hostetler, M. J.; Wingate, J. E.; Zhong, C. J.; Harris, J. E.; Vachet, R. W.; Clark, M. R.; Londono, J. D.; Green, S. J.; Stokes, J. J.; Wignall, G. D.; Glish, G. L.; Porter, M. D.; Evans, N. D.; Murray, R. W. *Langmuir* **1998**, *14*, 17.

18. (a) Cho, E. C.; Zhang, Q.; Xia, Y. N. *Nat. Nanotechnol.* **2011**, *6*, 385. (b) Kim, C.; Agasti, S. S.; Zhu, Z. J.; Isaacs, L.; Rotello, V. M. *Nat. Chem.* **2010**, *2*, 962.

19. (a) Alkilany, A. M.; Nagaria, P. K.; Hexel, C. R.; Shaw, T. J.; Murphy, C. J.; Wyatt, M. D. *Small* **2009**, *5*, 701. (b) Kim, K. J.; Malik, A. B. *Am. J. Physiol. Lung Cell Mol. Physiol.* **2003**, *284*, L247. (c) Panyam, J.; Labhasetwar, V. *Pharm. Res.* **2003**, *20*, 212.

20. (a) Araki, N.; Johnson, M. T.; Swanson, J. A. *J. Cell. Biol.* **1996**, *135*, 1249. (b) Khandelwal, P.; Ruiz, W. G.; Apodaca, G. *Embo J.* **2010**, *29*, 1961.

21. Chen, J.; Li, G.; Lu, J.; Chen, L.; Huang, Y.; Wu, H. L.; Zhang, J. X.; Lu, D. R. *Biochem. Biophys. Res. Commun.* **2006**, *347*, 931.

22. Schafer, D. A. *Curr. Opin. Cell Biol.* **2002**, *14*, 76.

23. (a) Ruan, G.; Agrawal, A.; Marcus, A. I.; Nie, S. *J. Am. Chem. Soc.* **2007**, *129*, 14759. (b) dos Santos, T.; Varela, J.; Lynch, I.; Salvati, A.; Dawson, K. A. *Plos One* **2011**, *6*, e24438.

24. Fujimoto, L. M.; Roth, R.; Heuser, J. E.; Schmid, S. L. *Traffic* **2000**, *1*, 161.

25. Hasegawa, S.; Hirashima, N.; Nakanishi, M. *Gene Ther.* **2001**, *8*, 1669.

26. Harush-Frenkel, O.; Debotton, N.; Benita, S.; Altschuler, Y. *Biochem Biophys Res Commun* **2007**, *353*, 26.

27 (a) Qian, Z. M.; Li, H. Y.; Sun, H. Z.; Ho, K. *Pharmacol. Rev.* **2002**, *54*, 561. (b) Stuart, A. D.; Brown, T. D. K. *J. Virol.* **2006**, *80*, 7500.

28. (a) Brandenberger, C.; Muhlfeld, C.; Ali, Z.; Lenz, A. G.; Schmid, O.; Parak, W. J.; Gehr, P.; Rothen-Rutishauser, B. *Small* **2010**, *6*, 1669. (b) Rodal, S. K.; Skretting, G.; Garred, O.; Vilhardt, F.; van Deurs, B.; Sandvig, K. *Mol. Biol. Cell* **1999**, *10*, 961.

29. Bhattacharyya, S.; Singh, R. D.; Pagano, R.; Robertson, J. D.; Bhattacharya, R.; Mukherjee, P. *Angew. Chem. Int. Ed.* **2012**, *51*, 1563.

30. (a) Mayor, S.; Pagano, R. E. *Nat. Rev. Mol. Cell Biol.* **2007**, *8*, 603. (b) Howes, M. T.; Mayor, S.; Parton, R. G. *Curr. Opin. Cell Biol.* **2010**, *22*, 519.

31. Macia, E.; Ehrlich, M.; Massol, R.; Boucrot, E.; Brunner, C.; Kirchhausen, T. *Dev. Cell.* **2006**, *10*, 839.

32. George, S. R.; O'Dowd, B. F.; Lee, S. R. *Nat. Rev. Drug Discov.* **2002**, *1*, 808.

33. Murphy, J. E.; Tedbury, P. R.; Homer-Vanniasinkam, S.; Walker, J. H.; Ponnambalam, S. *Atherosclerosis* **2005**, *182*, 1.

34. (a) Franca, A.; Aggarwal, P.; Barsov, E. V.; Kozlov, S. V.; Dobrovolskaia, M. A.; Gonzalez-Fernandez, A. *Nanomedicine* **2011**, *6*, 1175. (b) Patel, P. C.; Giljohann, D. A.; Daniel, W. L.; Zheng, D.; Prigodich, A. E.; Mirkin, C. A. *Bioconjugate Chem.* **2010**, *21*, 2250.

35. (a) Raynal, I.; Prigent, P.; Peyramaure, S.; Najid, A.; Rebuzzi, C.; Corot, C. *Invest. Radiol.* **2004**, *39*, 56. (b) Haisma, H. J.; Kamps, J. A. A. M.; Kamps, G. K.; Plantinga, J. A.; Rots, M. G.; Bellu, A. R. *J. Gen. Virol.* **2008**, *89*, 1097. (c) Liu, Y. P.; Tong, C.; Dispenzieri, A.; Federspiel, M. J.; Russell, S. J.; Peng, K. W. *Cancer Gene Ther.* **2012**, *19*, 202.

36. Gunther, E. C.; Von Bartheld, C. S.; Goodman, L. J.; Johnson, J. E.; Bothwell, M. *Neuroscience* **2000**, *100*, 569.

37. Mogami, H.; Mills, C. L.; Gallagher, D. V. *Biochem. J.* **1997**, *324*, 645.

38. (a) Banquy, X.; Suarez, F.; Argaw, A.; Rabanel, J. M.; Grutter, P.; Bouchard, J. F.; Hildgen, P.; Giasson, S. *Soft Matter* **2009**, *5*, 3984. (b) McLendon, P. M.; Fichter, K. M.; Reineke, T. M. *Mol. Pharm.* **2010**, *7*, 738.

39. Brust, M.; Fink, J.; Bethell, D.; Schiffrin, D. J.; Kiely, C. *J. Chem. Soc., Chem. Commun.* **1995**, 1655.

40. Hostetler, M. J.; Templeton, A. C.; Murray, R. W. *Langmuir* **1999**, *15*, 3782.

41. (a) Zhang, L. W.; Monteiro-Riviere, N. A. *Toxicol. Sci.* **2009**, *110*, 138. (b) Lunov, O.; Syrovets, T.; Loos, C.; Beil, J.; Delecher, M.; Tron, K.; Nienhaus, G. U.; Musyanovych, A.; Mailander, V.; Landfester, K.; Simmet, T. *Acs Nano* **2011**, *5*, 1657. (c) Gratton, S. E. A.; Ropp, P. A.; Pohlhaus, P. D.; Luft, J. C.; Madden, V. J.; Napier, M. E.; DeSimone, J. M. *Proc. Natl. Acad. Sci. U.S.A.* **2008**, *105*, 11613.

CHAPTER 3

THE ROLE OF SURFACE FUNCTIONALITY ON ACUTE CYTOTOXICITY, ROS GENERATION AND DNA DAMAGE BY CATIONIC GOLD NANOPARTICLES

3.1. Introduction

Gold nanoparticles (AuNPs) are promising materials for biomedical applications[1,2] due to their tunable surface properties [3] and extraordinary stability.[4] Additionally, the inert core material reduces the potential for toxicity issues arising from particle degradation.[5] The size regime and concomitant geometrical outcomes including high degree of curvature, however, generates the potential for toxicity.[6],[7] Generally, the toxicity of AuNPs depends on size, shape, the degree to which they aggregate, and their surface properties.[8] Recently, several studies on the short-term cytotoxicity of AuNPs[9] and quantum dots[10] have focused on size,[11,12] shape,[13,14] and charge.[15] To date, however, issues such as ligand hydrophobicity have not been systematically explored.

In addition to acute toxicity arising from lysis and other disruptive events, DNA damage (genotoxicity) is an important issue in the application of nanomaterials. DNA damage provides both a useful strategy for anti-cancer drugs as well as a potential challenge for the design of non-cytotoxic therapeutics. Recently, El-Sayed and coworkers has shown that AuNPs with nuclear targeting motifs elicit significant damage of DNA and concomitant programmed cell death.[16] This outcome mirrors the behavior of anticancer drugs such as cisplatin and analogs.[17] As such, AuNPs can be envisioned as therapeutic agents in their own right as well serving as carriers for other drugs and biomolecules.[18] Taken together, an in-depth understanding of how NPs interact with cell surfaces and cellular organelles is central to their applications in biomedicine. [19]

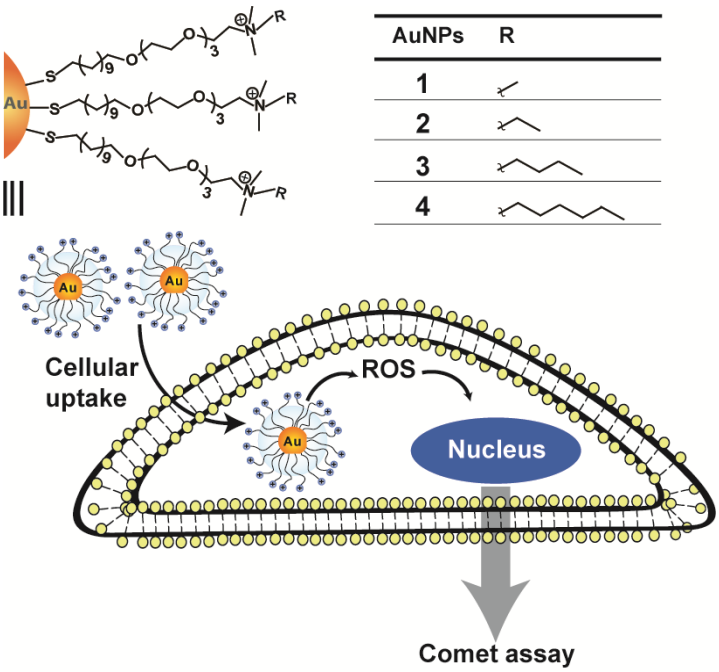

Figure 3.1. A series of AuNPs used in this study and a proposed mechanism of DNA damage determined by comet assay.

Recently, several reports have described varying degrees of transfection efficiency of cationic lipids by increasing the chain length and hydrophobicity.[20] Hence, to examine the effect of surface hydrophobicity on acute and long-term nanoparticle cytotoxicity, we have synthesized a series of 2 nm core AuNPs that feature an quaternary ammonium functionality with a systematically varied (C1-C6) hydrophobic alkyl tail (Figure 3.1). We have quantified the acute cytotoxicity of these AuNPs through mitochondrial activity assay, and the potential for long-term toxicity through quantification of reactive oxygen species (ROS) generation and DNA damage. Results are strongly dependent upon side chain structure, with greater acute toxicity and decreased DNA damage observed with increasing hydrophobicity. Significantly, these AuNPs can generate significant amounts of reactive oxygen species (ROS) that oxidatively damage DNA at concentrations that do not affect mitochondrial activity. These results suggest that caution is needed in the use of small AuNPs as carriers. Importantly, these results indicate the potential utility of these systems as cytotoxic therapeutic agents for cancer therapy.

3.2. Results and Discussion

The required AuNPs were synthesized via place exchange[21] of pentanethiol capped AuNPs (~2 nm) fabricated by Brust-Schiffrin reduction method.[22] Acute toxicity of the nanoparticles was determined through the alamar blue assay, a method based on mitochondrial activity. HeLa cells were treated with AuNPs dispersed in culture media with the concentrations ranging from 0-10 μM and incubated for 24 h. As shown in Figure 3.2, cellular viability decreases with increasing alkyl chain length, i.e. AuNP **1** is the least toxic (IC_{50} = 6 μM) while AuNP **4** is the most toxic (IC_{50} = 0.71 μM).

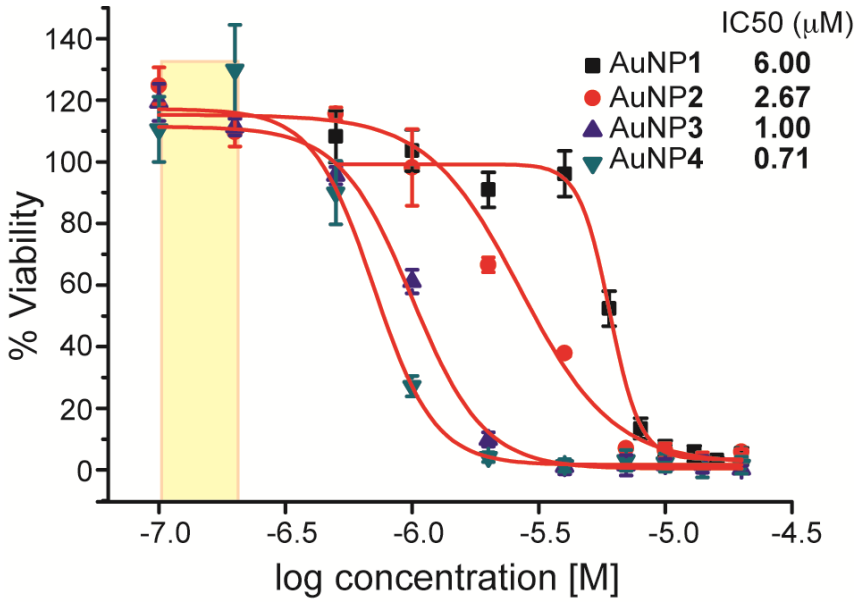

Figure 3.2. Cytotoxicity of AuNP **1-4** in HeLa cells determined by alamar blue assay and IC_{50} of particular AuNPs. The box represents the concentration range used in the ROS generation and DNA damage study.

In general, nanomaterials that retain >80% cell viability are considered safe for use in biological applications.[23] We next determined whether nanoparticles in this concentration range are capable of generating endogenous ROS and further causing DNA damage. As cellular uptake of these nanomaterials depends upon surface functionality,[24,25] we first used ICP-MS to

determine the extracellular concentrations of nanoparticle required to obtain a constant intracellular AuNP concentration (214 ng/well, Figure 3.3a). The calculated concentrations yielding 214 ng/well of intracellular gold were 100, 123, 148, and 165 nM for AuNP **1** to AuNP **4**, respectively, and were in the regime where treatment with all particles provided 100% viability.

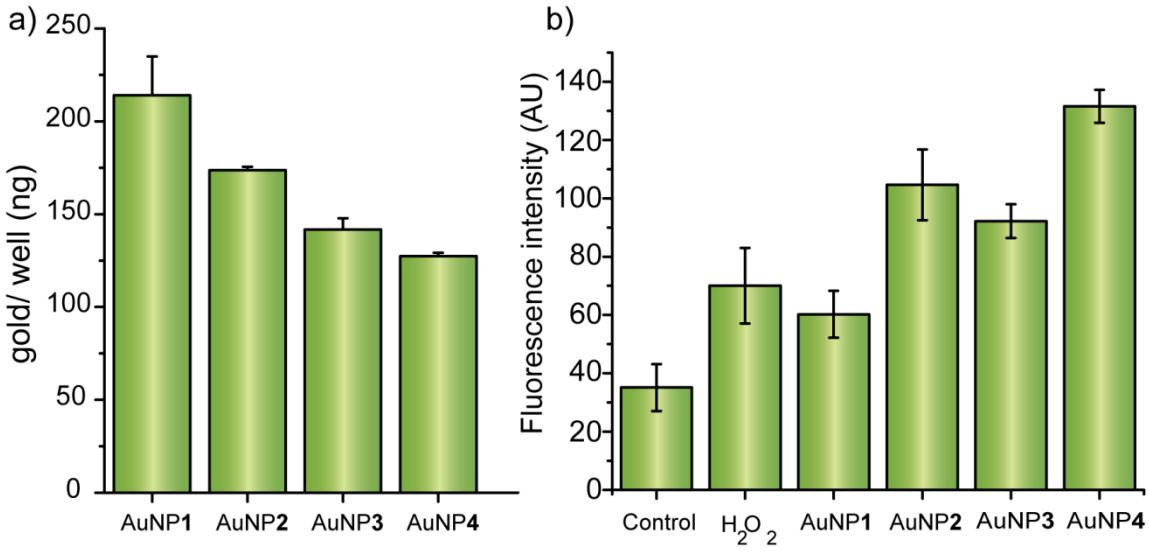

Figure 3.3. a) Uptake of AuNP**1-4** in HeLa cells b**)** ROS in HeLa cells determined by the oxidation of H_2DCFDA dye. The intracellular gold in each AuNPs was 214 ng/well. The controls were cells alone and cells treated with exogenous H_2O_2 (0.3% v/v). The data were statistically analyzed and significant ROS level difference was found between AuNP **1** and AuNP **4** (t=12.57, p=0.0002).

Endogenous ROS production was quantified using 2',7'-dichlorodihydrofluorescein diacetate (H_2DCFDA).[26] ROS species convert non-fluorescent H_2DCFDA to its fluorescent 2',7'-dichlorofluorescein (DCF) that can be quantified using a micro plate reader. Again, HeLa cells were treated with AuNPs dispersed in the cell culture media and incubated for 24 h. From Figure 3.3 it can be seen that the production of ROS was dependent on the AuNPs functionalization. The results indicate that increasing hydrophobicity increases ROS production, a result that mirrors mitochondrial activity albeit at much lower concentrations.

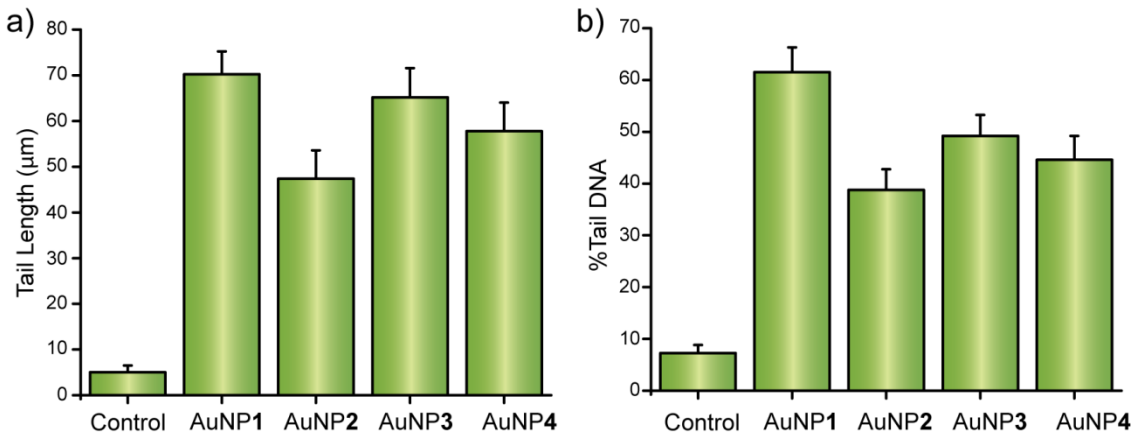

Figure 3.4. a) Tail Length of AuNP **1-4** from the comet assay b) % Tail DNA of AuNP **1-4** from the comet assay. Statistical analysis by ANOVA and post hoc t-tests with Bonferoni Correction for multiple comparisons revealed all of the nanoparticles caused significant DNA damage compared to control. ($p<0.001$)

Having established that hydrophobicity plays an important role in the generation of ROS and hence *potential* genotoxicity, we next explored the effect of particle hydrophobicity on DNA damage. DNA damage was quantified through the single cell gel electrophoresis, using the comet assay.[27] This technique provides a versatile and sensitive method to detect DNA damage. As with the ROS studies, the cells were incubated with AuNPs for 24 h. The cells were then trypsinized, embedded in agarose gel, and then lysed prior to performing gel electrophoresis. The DNA embedded in the gels was stained with SYBR Green dye and imaged by fluorescence microscopy (40X magnification) (Figure 3.5). The data were analyzed by Komet software. We observed that all four AuNPs significantly damage DNA in comparison to the control, as indicated by both and Tail Length (Figure 3.4a) and % Tail DNA (Figure 3.4b). Interestingly, AuNP **1** caused significantly greater DNA damage than the rest of the AuNPs, contrasting with data derived from the mitochondrial activity (Figure 3.2) and ROS generation assay (Figure 3.3b).

In addition, the percent of damaged cells was defined as those with values of % Tail DNA and Tail Length greater than two standard deviations above the mean of the control group values. Again, AuNP **1** resulted in the greatest percent of damaged cells (Figure 3.5). The degree of DNA damage is comparable to mercaptoundecanoic acid-functionalized quantum dots (tail

length~ 76±3.52 μm, @200 μg/mL)[10] Notably, AuNP **1** causes DNA damage similar to cisplatin (79.7±8% DNA in Tail) when administered to cells at concentrations that yield 75% cell viability.[28]

3.3. Conclusions

We have determined that both the acute cytotoxicity and genotoxicity of positively charged AuNPs depend on the hydrophobicity of the ligands attached. Increasing the hydrophobicity of the particles increased their cytotoxicity. Increasing hydrophobicity likewise increased ROS production, even at AuNP concentrations where 100% cell viability was observed. Interestingly, DNA damage *decreased* with increasing particle hydrophobicity. In literature, conflicting cytotoxicity and DNA damage result has been reported between structurally similar complexes.[28] In addition, cells have *in vivo* mechanisms that maintain homeostasis.[29] Moreover, treatment with AuNPs induces the endogenous ROS production. This oxidative stress environment could initiate the autophagic process,[30] which can destroy foreign molecules to avoid cell death. This process may contribute cell survival in an oxidative environment of NPs. Therefore, AuNP 4 which produces more ROS, can be presumably degraded due to autophagy and will be less available to damage DNA. Taken together, these studies indicate that AuNPs can be employed not only as carriers but also as potential therapeutics that exploit their capability to elicit cell function and generate cytotoxic and genotoxic responses.

3.4. Experimental Section

Cell culture: HeLa cells were cultured at 37°C under a humidified atmosphere of 5% CO_2. The cells were grown in low glucose Dulbecco's Modified Eagle's Medium (DMEM, 4.0 g/L glucose) containing 10% fetal bovine serum and 1% antibiotics (100 U/ml penicillin and 100

μg/ml streptomycin). The cells were maintained in the above media and subcultured once every four days.

Alamar blue assay: The cell viability was evaluated by using an alamar blue assay according to the manufacturer's protocol (Invitrogen Biosource, USA). In a typical experiment, cells were seeded at 3000 cells/well in a 96 well-plate 24 h prior to the experiment. On the following day, the old media was aspirated and cells were washed one time with cold PBS before putting the different concentrations of AuNP **1**, AuNP **2**, AuNP **3** and AuNP **4** ranging from 0-10 μM dispersed in the pre-warmed serum-containing media. The cells were again incubated 24 h at 37°C under a humidified atmosphere of 5% CO_2. On the next day, after thoroughly washing the cells three times with PBS buffer, the cells were treated with 220 μL of 10% alamar blue in serum-containing media. Subsequently, the cells were incubated at 37°C under a humidified atmosphere of 5% CO_2 for 3 h. After 3 h of incubation, 200 μL of solution from each wells was taken out and placed in a 96-well black microplate. Red fluorescence, resulting from the reduction of alamar blue solution, was valued (excitation/emission: 535 nm/590 nm) on a SpectroMax M5 microplate reader (Molecular Device) to determine the cellular viability. Each experiment was done in triplicate.

Endogenous reactive oxygen species (ROS): The ROS was determined through a microplate reader. HeLa cells were plated into a 24-well plate (20K /well) for 24 h prior the experiment. On the following day, cells were treated with AuNPs with the concentration of 100, 123, 148, and 165 nM for AuNP **1** to AuNP **4**, respectively. As a positive control experiment, cells were treated with 0.3% H_2O_2 suspended in culture media and incubate for 30 min at 37°C before performing the assay. After 24 h incubation, cells were wash with PBS 3 times and were subsequently treated with 2',7'-dichlorodihydrofluorescein diacetate, H_2DCFDA (Molecular Probes/ Invitrogen) (250 mL, 5 μM/well). Experiments were done in triplicate. After incubating for 30 min, the cells were washed by PBS and lysed with cell lysis buffer (Gene Therapy

Systems). 200 μL of solution from each well was transferred to a 96-well black microplate. Fluorescence intensity, resulting from the oxidation of dye, was valued (excitation/emission: 488 nm/520 nm) on a SpectroMax M5 microplate reader (Molecular Device) to determine the level of ROS. The level of ROS production by AuNPs was compared using a one way ANOVA and post hoc t-tests with a Bonferoni Correction for multiple comparisons. All four AuNPs resulted in a significant increase in ROS levels (ANOVA; F=45.08; df=5, 11). Moreover, ROS produced by AuNP **1** was significantly less than AuNP **2** (p=0.006), AuNP **3** (p=0.005), & AuNP **4** (p=0.0001).

Comet assay: For the comet assay, the HeLa cells were maintained as mentioned above. HeLa cells (20K cells/well) were plated in a 24-well plate for 24 h prior to performing the experiment. On the day of the experiment, cells were washed using cold PBS once. Thereafter, AuNPs were dispersed in pre-warmed serum-containing media with the final concentration determined according to ROS experiments. Cells were treated with AuNP solution and kept in cell culture incubator for 24 h. For the comet assay, cells were washed in PBS three times and trypsinized by trypsin EDTA 1X (MediaTech, Inc, USA). Cells were collected by centrifugation at 1000 rpm, 5 min. After centrifugation, cells were dispersed in PBS and embedded in 1% low melting point agarose (Agarose Type I-B, Sigma Aldrich). The agarose gel was transferred to CometSlide^{TM} HT (Trevigen, USA) and kept in 4°C refrigerator for 10 min. Slides were placed in a cold lysis solution (2.5 M NaCl, 80 mM Na_2-EDTA, 1 mM Tris-HCl, and 1% Triton X-100, pH 10) and kept at 4°C in the dark for 24 h. Electrophoresis was performed in 0.3 M NaOH, 0.5 mM Na_2-EDTA, and pH 13 for 35 min at 20 V, 300 mA. The slides were then neutralized and stained with SYBR Green dye (Invitrogen, USA). The comet images were pictured for 34, 52, 59, 76 nuclei for AuNP **1-4**, respectively using a fluorescence microscope (40X magnification, Nikon E600 microscope stand) with a green filter. The data were analyzed through Komet software. One-way analysis of variance revealed significant effects of treatment group for both tail length (F=10.33; df=243, 4; P<0.001) and % tail DNA (F=12.18; df=242, 4; P<0.001). Post

hoc t-tests with Bonferoni Correction for multiple comparisons demonstrated that all of the nanoparticles caused significant DNA damage.

3.5. Supplementary Information

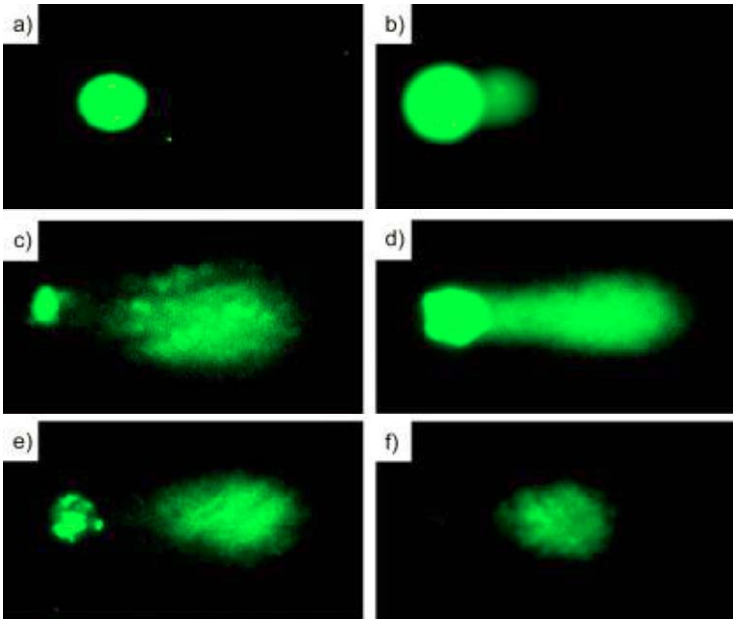

Figure 3.5. Optical images of comet assay from each treatment. a) cell alone, b) cell alone, c)AuNP **1**, d) AuNP **2**, e) AuNP **3**, f) AuNP **4**.

3.5. References

1. Rosi, N. L.; Mirkin, C. A. *Chem. Rev.* **2005**, *105*, 1547.

2. De, M.; Ghosh, P. S.; Rotello, V. M. *Adv. Mater.* **2008**, *20*, 4225.

3. Templeton, A. C.; Wuelfing, M. P.; Murray, R. W. *Acc. Chem. Res.* **2000**, *33*, 27.

4. Zheng, M.; Davidson, F.; Huang, X. Y. *J. Am. Chem. Soc.* **2003**, *125*, 7790.

5. (a) Connor, E. E.; Mwamuka, J.; Gole, A.; Murphy, C. J.; Wyatt, M. D. *Small* **2005**, *1*, 325. (b) Merchant, B. *Biologicals* **1998**, *26*, 49. (c) Shukla, R.; Bansal, V.; Chaudhary, M.; Basu, A.; Bhonde, R. R.; Sastry, M. *Langmuir* **2005**, *21*, 10644.

6. Nel, A.; Xia, T.; Madler, L.; Li, N. *Science* **2006**, *311*, 622.

7. Meng, H.; Xia, T.; George, S.; Nel, A. E. *Acs Nano* **2009**, *3*, 1620.

8. Lanone, S.; Boczkowski, J. *Curr. Mol. Med.* **2006**, *6*, 651.

9. Verma, A.; Stellacci, F. *Small* **2010**, *6*, 12.

10. (a) Pan, Y.; Leifert, A.; Ruau, D.; Neuss, S.; Bornemann, J.; Schmid, G.; Brandau, W.; Simon, U.; Jahnen-Dechent, W. *Small* **2009**, *5*, 2067. (b) Cho, W. S.; Cho, M. J.; Jeong, J.; Choi, M.; Cho, H. Y.; Han, B. S.; Kim, S. H.; Kim, H. O.; Lim, Y. T.; Chung, B. H.; Jeong, J. *Toxicol. Appl. Pharmacol.* **2009**, *236*, 16. (c) Pan, Y.; Neuss, S.; Leifert, A.; Fischler, M.; Wen, F.; Simon, U.; Schmid, G.; Brandau, W.; Jahnen-Dechent, W. *Small* **2007**, *3*, 1941. (d) Pernodet, N.; Fang, X. H.; Sun, Y.; Bakhtina, A.; Ramakrishnan, A.; Sokolov, J.; Ulman, A.; Rafailovich, M. *Small* **2006**, *2*, 766.

10. Hoshino, A.; Fujioka, K.; Oku, T.; Suga, M.; Sasaki, Y. F.; Ohta, T.; Yasuhara, M.; Suzuki, K.; Yamamoto, K. *Nano Lett.* **2004**, *4*, 2163.

11. Bar-Ilan, O.; Albrecht, R. M.; Fako, V. E.; Furgeson, D. Y. *Small* **2009**, *5*, 1897.

12. Yen, H. J.; Hsu, S. H.; Tsai, C. L. *Small* **2009**, *5*, 1553.

13. Hauck, T. S.; Ghazani, A. A.; Chan, W. C. W. *Small* **2008**, *4*, 153.

14. Arnida; Malugin, A.; Ghandehari, H. *J. Appl. Toxicol.* **2010**, *30*, 212.

15. Goodman, C. M.; McCusker, C. D.; Yilmaz, T.; Rotello, V. M. *Bioconjugate Chem.* **2004**, *15*, 897.

16. Kang, B.; Mackey, M. A.; El-Sayed, M. A. *J. Am. Chem. Soc.* **2010**, *132*, 1517.

17. Jamieson, E. R.; Lippard, S. J. *Chem. Rev.* **1999**, *99*, 2467.

18. (a) Agasti, S. S.; Chompoosor, A.; You, C. C.; Ghosh, P.; Kim, C. K.; Rotello, V. M. *J. Am. Chem. Soc.* **2009**, *131*, 5728. (b) Ghosh, P. S.; Kim, C. K.; Han, G.; Forbes, N. S.; Rotello, V. M. *Acs Nano* **2008**, *2*, 2213. (c) Ghosh, P.; Yang, X. C.; Arvizo, R.; Zhu, Z. J.; Agasti, S. S.; Mo, Z. H.; Rotello, V. M. *J. Am. Chem. Soc.* **2010**, *132*, 2642.

19. Nel, A. E.; Madler, L.; Velegol, D.; Xia, T.; Hoek, E. M. V.; Somasundaran, P.; Klaessig, F.; Castranova, V.; Thompson, M. *Nat. Mater.* **2009**, *8*, 543.

20. (a) Koynova, R.; Tenchov, B.; Wang, L.; MacDonald, R. C. *Mol. Pharm.* **2009**, *6*, 951. (b) Tenchov, B. G.; Wang, L.; Koynova, R.; MacDonald, R. C. *BBA-Biomembranes* **2008**, *1778*, 2405.

21. Hostetler, M. J.; Wingate, J. E.; Zhong, C. J.; Harris, J. E.; Vachet, R. W.; Clark, M. R.; Londono, J. D.; Green, S. J.; Stokes, J. J.; Wignall, G. D.; Glish, G. L.; Porter, M. D.; Evans, N. D.; Murray, R. W. *Langmuir* **1998**, *14*, 17.

22. Brust, M.; Fink, J.; Bethell, D.; Schiffrin, D. J.; Kiely, C. *J. Chem. Soc., Chem. Commun.* **1995**, 1655.

23. Thomas, M.; Klibanov, A. M. *Proc. Natl. Acad. Sci. U.S.A.* **2003**, *100*, 9138.

24. Nativo, P.; Prior, I. A.; Brust, M. *Acs Nano* **2008**, *2*, 1639.

25. Zhu, Z. J.; Ghosh, P. S.; Miranda, O. R.; Vachet, R. W.; Rotello, V. M. *J. Am. Chem. Soc.* **2008**, *130*, 14139.

26. Zhang, R.; Niu, Y. J.; Zhou, Y. K. *Toxicol. Lett.* **2010**, *192*, 108.

27. Tice, R. R.; Agurell, E.; Anderson, D.; Burlinson, B.; Hartmann, A.; Kobayashi, H.; Miyamae, Y.; Rojas, E.; Ryu, J. C.; Sasaki, Y. F. *Environ. Mol. Mutagen.* **2000**, *35*, 206.

28. Aguirre, J. D.; Angeles-Boza, A. M.; Chouai, A.; Pellois, J. P.; Turro, C.; Dunbar, K. R. *J. Am. Chem. Soc.* **2009**, *131*, 11353.

29. (a) Tsujimoto, Y.; Shimizu, S. *Cell Death Differ.* **2005**, *12*, 1528. (b) Chen, Y.; McMillan-Ward, E.; Kong, J.; Israels, S. J.; Gibson, S. B. *Cell Death Differ.* **2008**, *15*, 171.

30. Scherz-Shouval, R.; Shvets, E.; Fass, E.; Shorer, H.; Gil, L.; Elazar, Z. *Embo J.* **2007**, *26*, 1749.

CHAPTER 4

SERUM PROTEINS SUPPRESS THE HEMOLYTIC ACTIVITY OF HYDROPHILIC AND HYDROPHOBIC NANOPARTICLES

4.1. Introduction

Intravascular rupture of red blood cells (RBCs) upon systemic administration of therapeutic NPs can elevate plasma level of cell-free hemoglobin leading to endothelial cell dysfunction and vascular thrombosis.[1] This acute hemolysis can further cause hemolytic anemia that result in multiple organ failure[2] and death.[3] Several reports have recently demonstrated the hemolytic activities of therapeutic NPs both *in vitro*[4] and *in vivo*,[5] indicating potential adverse side-effects of NPs that can limit applications in nanomedicine. However, a lack of parametric study *in vitro* on NP hemolytic behavior makes their interaction profile difficult to predict *in vivo*.

Surface functionality of NPs is central to their effective use in therapeutic applications, imparting functional properties[6] and dictating their circulation profile in the blood stream.[7] However, in contrast to small molecule therapeutics the formation of a protein corona on the NP surface during blood circulation[8] alters surface chemical behavior of NPs and defines its physiological responses.[9] This interplay of NP surface functionality and the protein corona formed *in situ* would be expected to dictate the overall interaction of NPs with RBCs, regulating the hemolytic behavior of NPs. To date, however, there is no clear understanding how changes on NP surfaces coupled with the formation of protein corona control the hemolytic properties of NPs.[10]

Herein, we report the role of NP surface functionality on hemolytic activity in the presence and absence of plasma proteins. To this end, we have synthesized a class of cationic gold NPs of same core size (~2 nm), differing in their surface hydrophobicity (Figure 4.1). These NPs showed a direct increase in hemolytic activity with the increase of surface hydrophobicity in

the absence of plasma proteins. Significantly, the presence of protein corona dramatically altered the hemolytic activity of these NPs; hemolysis was only observed in the most hydrophobic of surface coverage. These studies demonstrate the importance of serum proteins in moderating hemolytic activity, expanding the range of particle surfaces that can be employed without hemolytic consequences.

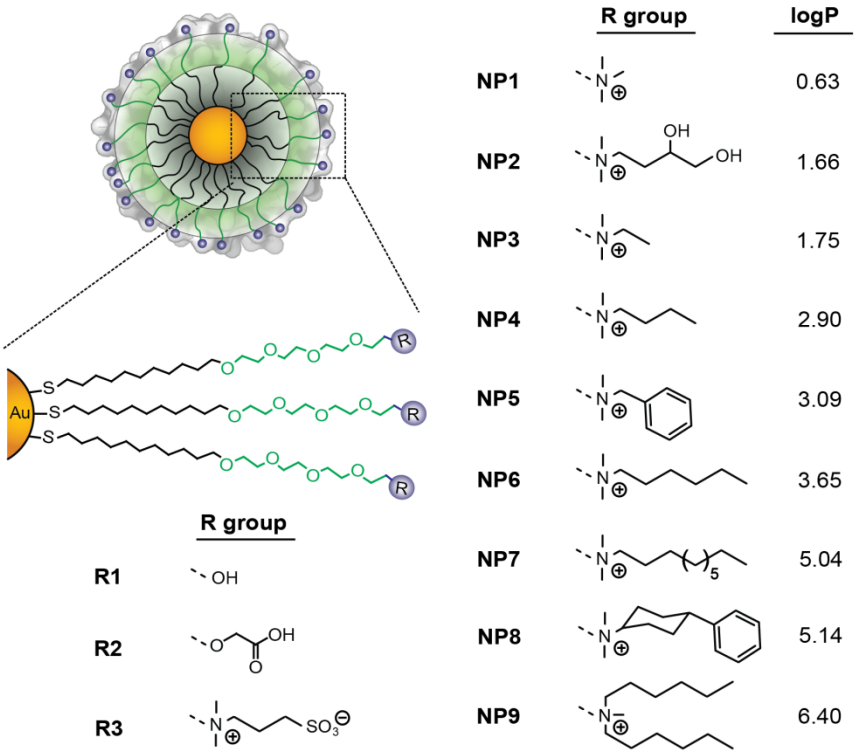

Figure 4.1. The structure of the NPs used to probe haemolytic activity of functionalized AuNPs. logP denotes the relative hydrophobic indices of R groups.

4.2. Results and Discussion

The NP surface hydrophobicity has a critical role in the cellular uptake,[11] toxicity,[12] and immune responses[13] of nanomaterials. To understand the role of NP surface hydrophobicity on the blood compatibility, a family of nine cationic NPs was synthesized systematically changing the degree of surface hydrophobicity by the use of specific chemical groups (Figure 4.1).[14] This chemical approach allows us to control the nature of the monolayer (nanoparticle surface), while

maintaining the other physico-chemical properties (e.g. size and surface charge) constant. Using this system, the NP properties can be translated into numerical descriptors, as demonstrated previously by interfacial tension experiments.[15] As such, the logP of the headgroups (R groups, Figure 4.1) was employed to describe the relative hydrophobic nature of the NP surface.

In prior studies, we have demonstrated that cationic NPs showed significantly higher hemolysis compared to anionic counterpart.[16] To this end, NPs with different surface charge e.g. cationic, anionic, neutral, and zwitterionic (500 nM each) were incubated with RBCs for 30 min and the absorbance of released hemoglobin from the hemolyzed RBCs were measured at 570 nm.[17] We observed a significantly higher hemolytic activity of cationic NPs compared to NPs with other surface charges (anionic, neutral, and zwitterionic) (Figure 4.2), corroborating previous reports.[18]

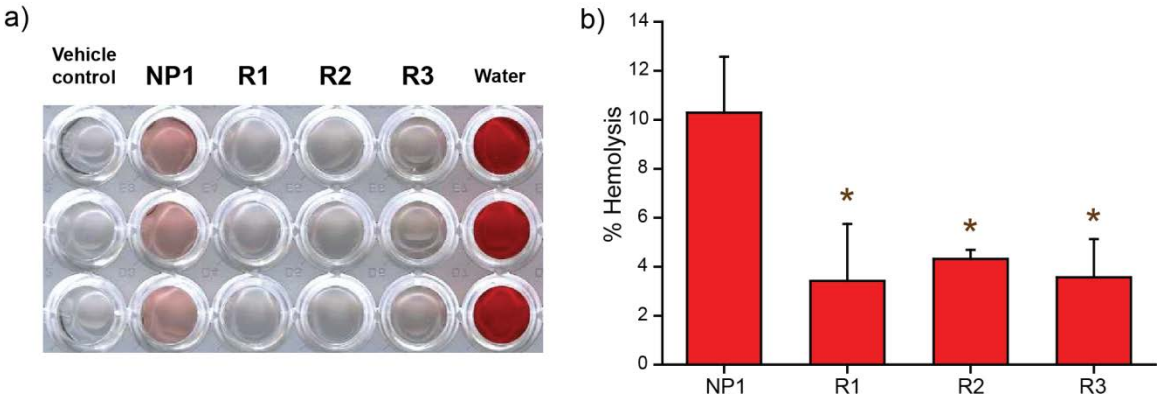

Figure 4.2. The effect of the nanoparticle surface charge on hemolysis. a) Physical observation of the supernatant after nanoparticle addition and centrifugation. b) Values of hemolysis relative to positive control. Experiments were performed by triplicate. Extreme left and right values are negative control (no nanoparticles) and positive control (water).

The role of NP surface hydrophobicity on hemolytic behavior was established incubating NP1-NP9 (500 nM each) with RBCs as mentioned above. A direct increase in hemolytic activity was observed for NP1-NP9 with the increase of hydrophobicity (Figure 4.3), demonstrating the role of NP surface hydrophobicity on the hemolysis. Significantly, NPs with similar headgroup logP but different chemical functionalities e.g. NP2 and NP3 demonstrated

different degree of hemolysis (~4.5% and 13.5% respectively), evidencing the role of specific functional groups on the observed hemolytic behavior.

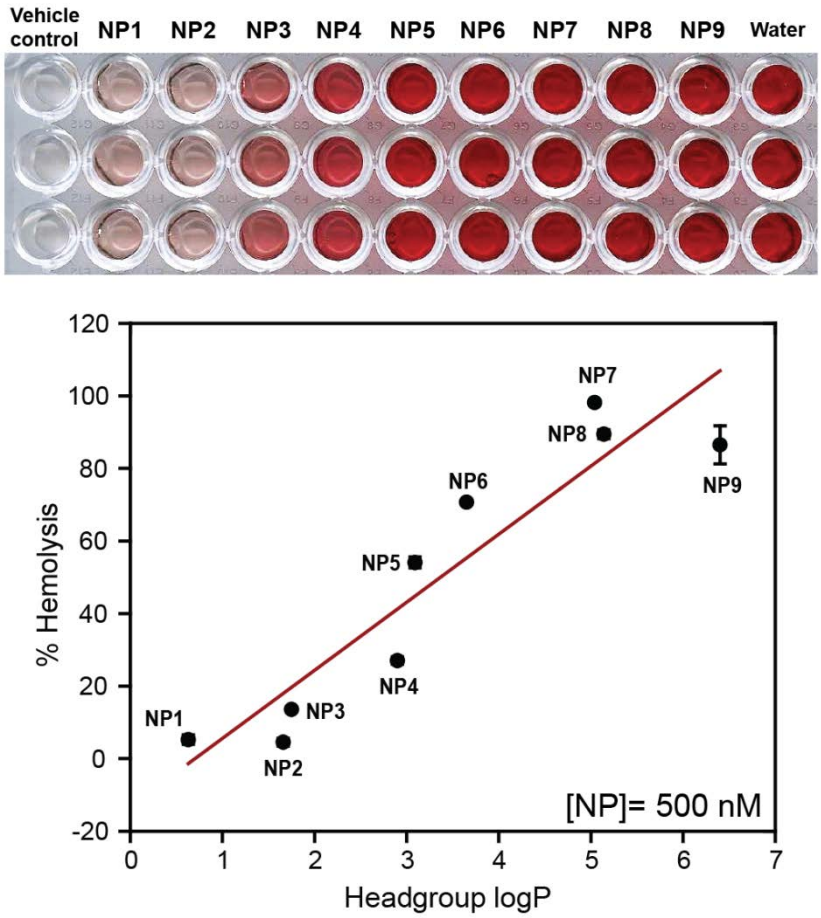

Figure 4.3. Hemolytic activities of NP1-NP9 (500 nM each) in the absence of plasma proteins. RBCs were incubated with NPs for 30 min in PBS at 37 ˚C and the mixture was centrifuged to detect the cell-free hemoglobin in the supernatant. % Hemolysis was calculated using water as the positive control. Error bars represent standard deviation (n=3).

The dose-dependent hemolytic behavior of these NPs was investigated exposing RBCs to a range of concentrations of NPs from 8 nM to 500 nM. As shown in Figure 4.4, a dose-dependent increase of hemolysis was observed for all NPs. NP1-NP3 did not show significant hemolysis at the highest concentration tested (500 nM), demonstrating biocompatibility of these particles towards RBCs. Significantly, a sigmoidal dose-response curve was observed for more hydrophobic NPs, demonstrating the co-operative nature of hemolytic process for these NPs.[19]

This result demonstrated that the subtle changes on NP surfaces can modulate the interaction profile with RBCs, leading to different hemolytic profile.

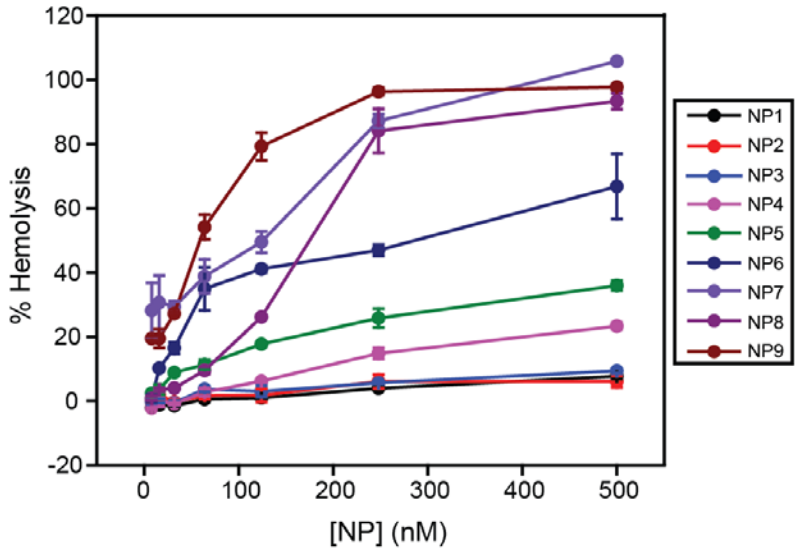

Figure 4.4. Dose-dependent hemolytic activity of NP1-NP9 in the absence of plasma proteins. % Hemolysis was calculated using water as the positive control. Error bars represent standard deviation (n=3).

Binding of plasma proteins on NP can mask the chemical nature of the NP surface, altering their activity *in vivo*.[20] The hemolytic activity of NP1-NP9 was further studied in the presence of 55% of plasma protein, a condition NPs will meet while administered in the blood stream. NPs were pre-incubated with 55% plasma in PBS for 30 min and then added to the RBCs. The pre-incubation time was chosen to have certainty of the protein absorption, although protein coronas form within minutes after NP exposure.[21] Following incubation with RBCs, the absorbance of the supernatant was measured at 570 nm to monitor the extent of hemolysis (*vide supra*). In presence of plasma, little to no hemolysis was observed for NP1-NP6 (Figure 4.5). Significantly, NP6 that showed ~70% hemolysis in the absence of plasma protein, demonstrated no hemolytic activity in the presence of plasma even after 24 hr, a striking example of the effect of protein corona formation on NP surface. Likewise, NP7-NP9 demonstrated significant decrease in hemolytic activities (more than 20-fold) in presence of plasma within 30 minutes. However, NP7-NP9 still showed ~5% hemolysis within 30 min, demonstrating hemolytic

potential of these NPs even in the presence of plasma proteins. This behavior was more pronounced after 24 hr where NP7 and NP9 showed severe hemolysis (Figure 4.5). Significantly, NP7 and NP8 showed different hemolytic activities after 24 hr albeit their similar headgroup hydrophobicity, presumably due to the NP aggregation in high protein concentration and/or selective amount of protein adsorption on NP surface. Nonetheless, this study signifies the interplay of the chemical functionalities on NP surface and the protein corona formed *in situ*, making NPs 'silent' towards hemolytic consequences. However, NPs with high degree of surface hydrophobicity (headgroup logP > 4) demonstrated severe hemolysis, providing a limit of the NP surface hydrophobicities tested in this study.

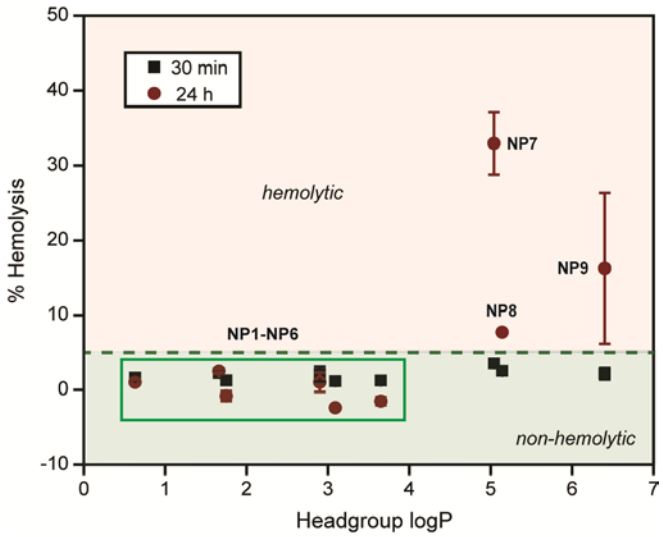

Figure 4.5. Hemolytic activities of NP1-NP9 (500 nM each) in the presence of plasma proteins. NPs were pre-incubated with 55% of plasma in PBS following incubation with RBCs for 30 min and 24 hr at 37 ˚C. The mixture was centrifuged to detect the cell-free hemoglobin in the supernatant. % Hemolysis was calculated using water as positive control. Error bars represent standard deviation (n=3).

4.3. Conclusions

In summary, we have demonstrated the critical synergy between NP surface chemical functionalities and the protein corona, leading to dramatically attenuated hemolytic behaviour of NPs. In the absence of plasma proteins, a linear hemolytic profile was observed with increasing

NP surface hydrophobicity. Significantly, the presence of plasma protein passivated both hydrophilic and hydrophobic NP surfaces leading to no hemolysis within 30 min. NPs with the highest degrees of hydrophobicity (headgroup logP>4), however, maintained their hemolytic properties (24 hr) presumably due to aggregation in the presence of plasma proteins. This study signifies the protective role of protein corona for improved blood compatibility and provides extended design parameters for therapeutic nanomaterials without toxic consequences.

4.4. Experimental Section

Nanoparticle synthesis: Gold nanoparticles cores (d~2nm) stabilized with a monolayer of 1-pentanethiol were synthesized following the Brust-Schiffrin methodology.[22] All the impurities were removed according to our own protocol to certify that the phase-transfer catalyst do not interfere in the biological tests.[23] To functionalize the cores with the desired ligands, a Murray place-exchange reaction[24] was performed by dissolving the thiolated ligand in dry DCM with the gold cores, stirring for 3 days at room temperature (5:1 w/w ratio of ligand/gold cores). DCM was then evaporated under reduced pressure and the residue was dissolved in distilled water. Dialysis was performed during 5 days (membrane MWCO = 10,000) to remove excess of ligand and salts remaining in the nanoparticle solution. After dialysis, the particles were lyophilized and dissolved in deionized MQ water. Nanoparticle concentration was obtained following the reported procedure.[25] The ligands were synthesized according to our previous reports.[26]

Hemolysis assay in the absence of plasma proteins: Citrate-stabilized human whole blood (pooled, mixed gender) was purchased from Bioreclamation LLC, NY and processed as soon as received. 10 mL of phosphate buffered saline (PBS) was added to the blood and centrifuged at 5000 r.pm. for 5 minutes. The supernant was carefully discarded and the red blood cells (RBCs) were dispersed in 10 mL of PBS. This step was repeated at least five times. The

purified RBCs were diluted in 10 mL of PBS and kept on ice during the sample preparation. 0.1 mL of RBC solution was added to 0.4 mL of nanoparticle (NP) solution in PBS in 1.5 mL centrifuge tube (Fisher) and mixed gently by pipetting. RBCs incubated with PBS and water were used as negative and positive control, respectively. All NP samples as well as controls were prepared in triplicate. The mixture was incubated at 37 ˚C for 30 minutes while shaking at 150 r.p.m. After incubation period, the solution was centrifuged at 4000 r.p.m. for 5 minutes and 100 µL of supernatant was transferred to a 96-well plate. The absorbance value of the supernatant was measured at 570 nm using a microplate reader (SpectraMax M2, Molecular devices) with absorbance at 655 nm as a reference. The percent hemolysis was calculated using the following formula:

% Hemolysis = ((sample absorbance-negative control absorbance)) / ((positive control absorbance-negative control absorbance)) × 100.

Hemolysis assay in the presence of plasma proteins: Human plasma (pooled, mixed gender) were purchased from Biochemed Pharmaceuticals, VA and kept at -20 ˚C for further use. NPs were pre-incubated in 55% of plasma solution in PBS (v/v) for 30 minutes at 37 ˚C. After the pre-incubation period, 0.1 mL of washed RBCs were added to the solution and further incubated for 30 minutes or 24 hours. The same procedure was followed to determine the hemolysis in the presence of plasma (*vide supra*).

4.5. References

1. Rother, R. P.; Bell, L.; Hillmen, P.; Gladwin, M. T. *JAMA* **2005**, *293*, 1653.

2. (a) Stroncek, D.; Procter, J. L.; Johnson, J. *Am. J. Hematol.* **2000**, *64*, 67. (b) Saitoh, D.; Kadota, T.; Senoh, A.; Takahara, T.; Okada, Y.; Mimura, K.; Yamashita, H.; Ohno, H.; Inoue, M. *Am. J. Emerg. Med.* **1993**, *11*, 355. (c) Scharte, M.; Fink, M. P. *Crit. Care Med.* **2003**, *31*, S651.

3. (a) Perkins, J. *Asian J. Tranfus. Sci.* **2008**, *2*, 20. (b) Yuerek, S.; Riess, H.; Kreher, S.; Doerken, B.; Salama, A. *Transfusion Med.* **2010**, *20*, 265.

4. (a) Love, S. A.; Thompson, J. W.; Haynes, C. L. *Nanomedicine* **2012**, *7*, 1355. (b) Choi, J.; Reipa, V.; Hitchins, V. M.; Goering, P. L.; Malinauskas, R. A. *Toxicol. Sci.* **2011**, *123*, 133. (c) Zhao, Y. N.; Sun, X. X.; Zhang, G. N.; Trewyn, B. G.; Slowing, I. I.; Lin, V. S. Y. *Acs Nano* **2011**, *5*, 1366.

5. (a) Lu, S. L.; Duffin, R.; Poland, C.; Daly, P.; Murphy, F.; Drost, E.; MacNee, W.; Stone, V.; Donaldson, K. *Environ. Health Perspect.* **2009**, *117*, 241. (b) Li, Y. T.; Liu, J.; Zhong, Y. J.; Zhang, J.; Wang, Z. Y.; Wang, L.; An, Y. L.; Lin, M.; Gao, Z. Q.; Zhang, D. S. *Int. J. Nanomedicine* **2011**, *6*, 2805.

6. (a) Saha, K.; Bajaj, A.; Duncan, B.; Rotello, V. M. *Small* **2011**, *7*, 1903. (b) Mout, R.; Moyano, D. F.; Rana, S.; Rotello, V. M. *Chem. Soc. Rev.* **2012**, *41*, 2539.

7. Yoo, J. W.; Chambers, E.; Mitragotri, S. *Curr. Pharm. Des.* **2010**, *16*, 2298.

8. (a) Walkey, C. D.; Chan, W. C. W. *Chem. Soc. Rev.* **2012**, *41*, 2780. (b) Monopoli, M. P.; Aberg, C.; Salvati, A.; Dawson, K. A. *Nat. Nanotechnol.* **2012**, *7*, 779. (c) Arvizo, R. R.; Giri, K.; Moyano, D.; Miranda, O. R.; Madden, B.; McCormick, D. J.; Bhattacharya, R.; Rotello, V. M.; Kocher, J. P.; Mukherjee, P. *Plos One* **2012**, *7*.

9. (a) Salvador-Morales, C.; Flahaut, E.; Sim, E.; Sloan, J.; Green, M. L. H.; Sim, R. B. *Mol. Immunol.* **2006**, *43*, 193. (b) Owens, D. E.; Peppas, N. A. *Int. J. Pharm.* **2006**, *307*, 93.

10. (a) Joglekar, M.; Roggers, R. A.; Zhao, Y. N.; Trewyn, B. G. *Rsc Advances* **2013**, *3*, 2454. (b) Kwon, T.; Woo, H. J.; Kim, Y. H.; Lee, H. J.; Park, K. H.; Park, S.; Youn, B. *J. Nanosci. Nanotechnol.* **2012**, *12*, 6168.

11. Zhu, Z. J.; Posati, T.; Moyano, D. F.; Tang, R.; Yan, B.; Vachet, R. W.; Rotello, V. M. *Small* **2012**, *8*, 2659.

12. Chompoosor, A.; Saha, K.; Ghosh, P. S.; Macarthy, D. J.; Miranda, O. R.; Zhu, Z. J.; Arcaro, K. F.; Rotello, V. M. *Small* **2010**, *6*, 2246.

13. Moyano, D. F.; Goldsmith, M.; Solfiell, D. J.; Landesman-Milo, D.; Miranda, O. R.; Peer, D.; Rotello, V. M. *J. Am. Chem. Soc.* **2012**, *134*, 3965.

14. Moyano, D. F.; Rotello, V. M. *Langmuir* **2011**, *27*, 10376.

15. Rana, S.; Yu, X.; Patra, D.; Moyano, D. F.; Miranda, O. R.; Hussain, I.; Rotello, V. M. *Langmuir* **2012**, *28*, 2023.

16. Goodman, C. M.; McCusker, C. D.; Yilmaz, T.; Rotello, V. M. *Bioconjugate Chem.* **2004**, *15*, 897.

17. (a) Lin, Y. S.; Haynes, C. L. *Chem. Mater.* **2009**, *21*, 3979. (b) Lin, Y. S.; Haynes, C. L. *J. Am. Chem. Soc.* **2010**, *132*, 4834. (c) Yu, T.; Malugin, A.; Ghandehari, H. *Acs Nano* **2011**, *5*, 5717.

18. (a) Arvizo, R. R.; Miranda, O. R.; Thompson, M. A.; Pabelick, C. M.; Bhattacharya, R.; Robertson, J. D.; Rotello, V. M.; Prakash, Y. S.; Mukherjee, P. *Nano Lett.* **2010**, *10*, 2543. (b) Schaeublin, N. M.; Braydich-Stolle, L. K.; Schrand, A. M.; Miller, J. M.; Hutchison, J.; Schlager, J. J.; Hussain, S. M. *Nanoscale* **2011**, *3*, 410. (c) Leroueil, P. R.; Berry, S. A.; Duthie, K.; Han, G.; Rotello, V. M.; McNerny, D. Q.; Baker, J. R.; Orr, B. G.; Holl, M. M. B. *Nano Lett.* **2008**, *8*, 420.

19. Andreeva, Z. I.; Nesterenko, V. F.; Fomkina, M. G.; Ternovsky, V. I.; Suzina, N. E.; Bakulina, A. Y.; Solonin, A. S.; Sineva, E. V. *BBA-Biomembranes* **2007**, *1768*, 253.

20. (a) Lynch, I.; Dawson, K. A. *Nano Today* **2008**, *3*, 40. (b) Mahmoudi, M.; Lynch, I.; Ejtehadi, M. R.; Monopoli, M. P.; Bombelli, F. B.; Laurent, S. *Chem. Rev.* **2011**, *111*, 5610.

21. (a) Dell'Orco, D.; Lundqvist, M.; Oslakovic, C.; Cedervall, T.; Linse, S. *Plos One* **2010**, *5*. (b) Barran-Berdon, A. L.; Pozzi, D.; Caracciolo, G.; Capriotti, A. L.; Caruso, G.; Cavaliere, C.; Riccioli, A.; Palchetti, S.; Lagana, A. *Langmuir* **2013**, *29*, 6485.

22. Brust, M.; Fink, J.; Bethell, D.; Schiffrin, D. J.; Kiely, C. *J. Chem. Soc., Chem. Commun.* **1995**, 1655.

23. Moyano, D. F.; Duncan, B.; Rotello, V. M. *Methods Mol. Biol.* **2013**, *1025*, 3.

24. Hostetler, M. J.; Wingate, J. E.; Zhong, C. J.; Harris, J. E.; Vachet, R. W.; Clark, M. R.; Londono, J. D.; Green, S. J.; Stokes, J. J.; Wignall, G. D.; Glish, G. L.; Porter, M. D.; Evans, N. D.; Murray, R. W. *Langmuir* **1998**, *14*, 17.

25. Liu, X. O.; Atwater, M.; Wang, J. H.; Huo, Q. *Colloids Surf. B* **2007**, *58*, 3.

26. You, C. C.; Miranda, O. R.; Gider, B.; Ghosh, P. S.; Kim, I. B.; Erdogan, B.; Krovi, S. A.; Bunz, U. H. F.; Rotello, V. M. *Nat. Nanotechnol.* **2007**, *2*, 318.

CHAPTER 5

NANOPARTICLE SURFACE FUNCTIONALITY DICTATES PROTEIN CORONA FORMATION AND MACROPHAGE RECOGNITION

5.1. Introduction

When NPs (NPs) are exposed to complex biofluids (e.g. blood, plasma), it immediately adsorbs proteins on its surface, forming a layer of proteins, namely “protein corona" that effectively mask the original chemical nature.[1] This non-specific adsorption of proteins on NP surfaces is highly critical for delivery applications because the adsorption of opsonin proteins from blood (e.g. immunoglobulins) increase the clearance rate of NPs via the reticulo-endothelial system and decrease the pharmacokinetic half-life of NPs *in vivo*.[2] Blood plasma contains thousands of proteins that can bind to NPs with the interaction profile strongly depending on the NP surface chemistry.[3] For example, positively charged polystyrene particles were shown to interact with proteins with isoelectric points less than 5.5 (e.g. serum albumin) while negatively charged particles preferentially bind to proteins with isoelectric points higher than 5.5 (e.g. IgG).[4] This demonstrates the binding of NPs to proteins can be electrostatic in nature. Moreover, negatively charged polymeric NPs of similar size and hydrophobicity adsorb higher amount of proteins on their surfaces with increasing surface charge density; however, the identity of the adsorbed proteins were very similar.[5]

The hydrophobicity of the NP surface is also a key parameter in NP-protein interactions.[6] For example, hydrophobic *N*-isopropylacrylamide-co-*N*-tert-butylacrylamide (NIPAM/BAM) copolymer NPs were shown to adsorb a higher amount of protein on their surfaces than their hydrophilic counterparts,[7] presumably due to greater affinity and/or increased number of binding sites on hydrophobic NP surfaces.[8] The identity of the protein corona formed on the surface is also dependent on the NP surface hydrophobicity. For example, hydrophobic NPs adsorb

apolipoproteins on their surface while adsorption of more abundant hydrophilic proteins including albumin and IgG were observed in the corona of hydrophilic NPs.[9]

In addition to charge and hydrophobicity, the presence of specific functional groups on NP surface also dictates the interaction of proteins with NPs. For example, Shea *et al.* have synthesized three different cationic NIPAM polymeric NPs featuring guanidinium, primary amino, and quaternary ammonium functional groups. A significant higher binding was observed for the guanidinium functionalized polymer NPs towards fibrinogen. This specific chemical structure-dependent interaction was due to the strong interactions of guanidinium groups with surface carboxylate groups on fibrinogen. [10] Likewise, methylstyrene-featuring NPs (~90 nm) showed significantly higher binding of plasma proteins compared to tert-butylstyrene functionalized NPs of similar charge.[6]

Even though numerous studies have documented the effect of surface chemistry on the formation of plasma protein coronas, a clear structure-function relationship still remains elusive. The use of disorganized array of particle sizes, shapes, and coverages with little to no therapeutic values also makes it challenging to deduce general conclusion that can be applied to 'real' drug delivery systems. In prior studies, we have shown that blood half life of surface engineered cationic gold NPs is lower than NPs featuring other charges (Neutral, anionic, and negative).[11] Moreover, the biodistribution of the surface engineered cationic NPs were strictly dependent on their surface hydrophobicity; gold NPs featuring the most hydrophobic headgroup had significant accumulation in liver while AuNPs with moderate hydrophobicity showed higher accumulation in spleen.[12] The significant accumulation of these NPs in liver and spleen also suggests their rapid uptake by liver and splenic macrophages and subsequent phagocytic clearance. Therefore, understanding the effect of engineered surface functionality on macrophage recognition can aid in design delivery vehicles with improved selectivity and longer pharmacokinetic profile.

Herein, we have studied a systematic understanding of the role of NP surface functionality on the formation of protein corona and investigated the uptake of NPs in

macrophage cells. Using a semi-quantitative proteomics approach we have shown that the specific chemical moieties on the NP surface adsorb a variety of proteins of different amount and identity. In particular, NPs with similar hydrophobicity but constitutional isomers also showed different corona type and uptake pattern, arising due to the recognition of specific functional group on NP surface.

5.2. Results and Discussion

All NPs were synthesized from a 2 nm core pentanethiol capped gold NPs[13] via place exchange reaction[14] and have similar hydrodynamic diameter and zeta potential value, making them an ideal platform to study the sole effect of NP surface functionality. A critical point in the design of these NPs is the inclusion of a non-interacting biocompatible spacer tetra(ethylene glycol) that prevents aggregation, and more importantly, allows specific chemical groups to be exposed to the NP surface (the interacting zone). Hydrophobicity was chosen as the chemical variable due to the significant role played by this parameter at the nano-bio interface, including protein-NP interaction,[15,16] cellular uptake,[17] toxicity,[18,19] and immune system recognition.[20,21] (Figure 5.1). Most importantly, the atomic level control of the design allowed us to fabricate NP bearing constitutional isomeric headgroups (e.g. NP5 and NP6) to probe their effect on the protein binding and macrophage uptake.

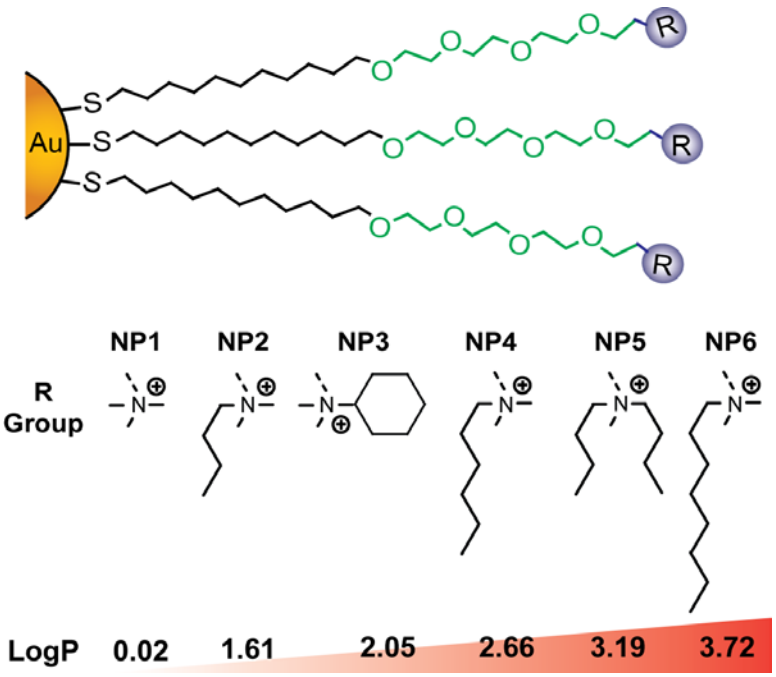

Figure 5.1. Gold NPs used in this study to investigate the identity of protein corona formation and macrophage uptake. LogP denotes the relative hydrophobic index of the functional headgroups.

Previously we have demonstrated that cationic NPs can effectively bind to the anionic proteins at physiological pH.[22] However, this one model protein can not address the complex nature of NP-protein interaction in serum which contains thousands of proteins. To this end, we have studied the protein interaction in 10% and 50% serum, mimicking *in vitro* and *in vivo* conditions. Previous literature have demonstrated that NP-bound serum proteins have two different layer, 'soft' corona (reversibly bound proteins) and 'hard' corona (irreversibly bound proteins).[23] Hard corona proteins tend to stick with NPs for longer time and dictate the NP biodistribution and macrophage uptake. We have studied the identity of hard corona proteins using liquid chromatography tandem mass spectrometry (LC-MS/MS).[24] The NPs were incubated with different concentrations of serum proteins followed by centrifugation, and then washed multiple times to remove soft corona proteins and were subjected to LC-MS/MS analysis.

Table 5.1. Abundant proteins observed in the hard corona of NP1 to NP6

Mw	Proteins	Gene	pI	Function
30778	Apolipoprotein A-I	APOA1	5.72	Lipid transport
10852	Apolipoprotein C-III	APOC3	5.23	Lipid transport
11609	Ig kappa chain C region	IGKC	9.01	Immune response
51790	Ig mu chain C region	IGHM	6.56	Immune response
8168	Immunoglobulin J chain	IGJ	5.09	Immune response
187147	Complement C3	C3	6.02	Complement activation
26459	Complement C1q subcomponent subunit B	C1QB	8.83	Complement activation

Although other studies identified numerous proteins in the hard corona composition,[25] we have successfully identified nearly 100 different types of proteins in our NP samples. Table 5.1 demonstrates the highly abundant proteins bound to all of the NPs irrespective of their surface functionality. First, the analysis showed that the hard corona protein found on the NP surface does not correspond to their abundance in serum. For example, albumin is the most abundant protein in serum (comprises ~60-70% of serum proteins) but it was not the highest abundant protein in the corona. Instead, corona was enriched with mostly lipoproteins (~25% of total corona proteins) that have low abundance in serum (~5%). Second, the most abundant proteins adsorbed on NP surface have pI<7, demonstrating the binding is mostly due to the electrostatic association.

Figure 5.2 depicts a concise picture of the corona proteins identified when NPs were incubated in 10% serum sample. Clearly, the majority of the proteins observed in the corona are the proteins from extracellular region or space, attesting the reliability of the method of detection. The analysis also revealed that the majority of the proteins bound to all of the NPs irrespective of

their functionality are lipoproteins, immunoglobulins, and complement system proteins (70-80% of total proteins). Previous studies have demonstrated that NPs with higher hydrophobicity tend to bind more lipoproteins,[9] however, we observed a decreasing amount of bound lipoproteins on NPs with higher hydrophobicity, a strikingly opposite observation in case of surface engineered NPs. This provides direct evidence that the binding of functionalized NPs with serum proteins can be significantly altered compared to bare NPs. However, no direct trend was observed for NPs bound to other type of protein classes, demonstrating major influence of lipoproteins over other classes in the binding process towards hydrophobic NPs. Significantly NP5 and NP6 have distinctly different immunoglobulin binding profile despite being constitutional isomers, signifying that functionality of headgroup (branched vs linear) plays a critical role on protein corona formation. Likewise, NP3 and NP4 (cyclic *vs*. linear chain) also demonstrated different binding of coagulation and complement, attesting to the importance of monolayer functionality on the proteomic profile. In general, linear structured NPs adsorbed fewer proteins of different classes (acute phase, complement, coagulation, immunoglobulins) in 10% serum compared to their cyclic and branched counterpart (Figure 5.2), an important criterion that can be crucial for nanomaterial design for *in vivo* applications.

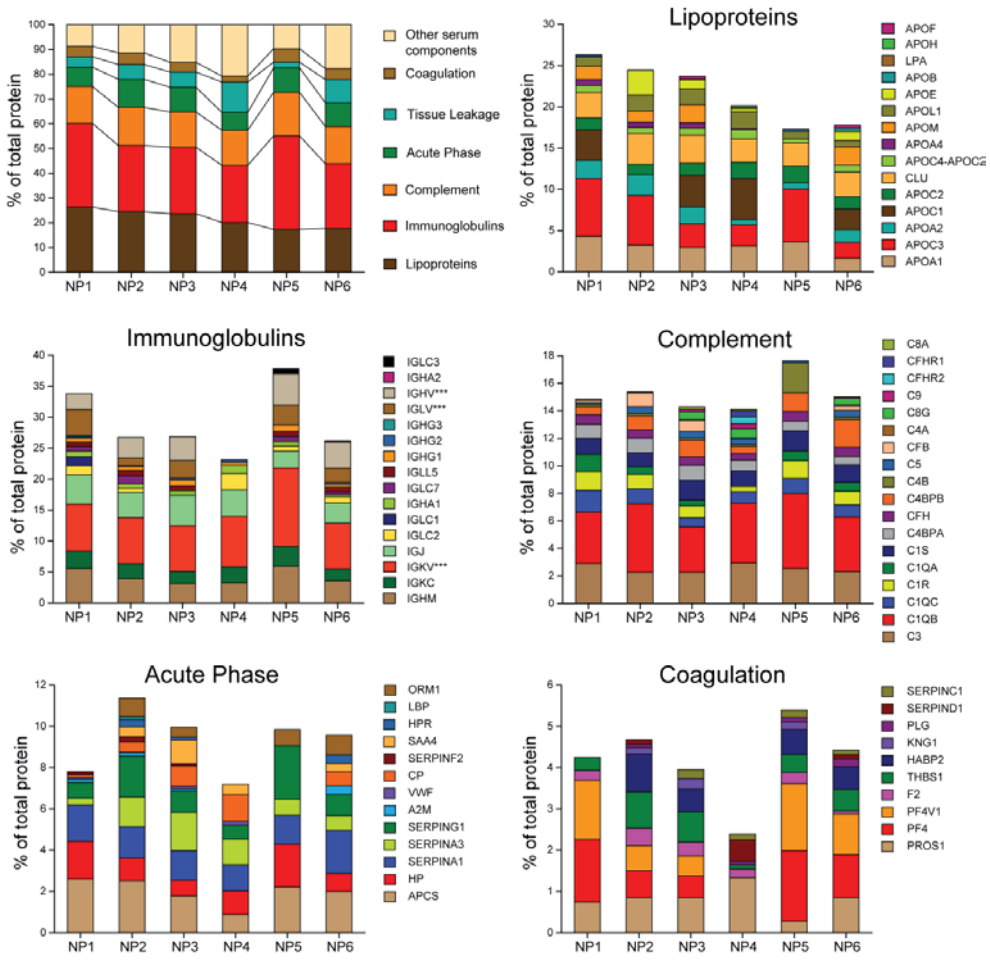

Figure 5.2. Classification of identified corona proteins for NP1-NP6 in 10% human serum**.** The proteins were classified in five major classes according to their biological function in blood.

The concentration of serum, however, is close to 50% in blood. We, therefore, further investigated the protein binding profile of our NPs in 50% human serum solution (Figure 5.3). Few important observations were noted in the data obtained in higher serum concentrations. First, the major difference between 10% and 50% data was the number of proteins identified on NPs in 50% serum is lower (50-60) than the 10% serum samples (70-100). This might be due to the fact that in diluted serum samples (10%) NPs have higher chances to interact with non-abundant proteins (interaction is more reversible) while at high serum concentrations the abundant proteins mask NP surfaces more efficiently (not fully reversible), thereby hindering access to other type of proteins in the serum. Second, the amount and the identity of the corona profile were significantly

varied in the presence of higher serum amount. For example, in 10% serum sample, hydrophobic NPs bound less lipoproteins but in 50% serum NP4 has the highest lipoproteins binding compared to other NPs. However, the common trend of lower binding of immunoglobulins and complement proteins can still be observed in case of linear structured NPs (NP4 and NP6) compared to the either branched (NP5) or cyclic (NP3) counterparts. Since immunoglobulins and complement factors are important classes of proteins known for facilitating opsonization process, this atomic level control of design can evade immune system recognition and improve pharmacokinetic profile of NPs in blood. Taken together, NP surface functionality dictates the binding of serum proteins on its surface. Importantly, NPs featuring constitutional isomeric headgroups showed different binding profile of serum proteins, indicating the significance of chemical design in developing therapeutic NPs. Linear structured hydrophobic NPs bound less immunoglobulins and complement proteins in both 10% and 50% serum samples, providing an important design parameter for *in vivo* applications.

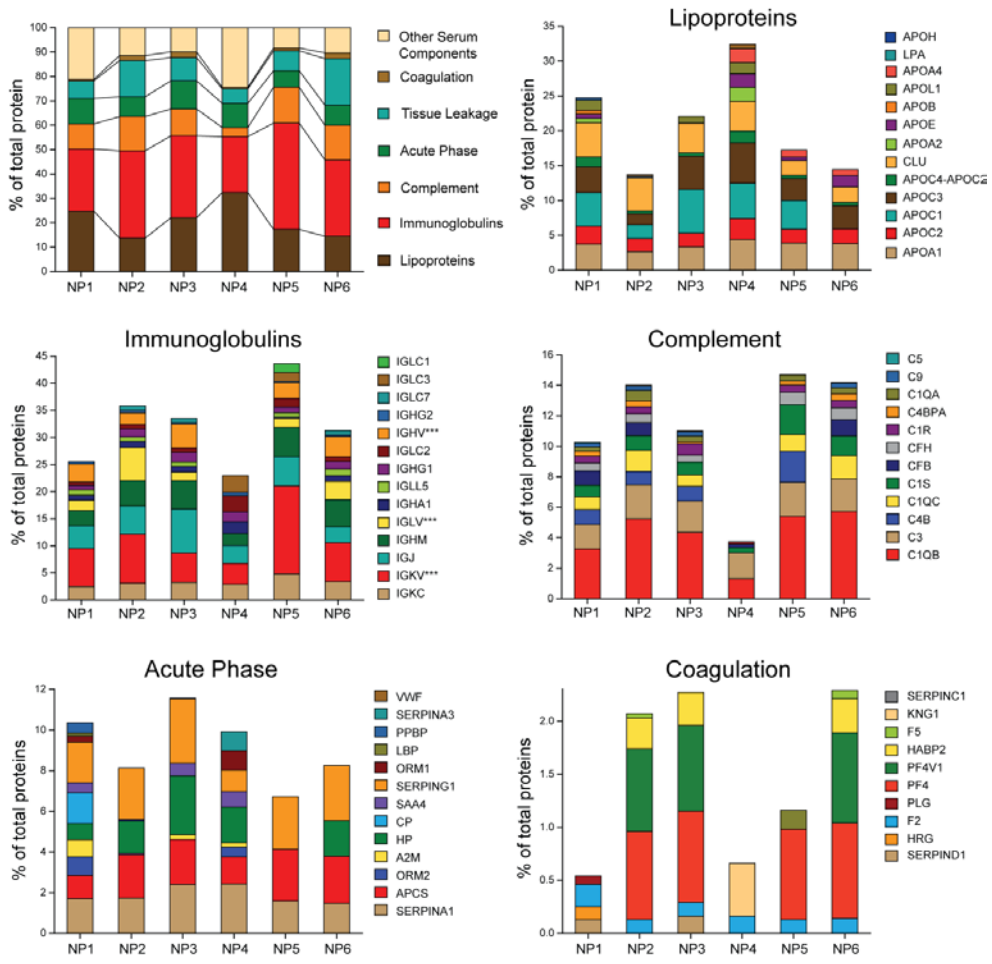

Figure 5.3. Classification of identified corona proteins for NP1-NP6 in 50% serum**.** The proteins were classified in five major classes according to their biological function in blood.

Opsonization of the foreign substances via immunoglobulins and complement proteins is the key step through which tissue resident macrophages can remove the foreign pathogens/substances from the blood.[26] Since all of the NPs tested in this study showed binding to immunoglobulins and complement factors, we hypothesized that the differential amount and identity of bound proteins can regulate the uptake of these NPs in macrophages. We have chosen a murine macrophage cell line RAW 264.7 to study the uptake both in the presence and absence of 10% serum. As depicted in figure 5.4a, NP uptake was strongly dependent on the surface functionality. Clearly, without serum the uptake of NP4 and NP6 was lower compared to their cyclic (NP3) and branched (NP5) counterpart, demonstrating the lack of recognition process of

linear surface functionality towards both proteins and cells. Interestingly, in the presence of serum, a nearly 20 fold decrease in uptake was observed (Figure 5.4b), indicating the effective masking of NP surface functionality by serum proteins and subsequent low uptake in macrophage cells. However, the hydrophobic NPs showed lower uptake compared to hydrophilic ones (NP1 and NP2) in the presence of serum proteins. This result mirrors our previous finding where a linear trend in NP surface hydrophobicity and cellular uptake was observed in HeLa cells.[17] Most importantly, although NP5 and NP6 showed similar uptake behavior in the absence of serum, a significant difference in uptake was observed in presence of serum, signifying the role of specific chemical group on NP surface on macrophage recognition.

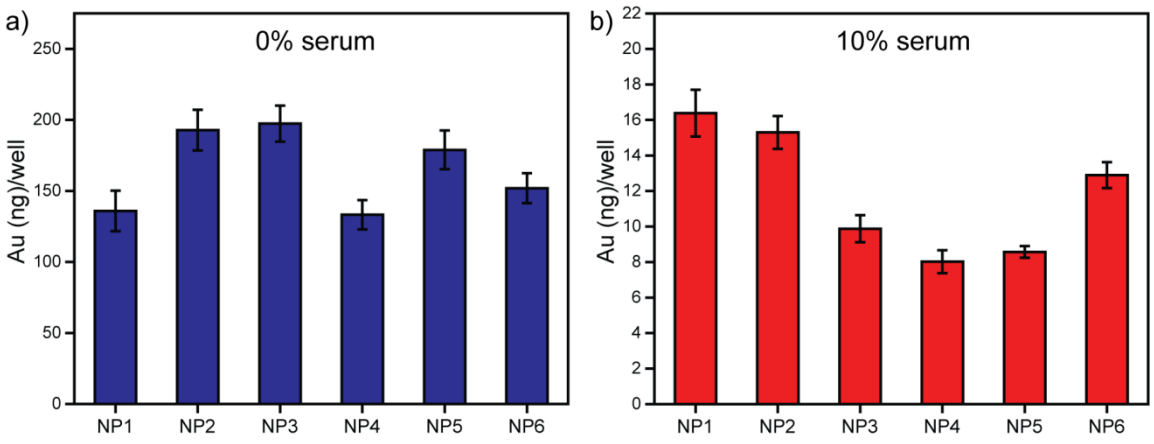

Figure 5.4. Uptake of NP1-NP6 (50 nM each) in murine macrophage cells RAW 264.7 after 3 h (a) without and (b) with 10% serum.

Recognition of specific chemical moieties by antigen presenting cells (e.g. macrophages) is central to the innate immune response.[27] To understand the effect of surface functional group towards macrophage recognition, we have studied the pro-inflammatory cytokine TNFα generation upon interaction with NP1-NP6 in RAW cells both in the presence and absence of serum proteins (Figure 5.5). Although we did not observe a strong immune response for most of the NPs at the concentration tested compared to the positive control lipopolysaccharide (LPS, 1μg/mL), NP4 produced a strikingly high amount of TNFα (~70% compared to LPS) in RAW

cells. This is presumably due to the direct recognition of cyclic headgroup on NP surface to the macrophage surface receptor Toll-like receptor 4. However, as expected, in the presence of serum the NP surface was masked and all NPs showed no TNFα production compared to the negative control (cell only). Taken together, the interplay of NP surface functionality and protein corona formation dictates the macrophage uptake and rescue cells from pro-inflammation.

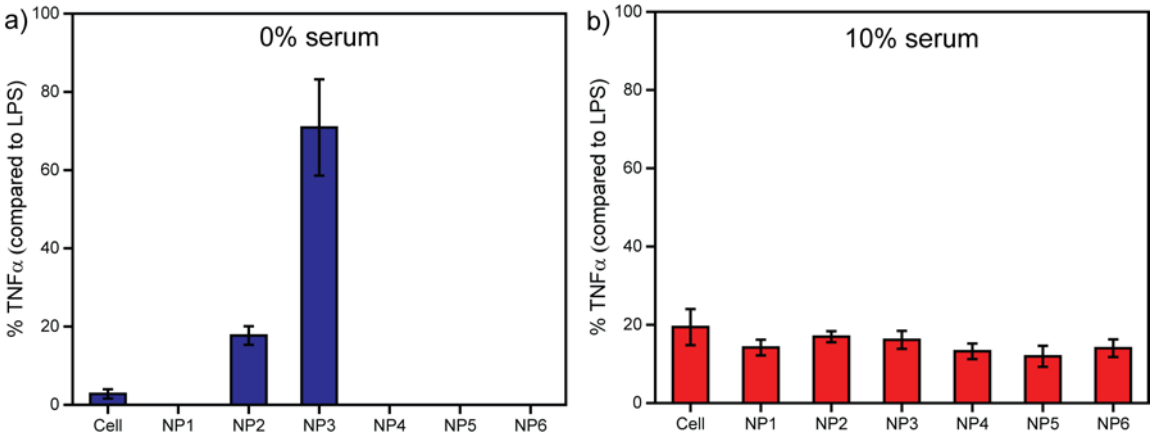

Figure 5.5. % Production of tumor necrosis factor alpha in RAW 264.7 cells after 6 h of incubation with NP1-NP6 (50 nM each) (a) without and (b) with 10% serum.

5.3. Conclusions

The surface functionality of NPs creates an effective interface between nanomaterials and biosystems. Using a semi-quantitative proteomics approach, we have demonstrated that the specific chemical moieties on the NP surface adsorb a variety of proteins of different amount and identity. Importantly, the linear functional group binds to fewer amounts of immunoglobulins and complement proteins compared to cyclic and branched counterpart in both low and high serum conditions, providing a design parameter for future delivery vehicles. Uptake in macrophage revealed a linear dependency of surface hydrophobicity; lower uptake was observed for NPs with higher hydrophobicity. Cyclic chemical group produced a strong pro-inflammatory response in the absence of serum, however, the presence of serum completely nullify the pro-inflammation.

Understanding the effect of surface functionality on NP interaction with serum proteins can predict the key pharmacokinetic parameters including biodistribution, recognition by mononuclear phagocytic system and subsequent clearance.

5.4. Experimental Section

NP synthesis: All NPs were synthesized according to previously published procedure. [28]

Protein isolation and mass spectrometric detection: 100 μL of AuNPs (1μM) were mixed with 900 μL of human serum (with various concentrations) and incubated for 1h at 37 ˚C. The mixture were then centrifuged at 13 000g at 15 ˚C for 30 min. The supernatant was removed and the collected corona coated AuNPs was redispersed in 500 μL of cold (15 ˚C) phosphate buffered saline (PBS). The solution was centrifuged again (at the same condition) and the collected particles was redispersed in 500 μL of cold (15 ˚C) PBS. After another centrifugation process, the hard corona coated particles were introduced to LC MS/MS procedure.

Mass spectrometric detection of NP-bound proteins: The liquid chromatography tandem mass sprectrometric characterization of NP bound proteins was performed according to the previously published procedure.[29] In order to obtain the total number of the LC MS/MS spectra for all of the peptides that are attributed to a matched protein, a semi-quantitative assessment of the protein amounts was conducted through application of spectral counting method. The normalized SpC amounts of each protein, identified in the MS study of smooth and jagged surfaces, were calculated by applying the following equation

$$NpSpCk = \left(\frac{\left({SpC}/{(M_w)_k}\right)}{\sum_{t=1}^{n}\left({SpC}/{(M_w)_t}\right)}\right) \times 100$$

Where NpSpCk is the normalized percentage of spectral count (i.e., raw counts of ions) for protein k, SpC is the spectral count identified, and Mw is the molecular weight (in kDa) of the

protein k. Using this equation, one can expect to obtain the protein size and to evaluate the real contribution of each protein to the hard corona composition.

Cellular uptake: RAW 264.7 cells (murine macrophage) were cultured at 37 °C under a humidified atmosphere of 5 % CO_2. The cells were grown in RPMI media containing 10 % fetal bovine serum (FBS) and 1% antibiotics (100 U/ml penicillin and 100 μg/ml streptomycin). For the uptake experiment, 250,000 cells/well were plated in a 48-well plate prior to the experiment. On the following day, cells were washed one time with PBS followed by NP treatment (50 nM/well) and further incubated with or without 10% serum for 3 h. Following incubation, cells were washed three times with PBS, lysed and the intracellular gold amount was measured using inductively coupled plasma mass spectrometry (Elan 6100, Perkin-Elmer, Shelton, CT, USA). Each cell uptake experiment was done in triplicate, and each replicate was measured 5 times by ICP-MS. ICP-MS operating conditions are as below: rf power 1600 W; plasma Ar Flow rate, 15 ml/min, nebulizer Ar flow rate, 0.98 ml/min and dwell time, 45 ms.

Cytokine measurement: RAW 264.7 cells were seeded at a density of 500000 cells/well prior to the experiment. On the following day, cells were washed one time with PBS followed by NP treatment (50 nM/well) and further incubated with or without 10% serum for 6 h. After incubation, the supernatant were collected from each well. TNFα expression was evaluated using ELISA. Briefly, 100uL of a solution of anti-mouse/rat TNF antibody (1:1000 from 0.5mg/mL stock) were poured into the wells of a 96 well plate and incubated at 4°C overnight. The plate was then washed 3 times using a solution of tween 20 (0.05% v/v), and 200uL of blocking solution (1% BSA in PBS) were added to the plate with incubation for 3 hours at room temperature. The plate was then washed again, and 100uL of the samples (undiluted media from the cell culture) were added to the wells along with TNFα standards. The plate was incubated overnight at 4°C and after that it was washed again. A solution of Biotin Human anti-mouse/rat antibody (1:1000 from 0.5mg/mL stock) was added to the plate and incubated at room temperature for 1 h. A new washing was performed and a solution of Avidin-HRP (100 uL of 1:500 from stock) was added to

the wells. After incubation for 1 h, a final washing step was performed and 100uL TMB substrate reagent set were added to the wells. When blue coloration started to appear 50uL of stop solution (2N H_2SO_4) were added. The absorbance of the samples was the recorded at 450nm on a Biotek synergy 2 plate reader.

5.5. References

1. a) Walkey, C. D.; Chan, W. C. W. *Chem. Soc. Rev.* **2012**, *41*, 2780. b) Monopoli, M. P.; Aberg, C.; Salvati, A.; Dawson, K. A. *Nat. Nanotechnol.* **2012**, *7*, 779.

2. a) Aggarwal, P.; Hall, J. B.; McLeland, C. B.; Dobrovolskaia, M. A.; McNeil, S. E. *Adv. Drug Delivery Rev.* **2009**, *61*, 428. b) Alexis, F.; Pridgen, E.; Molnar, L. K.; Farokhzad, O. C. *Mol. Pharm.* **2008**, *5*, 505.

3. a) Walkey, C. D.; Olsen, J. B.; Guo, H. B.; Emili, A.; Chan, W. C. W. *J. Am. Chem. Soc.* **2012**, *134*, 2139. (b) Walkey, C. D.; Olsen, J. B.; Song, F. Y.; Liu, R.; Guo, H. B.; Olsen, D. W. H.; Cohen, Y.; Emili, A.; Chan, W. C. W. *Acs Nano* **2014**, *8*, 2439.

4. Gessner, A.; Lieske, A.; Paulke, B. R.; Muller, R. H. *J. Biomed. Mater. Res. A* **2003**, *65*, 319.

5. Gessner, A.; Lieske, A.; Paulke, B.; Muller, R. *Eur J Pharm Biopharm* **2002**, *54*, 165.

6. Gessner, A.; Waicz, R.; Lieske, A.; Paulke, B. R.; Mader, K.; Muller, R. H. *Int. J. Pharm.* **2000**, *196*, 245.

7. Cedervall, T.; Lynch, I.; Lindman, S.; Berggard, T.; Thulin, E.; Nilsson, H.; Dawson, K. A.; Linse, S. *Proc. Natl. Acad. Sci. U.S.A.* **2007**, *104*, 2050.

8. Lindman, S.; Lynch, I.; Thulin, E.; Nilsson, H.; Dawson, K. A.; Linse, S. *Nano Lett.* **2007**, *7*, 914.

9. Cedervall, T.; Lynch, I.; Foy, M.; Berggad, T.; Donnelly, S. C.; Cagney, G.; Linse, S.; Dawson, K. A. *Angew. Chem. Int. Ed.* **2007**, *46*, 5754.

10. Yonamine, Y.; Yoshimatsu, K.; Lee, S. H.; Hoshino, Y.; Okahata, Y.; Shea, K. J. *ACS Appl. Mater. Interfaces* **2013**, *5*, 374.

11. Arvizo, R. R.; Miranda, O. R.; Moyano, D. F.; Walden, C. A.; Giri, K.; Bhattacharya, R.; Robertson, J. D.; Rotello, V. M.; Reid, J. M.; Mukherjee, P. *Plos One* **2011**, *6*, e24374.

12. Yan, B.; Kim, S. T.; Kim, C. S.; Saha, K.; Moyano, D. F.; Xing, Y. Q.; Jiang, Y.; Roberts, A. L.; Alfonso, F. S.; Rotello, V. M.; Vachet, R. W. *J. Am. Chem. Soc.* **2013**, *135*, 12564.

13. Brust, M.; Fink, J.; Bethell, D.; Schiffrin, D. J.; Kiely, C. *J. Chem. Soc., Chem. Commun.* **1995**, 1655.

14. Hostetler, M. J.; Wingate, J. E.; Zhong, C. J.; Harris, J. E.; Vachet, R. W.; Clark, M. R.; Londono, J. D.; Green, S. J.; Stokes, J. J.; Wignall, G. D.; Glish, G. L.; Porter, M. D.; Evans, N. D.; Murray, R. W. *Langmuir* **1998**, *14*, 17.

15. Maiti, S.; Das, K.; Dutta, S.; Das, P. K. *Chem. Eur. J.* **2012**, *18*, 15021.

16. Zuo, G.; Huang, Q.; Wei, G.; Zhou, R.; Fang, H. *ACS Nano* **2010**, *4*, 7508.

17. Zhu, Z. J.; Posati, T.; Moyano, D. F.; Tang, R.; Yan, B.; Vachet, R. W.; Rotello, V. M. *Small* **2012**, *8*, 2659.

18. Fubini, B.; Ghiazza, M.; Fenoglio, I. *Nanotoxicology* **2010**, *4*, 347.

19. Chompoosor, A.; Saha, K.; Ghosh, P. S.; Macarthy, D. J.; Miranda, O. R.; Zhu, Z. J.; Arcaro, K. F.; Rotello, V. M. *Small* **2010**, *6*, 2246.

20. Moyano, D. F.; Goldsmith, M.; Solfiell, D. J.; Landesman-Milo, D.; Miranda, O. R.; Peer, D.; Rotello, V. M. *J. Am. Chem. Soc.* **2012**, *134*, 3965.

21. Kreuter, J.; Liehl, E.; Berg, U.; Soliva, M.; Speiser, P. P. *Vaccine* **1988**, *6*, 253.

22. a) You, C. C.; Miranda, O. R.; Gider, B.; Ghosh, P. S.; Kim, I. B.; Erdogan, B.; Krovi, S. A.; Bunz, U. H. F.; Rotello, V. M. *Nat. Nanotechnol.* **2007**, *2*, 318. b) Bajaj, A.; Rana, S.; Miranda, O. R.; Yawe, J. C.; Jerry, D. J.; Bunz, U. H. F.; Rotello, V. M. *Chem. Sci.* **2010**, *1*, 134.

23. a) Milani, S.; Bombelli, F. B.; Pitek, A. S.; Dawson, K. A.; Radler, J. *Acs Nano* **2012**, *6*, 2532. b) Casals, E.; Puntes, V. F. *Nanomedicine* **2012**, *7*, 1917. c) Monopoli, M. P.; Pitek, A. S.; Lynch, I.; Dawson, K. A. *Methods Mol. Biol.* **2013**, *1025*, 137.

24. Monopoli, M. P.; Walczyk, D.; Campbell, A.; Elia, G.; Lynch, I.; Bombelli, F. B.; Dawson, K. A. *J. Am. Chem. Soc.* **2011**, *133*, 2525.

25. Dobrovolskaia, M. A.; Patri, A. K.; Zheng, J. W.; Clogston, J. D.; Ayub, N.; Aggarwal, P.; Neun, B. W.; Hall, J. B.; McNeil, S. E. *Nanomedicine* **2009**, *5*, 106.

26. Owens, D. E.; Peppas, N. A. *Int. J. Pharm.* **2006**, *307*, 93.

27. Matzinger, P. *Annu. rev. Immunol.* **1994**, *12*, 991.

28. Miranda, O. R.; Chen, H. T.; You, C. C.; Mortenson, D. E.; Yang, X. C.; Bunz, U. H. F.; Rotello, V. M. *J. Am. Chem. Soc.* **2010**, *132*, 5285.

29. Tenzer, S.; Docter, D.; Kuharev, J.; Musyanovych, A.; Fetz, V.; Hecht, R.; Schlenk, F.; Fischer, D.; Kiouptsi, K.; Reinhardt, C.; Landfester, K.; Schild, H.; Maskos, M.; Knauer, S. K.; Stauber, R. H. *Nat. Nanotechnol.* **2013**, *8*, 772.

CHAPTER 6

FABRICATION OF ZWITTERIONIC NANOPARTICLES WITH TUNABLE HYDROPHOBICITY

6.1. Introduction

Surface functionalization of nanoparticles (NPs) is an essential tool to modulate the behavior of these materials both *in vitro* and *in vivo*.[1, 2] The biodistribution,[3] toxicity[4] and clearance[5,6] of nanomaterials can be regulated through controlled chemical modifications. However, when NPs are exposed to biofluids, such as plasma or serum, proteins and other biomolecules adsorb on the surface of these materials (Figure 6.1a).[7-9] This *in situ* formation of a "protein corona" [10,11] masks the engineered functionalities on the nanoparticle surfaces, dramatically changing the nature of their interaction with biosystems.[12-14] For example, the targeting efficacy of antibody-functionalized NPs are compromised due to the high levels of opsonization.[15,16] Likewise, the study of correlations between surface functionality and biological activity is challenging, as the results are subject to the interplay between the chemical moieties and the corona, rather than depending on the functionalities themselves.[17,18]

Many approaches have been investigated to prevent the formation of the protein corona to provide NPs with non-fouling properties. One classical approach is the use of a non-charged poly(ethylene glycol) (PEG) polymer that prevents the NP from adsorbing proteins.[19,20] However, it has been observed that PEG-functionalized NPs do indeed interact with certain plasma proteins, inducing the activation of different immune responses.[21] Moreover, systematic changes in the surface properties of PEG functionalized NPs are difficult to achieve as the absence of charge allows the internalization of pendant hydrophobic functionalities, reducing exposure.[22] An alternative to the use of PEG is the incorporation of zwitterion functionalities onto the NP surface, including amino acids[23] and polybetaines.[24]The strong electrostatic binding of water with

zwitterions (as opposed to water hydrogen bonding with PEG) has been postulated as the rationale behind the high degree of stability and non-fouling properties observed with zwitterionic systems.[25] However, pH dependence of carboxy-based systems[26] and the difficulty of systematic functionalization[27,28] limit the ability to control surface properties while maintaining biocompatibility and corona-free character.

Herein, we report the synthesis and use of a new family of NP surface coverages that exhibit tunable hydrophobicity while preventing the formation of a protein corona. This nanoparticle ligand design maintains corona-free behavior at moderate protein levels and prevents the irreversible formation of "hard" corona at physiological serum concentrations, while allowing properties such as hydrophobicity to be varied. These "naked" particles allow a systematic molecular structure-based assessment of the effects caused directly by the NP surface, including cellular uptake and hemolytic activity.

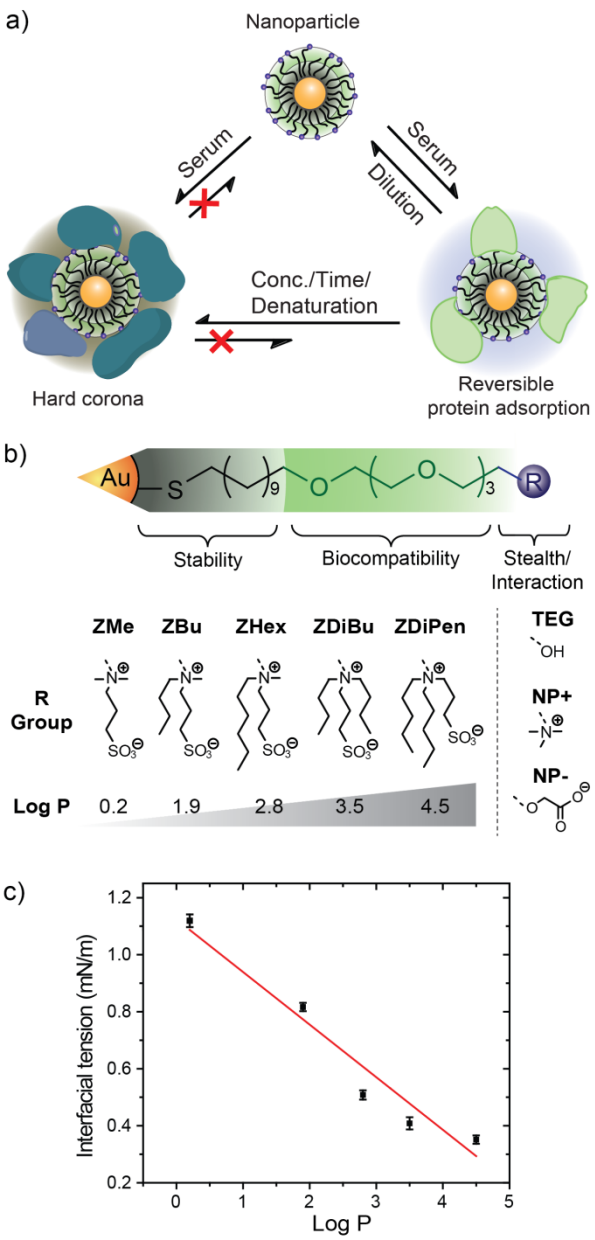

Figure 6.1. (a) Reversible adsorption of proteins and formation of irreversible hard corona over the NP surface. (b) Structures of the non-fouling NPs, along with TEG, NP+ and NP- controls. The ligand structure consists of a hydrophobic interior that confers stability to the NP core, an oligo(ethylene glycol) chain used as a first layer for biocompatibility, and the zwitterionic headgroups to confer ultra-fouling properties. The zwitterionic headgroups (the NP surface) differ only in their hydrophobicity, whose relative values can be estimated by the calculated Log P of the terminal functionality. (c) Correlation of the calculated Log P with toluene/water interfacial tension.

6.2. Results and Discussion

The chemical design of the NP ligand is based on a combination of a short oligo(ethylene glycol) spacer with sulfobetaine termini (Figure 6.1b). This combination has shown to provide better stealth properties to NPs compared to the ethylene glycol chains alone.[29] Hydrophobicity was chosen as the chemical variable due to the significant role played by this parameter at the nano-bio interface, including protein-NP interaction,[30,31] cellular uptake,[18] toxicity,[32,33] and immune system recognition.[34,35] The degree of surface hydrophobicity was controlled with these ligands by systematically engineering the quaternary ammonium nitrogen (Figure 6.1b). All particles were fabricated from a 2 nm gold core, a factor that contributes to the observed corona-free character, given the reduced protein adsorption[7] and the increased plasma stability of small nanoparticles.[36]

A numerical descriptor is commonly employed in SAR studies to represent the property that is being tested. Computational calculation of the n-octanol/water partition coefficient of the NP headgroups (Log P of R groups, Figure 6.1b) provides a readily accessible means to describe the relative hydrophobicity of NPs.[37] These calculated values were correlated with water/toluene interfacial tension (IFT) measurements, a technique that has been used to describe the effective surface hydrophobicity of NPs independent of the material of origin.[38] As can be observed in Figure 6.1c, the calculated Log P values and the experimental IFT results are essentially linearly correlated, indicating that the hydrophobicity of the NPs is predicted by the Log P descriptor. The very low threshold of values of the IFT of these NPs evidenced their high degree of amphiphilicity, a characteristic that is on favor of their colloidal stability despite the overall neutral zeta potential. ZDiPen represents the limit in terms of hydrophobicity: if the Log P of the headgroup is above 4.5 (IFT<0), or if the length of the straight-chain substituents is larger than six carbons, the NPs were insoluble in water.

To determine the preliminary interactions of the synthesized NPs with proteins,[26, 39] dynamic light scattering (DLS) measurements were recorded in the presence of 1% serum, the highest concentration that did not overwhelm the NP signal. The principal change in the DLS profile of serum after the addition of NP+ (cationic), NP- (anionic) and TEG (neutral oligo (ethylene glycol) capped particles) was the shift of the ~9 nm hydrodynamic diameter (d_h) peak to ~20 nm, evidencing the formation of discrete protein-NP complexes, namely the protein corona (Figure 6.2a and 6.2b). For NP+, the formation of a peak above 1000 nm was also observed indicating the presence of extended protein-NP aggregates. In contrast, only the peak at ~9 nm was observed with the zwitterionic NPs ZMe to ZDiPen (Figures 6.2a and 6.2b). These results can easily be contrasted by comparing the predicted histogram in the case where no corona is formed (the addition of the individual serum and NP histograms) with the experimental DLS distribution after mixing the NPs with serum (Figure 6.2c). As observed in Figure 6.2d, the subtraction of the experimental histograms from the predicted additive histograms shows that while NP+ presents residuals at the ~20 nm and ~1000 nm zones indicative of both aggregation and corona formation, ZMe has minimal residual, indicating the absence of corona at these protein levels.

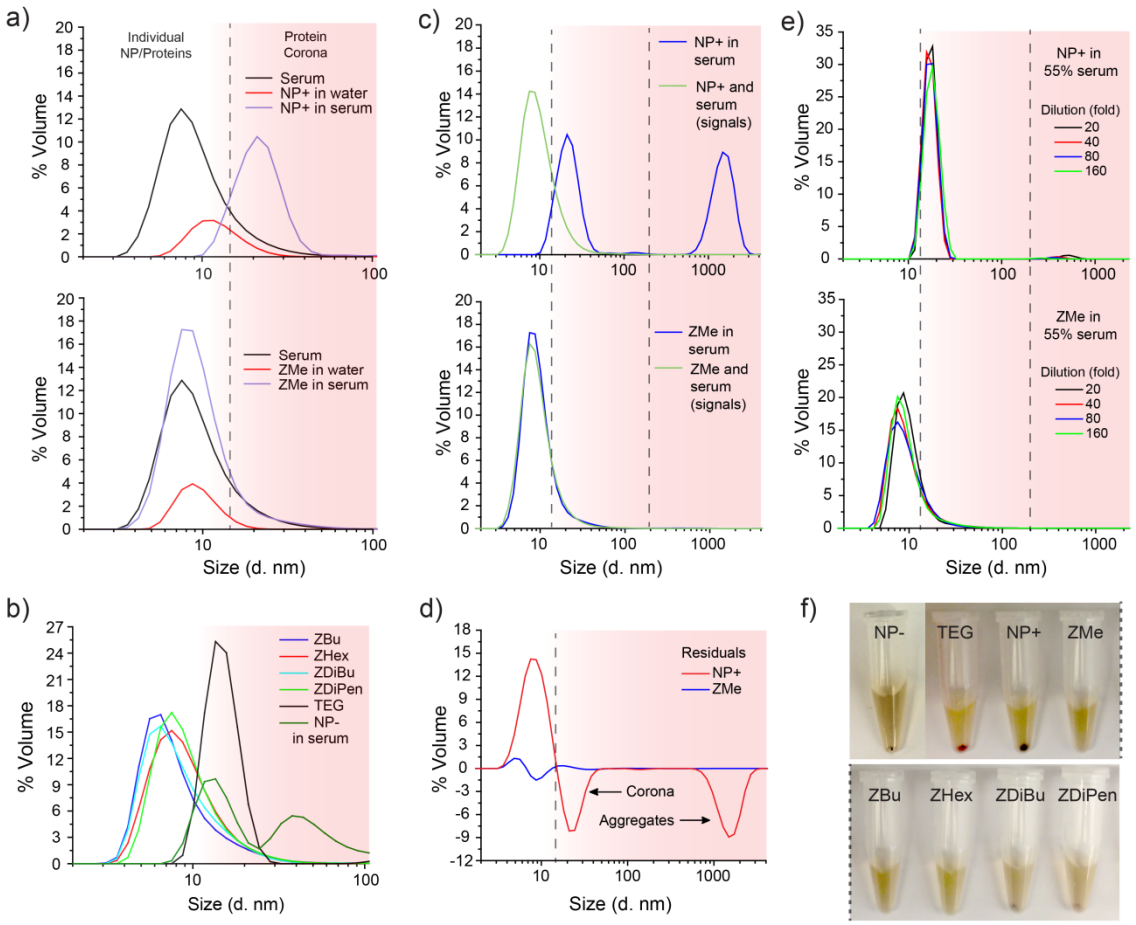

Figure 6.2. (a) Particle size distribution for cationic NP+ and zwitterionic particle ZMe in the presence and absence of serum proteins (1% serum, background) evidencing the formation of NP/protein complexes (~20 nm) with NP+ but not with ZMe (b) Lack of corona formation for zwitterionic particles in serum, and corona formation for TEG (lacking zwitterionic headgroup) and anionic NP-. (c) Comparison between the experimental DLS profiles of each NP in serum with the additive histogram of the combination of the individual serum and NP. (d) Residuals of the spectrums in serum after removing the individual NP and serum histograms, evidencing corona and aggregate formation for NP+ with minimal residual observed for ZMe (e) Dilution studies showing lack of hard corona formation for ZMe after incubation in 55% human serum, with contrasting behavior by the cationic NP+ particle. (f) Sedimentation experiments for the series of NPs in 55% plasma showing that zwitterionic NPs ZMe to ZDiPen did not aggregate, in contrast to NP+, NP-, and TEG that formed pellets.

Corona formation involves both reversible and irreversible (hard corona) adsorption of proteins on the NP surface (Figure 6.1a).[40, 41, 42] While we were unable to verify the lack of reversible protein adsorption at physiological serum concentrations, we were able to verify the absence of hard corona formation on zwitterionic NPs through incubation and dilution. For this

purpose, we incubated the set of NPs with 55% human serum at 37°C for 30 min, diluted the solutions and recorded DLS measurements to observe if irreversible protein-NP interactions had occurred for the controls and if crowding effects may alter the absence of corona for the zwitterionic NPs. As observed in Figure 6.2e, although the peak of the NP-protein conjugates (>1000 nm) for NP+ decreased when the sample was diluted, the peak at ~20 nm that describes discrete NP-protein complexes remained present after dilution, indicating a strong irreversible protein binding (hard corona). Similar results were obtained for NP- and TEG, suggesting that the larger protein-NP conjugates dissociated and only the discrete ones remained after dilution (Figure 6.4). In contrast, for NPs ZMe-ZDiPen (Figure 6.2e and 6.4), the ~9 nm peak was the only one observed, indicating the absence of an irreversible protein layer (hard corona).

Further studies using electrophoresis established that zwitterionic particles ZMe-ZDiPen are non-interacting in plasma (55% in PBS, v/v), a more complex matrix. As expected, the mobilities of cationic NP+ and anionic NP- were affected by the presence of proteins due to the corona formation. In contrast, similar mobilities were observed for the zwitterionic NPs in the presence and absence of plasma proteins (Figure 6.5). Likewise, TEG presented a minimal difference between the two conditions, and the subtle band movement in presence of protein presumably occurs due to NP aggregation. Despite these results, gel electrophoresis does not provide a definitive result on the absence of corona formation due to the poor mobility of all of the NPs in the agarose matrix. To further corroborate our hypothesis, sedimentation experiments were performed in the presence of 10%, 55% and undiluted plasma, mimicking *in vitro* and *in vivo* conditions.[42] As expected, while NP+ formed a pellet, NPs ZMe to ZDiPen presented minimal or no aggregates even at physiological plasma levels (Figure 6.2f and Figure 6.6a). These qualitative observations were validated by UV measurements of the supernatants before and after the sedimentation process (Figure 6.6b). NP- presented a pellet of smaller size than NP+, result that correlates with the observations by DLS and gel electrophoresis. Significantly, TEG NP presented sedimentation similar to the one observed for NP+. This outcome mirrors the

results from DLS experiments and is consistent with previous findings that postulate the recognition of PEG functionalities by proteins of the bloodstream.[21]

We wanted to observe if we were able to obtain pellets for the zwitterionic NPs using other variants of the sedimentation experiments, and also confirm that the sedimentation of NP+ was due to the formation of corona and no simple NP precipitation. To this end we repeated the sedimentation experiments using different sucrose gradients, a technique that has been used to separate NP/protein complexes from NPs alone.[14] Under these conditions we obtained similar results as with the direct sedimentation experiments, with a thick pellet only observed for NP+. We further ran a SDS-PAGE gel treating all the samples as if precipitation was observed, and from the results it can be observed that NP+ did adsorb proteins over the surface while ZMe-ZDiPen behave as the negative control (serum only, no NPs added, Figure 6.7). This further confirms the absence of irreversible protein adsorption over the surface of zwitterionic NPs at physiological protein levels. It is important to note that we did observe a very faint precipitation for the more hydrophobic NPs, however this precipitate was redissolved in the washing steps with PBS (intended to remove loosely bound proteins). This result indicates that even if NP/protein interactions are observed at large values of hydrophobicity, these interactions are reversible and no hard corona is formed.

Once the absence of corona was established, we investigated the effects of NP hydrophobicity on cellular uptake,[43] a phenomenon critically affected by the NP surface and the protein corona.[44, 45, 46] For this purpose, uptake studies were performed in serum-containing and serum-free media, conditions that critically affect the trend of uptake of NPs of varying hydrophobicity.[18] As seen in Figure 6.3a, there was an increase in cellular uptake with increasing surface hydrophobicity for both cases. In previous studies, when NPs were exposed to the cells in serum-free conditions, increasing hydrophobicity increased cell uptake, similar to the results that we obtained.[18] However when the studies were performed in media with serum, increasing the hydrophobicity of NPs lead to greater protein adsorption over the NP surface,[47] which in turn

reduced the cellular uptake.[48,49] In contrast to these prior systems, we obtained similar cellular uptake trends for NPs ZMe-ZDiPen both in the presence and absence of serum. This result indicates that direct correlations between the NP surface chemistry and biological responses can be assessed using these NPs, providing further proof of the absence of proteins on the NP surfaces and the direct presentation of the chemical motifs to the cell surface. As expected, overall uptake was low[50] and there was a marked difference in the absolute amount of NP uptake in the presence and absence of serum (~2 fold higher uptake without serum). This latter phenomenon has been observed previously for other particles independent of their charge,[51,52] possibly due to non-specific binding of proteins and NPs to the cell membrane, a competitive process that slows the uptake of NPs when proteins are present.[52, 17] Finally, it is important to note that at the condition of the study the nanoparticles were non-cytotoxic (Figure 6.8).

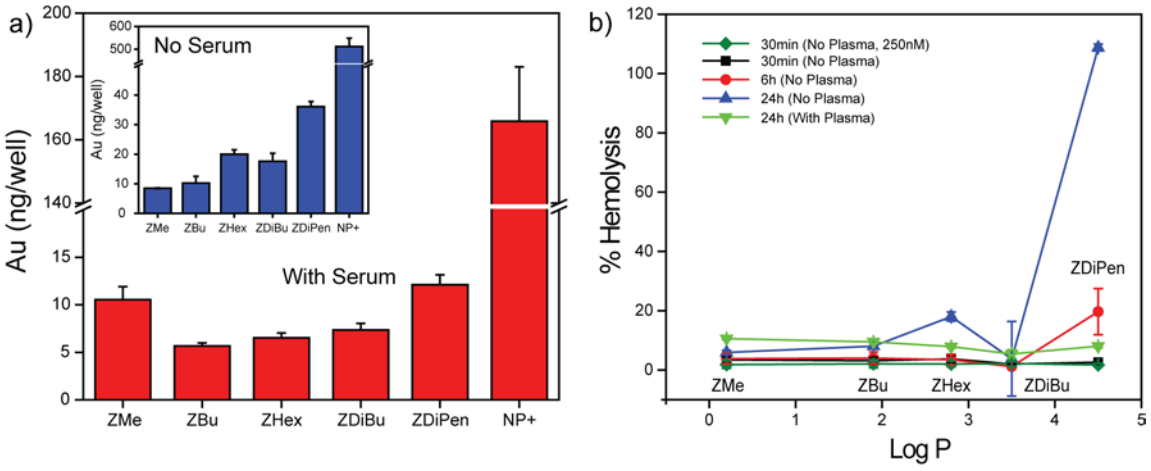

Figure 6.3. (a) Cellular uptake (MCF-7 cells, 3h) of zwitterionic NPs ZMe to ZDiPen and NP+ in presence and absence (inset) of serum, showing similar uptake trends for both experimental conditions. (b) Hemolytic activity of the NPs at different time points and in the presence and absence of plasma (NPs at a concentration of 500nM unless otherwise stated).

Due to the corona-free character, these NPs have the potential for long circulation times[53] increasing the possibility of hemolytic activity. As such, hemolytic assays were performed as a

means to probe the compatibility of the NPs with red blood cells (RBCs).[54, 55] NPs ZMe to ZDiPen were incubated with RBCs isolated from commercially purchased human whole blood. The experiments were performed both in the presence and in the absence of blood plasma. [56] The results (Figure 6.3b) provide evidence that no significant cell lysis was elicited by the zwitterionic NPs either in the presence or in the absence of plasma. Hemolytic activity was only observed for the more hydrophobic NP (ZDiPen) at 24h without plasma proteins, consistent with a critical change in the behavior of NPs at extreme values of hydrophobicity. However, it is important to note that during the half-life that is expected for these particles (~6h),[37] no significant hemolytic response was observed in the presence of plasma proteins for the zwitterionic NPs.

6.3. Conclusions

In summary, we have demonstrated that sulfobetaine headgroups can be engineered to provide particles with controlled hydrophobicity. These particles do not adsorb proteins at moderate serum protein concentrations nor do they form a hard corona at physiological serum conditions. The ligand design provides the potential to directly control the interaction of the nanomaterials with biosystems without interference from protein binding. As such, these coverages provide promising scaffolds for delivery vehicles and self-therapeutic systems. They also open new avenues for probing the fundamental nature of the nano-bio interface through direct interfacing of synthetic and biological components without intermediary complications arising from the protein corona.

6.4. Experimental Section

Nanoparticle synthesis and characterization: To a solution of gold nanoparticle (NP) cores coated with a monolayer of 1-pentanethiol (~2nm core diameter, synthesized by the Brust-

Schiffrin methodology[57] and purified to remove the phase transfer catalyst[58]) in dry dichloromethane (DCM) and methanol (MeOH) (9.5:0.5), a solution of the respective ligands in the same solvent was added, maintaining an inert atmosphere and constantly stirring for 3 days (5:1 w/w ratio of ligand/gold cores).[59] The solvent was evaporated and the remaining dark residue was washed several times with DCM or ethyl acetate until no smell was detected (removal of 1-pentanethiol). The nanoparticles were dispersed in distilled water, and dispensed into a membrane bag (~10,000 pore size) for dialysis purification for 5 days. Water was removed by lyophilization and the final product was redispersed in MQ deionized water (or D_2O), and the concentration of the final solution was determined using UV absorption according to the reported procedure.[60] The functionalized gold nanoparticles were characterized by ^{1}HNMR (Bruker Avance 400 MHz, 600 scans, [NP]=20μM), MALDI-MS (Bruker Autoflex III MALDI-TOF MS, 200 shots-20 off-laser 55%, suppress up to 400Da), DLS and ZP (Malvern NanoZeta Sizer, [NP]=1 μM) to observe the chemical composition of the monolayer, the hydrodynamic size, and the surface zeta potential. The LogP values of the ligand headgroups (R groups of Figure 6.1) were estimated using ChemDraw Ultra 12.0.

Interfacial Tension. The dynamic interfacial tension of the NPs at the toluene−water interface was measured by the pendant drop method using an OCA20 measuring instrument (Dataphysics, Stuttgart). A syringe filled with an aqueous solution of NPs (1μM) connected to a blunt needle was fixed vertically with the needle immersed in the toluene phase. A small amount of solution was injected from the syringe to form a drop. The variation of drop shape with time until equilibrium (interfacial tension) and drop fall was captured by automated camera. The measurements were performed in triplicate.

Dynamic Light Scattering. DLS profiles were recorded in 1% human serum (~16 μM protein concentration) diluted in phosphate buffered saline (PBS, pH 7.4) at 37 °C with NPs at a concentration of 1μM using a Malvern Zetasizer Nano ZS. For the dilution profiles, NPs at a

concentration of 50 μM were incubated for 30 min at 37 °C in 55% human serum, then diluted accordingly. The subtraction of the individual NP and serum spectrums from the 'NP in serum' results, was done point by point using normalized data to take into account the concentration of each species (spectra of individual NPs and serum reported as normalized). The results are reported as %Number when individual NPs are analyzed (characterization) and as %Volume for the NP/Protein mixtures due to the dependence on the different refractive index of each entity.

Sedimentation. To a solution of 10%, 55% plasma (in PBS) and undiluted plasma, NPs were added to achieve a final concentration of 500nM (500μL total volume). The solutions were incubated for 5 minutes, and the tubes were subjected to centrifugation for 30 min at 14,000 r.p.m. After centrifugation, 200 μL of the supernatant was transferred to a 96-well plate alongside 200 μL of the same mixture before the centrifugation. The absorbance values were measured at 506 nm, which is the wavelength at which NP concentration is determined. The absorbance generated by the proteins was subtracted using a blank protein sample with no particles. UV differences were significant only at 10% plasma, as the proteins have much more interference at 55% plasma. All NPs and blank samples were prepared in triplicate. For the sucrose gradients, NP samples in undiluted serum/plasma were centrifuged at 14,000 rpm during 30 min using a sequential gradient of 24%, 12% and 6% sucrose, and a sharp gradient of 24% for the gel. Ultracentrifugation experiments were run at 60,000 rpm for 1h.

Agarose gel electrophoresis. Agarose gels were prepared in PBS at a 0.5% final agarose concentration. NPs at a concentration of 1 μM were incubated with or without 55% plasma in PBS for 15 min, and 2 uL of 50% glycerol were added to the solution to ensure proper gel loading. The mixture was loaded in each well and the gels were run at a constant voltage of 100V for 30 min.

Protein isolation from NPs and SDS-polyacrylamide gel electrophoresis. NP+ and NPs ZMe-ZDiPen (0.5μM) were incubated in undiluted human serum for 24h at 37°C. After incubation, serum-NP mixtures were loaded onto a sucrose cushion (24%) to rapidly separate NP-

protein complexes from serum by centrifugation at 14,000rpm for 30min.[14] The supernatant was carefully removed and the residues were washed with 1mL PBS three times. Proteins were eluted from the nanoparticles by adding 4x Laemmli sample buffer (Biorad 161-0747) with 2-mercaptoethanol to the pellet and subsequent incubation at 95°C for 5min. For 1D gel electrophoresis, 20µL of recovered proteins in sample buffer were separated on a 12% SDS-PAGE gel. Gels were run at the constant voltage of 150V for 1h and silver staining was performed to visualize the bands according to the previously published protocol.[61] A 0.1% human serum sample was also run for comparison.

Cellular uptake. MCF7 cells (breast adenocarcinoma) were cultured at 37 °C under a humidified atmosphere of 5 % CO_2. The cells were grown in low glucose Dulbecco's Modified Eagle's Medium (DMEM, 1.0 g/L glucose) containing 10 % fetal bovine serum (FBS) and 1% antibiotics (100 U/ml penicillin and 100 µg/ml streptomycin). For the uptake experiment, 20,000 cells/well were plated in a 48-well plate prior to the experiment. On the following day, cells were washed one time with PBS followed by NP treatment (25 nM/well) and further incubated with or without 10% serum for 3 h (or 24 h). Following incubation, cells were lysed and the intracellular gold amount was measured using inductively coupled plasma mass spectrometry (Elan 6100, Perkin-Elmer, Shelton, CT, USA). Each cell uptake experiment was done in triplicate, and each replicate was measured 5 times by ICP-MS. ICP-MS operating conditions are as below: rf power 1600 W; plasma Ar Flow rate, 15 ml/min, nebulizer Ar flow rate, 0.98 ml/min and dwell time, 45 ms.

Hemolysis. Red blood cells (RBCs) were purified from citrate-stabilized human whole blood (pooled, mixed gender) by multiple cycles of centrifugation and dilution in PBS (5000 r.p.m., 5 min). The purified RBCs were then diluted in 10 mL of PBS and kept on ice during the sample preparation. 0.1 mL of RBC solution was added to 0.4 mL of NP solution in PBS in a 1.5 mL centrifuge tube (Fisher) and mixed gently by pipetting (NPs at a final concentration of 250 nM and 500 nM). RBCs incubated with PBS and water were used as negative and positive control

respectively. All NP samples as well as controls were prepared in triplicate. The mixture was incubated at 37 ˚C for 30 min, 6h and 24h while shaking at 150 r.p.m. After incubating, the solution was centrifuged at 4000 r.p.m. for 5 minutes and 100 μL of supernatant was transferred to a 96-well plate. The absorbance value of the supernatant was measured at 570 nm using a microplate reader (SpectraMax M2, Molecular Devices) with absorbance at 655 nm as a reference. To determine hemolysis in the presence of plasma, NPs were pre-incubated in 55% of plasma solution in PBS (v/v) for 30 minutes at 37 ˚C. After the pre-incubation period, 0.1 mL of washed RBCs were added to the solution and further incubated for 24 hours. The percent hemolysis was calculated using the following formula:

$$\%\text{Hemolysis} = ((\text{sample absorbance} - \text{negative control absorbance})) / ((\text{positive control absorbance} - \text{negative control absorbance})) \times 100.$$

To corroborate that the lack of hemolytic properties was not due to precipitation of NPs in the presence of RBC, sedimentation experiments were done in PBS both in the presence and absence of RBCs. A control with no NPs was used to remove the background. As observed in Figure S23, the differences in the absorbance in the presence and absence of RBCs are not significant, indicating that NPs remained in the solution for both cases.

Cell viability: The cell viability was determined by alamar blue assay according to manufacturer protocol (Life Technologies, DAL1100). MCF7 cells (15000 cells/well) were seeded in a 96-well plate 24 hours prior to the experiment. On the following day, the old media was aspirated and the cells were washed with PBS for one time. NPs ZMe-ZDiPen (25 nM each) were then incubated with the cells in 10% serum containing media for 24 h at 37 °C. After the incubation period, the cells were washed three times with PBS and 220 μL of 10 % alamar blue solution in serum containing media was added to each well and cells were further incubated at 37 ˚C for 3 hours. After 3 hours, 200 μL of solution from each well were taken out and loaded in a 96- well black microplate. Red fluorescence, resulting from the reduction of the alamar blue

solution by viable cells was measured (Ex: 560 nm, Em: 590 nm) on a SpectroMax M2 microplate reader (Molecular Device). Viability (%) of NP-treated cells was calculated taking untreated cells as 100 % viable. All experiments were performed using at least four parallel replicates.

6.5. Supplementary Information

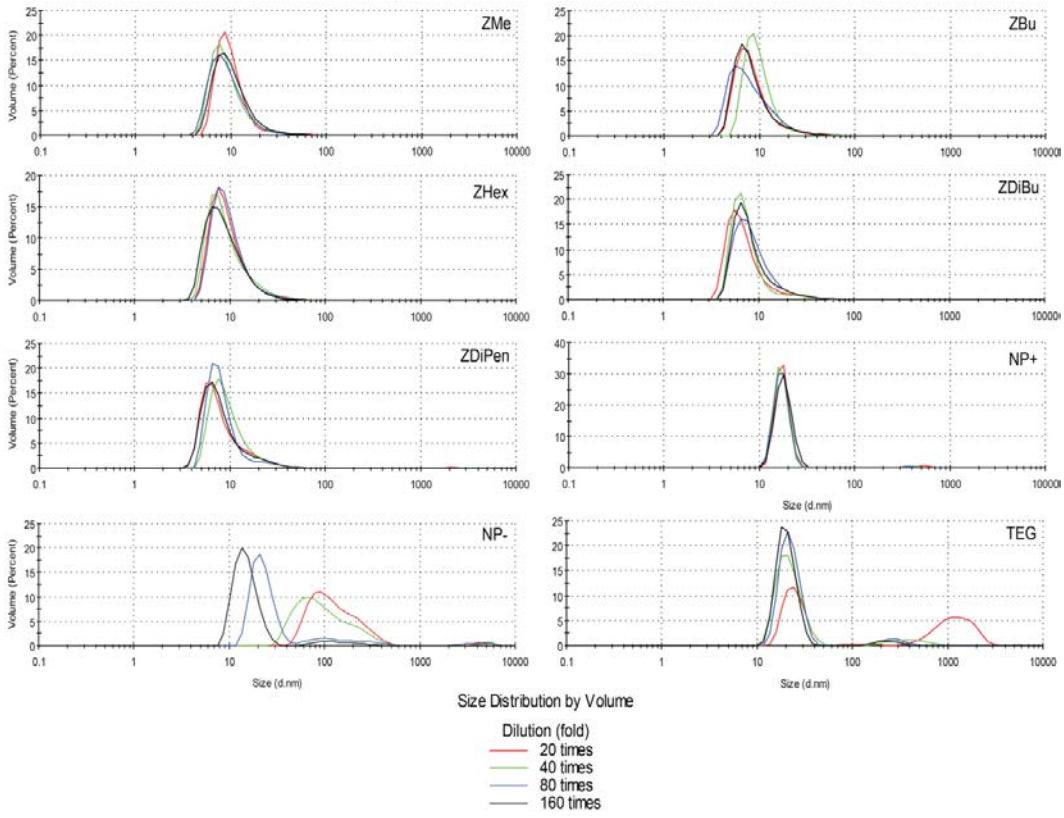

Figure 6.4. DLS profiles (% Volume) of the series of NPs after incubation in 55% human serum and successive dilutions, evidencing the absence of protein corona for ZMe-ZDiPen while NP+, NP- and TEG present NP/protein complexes.

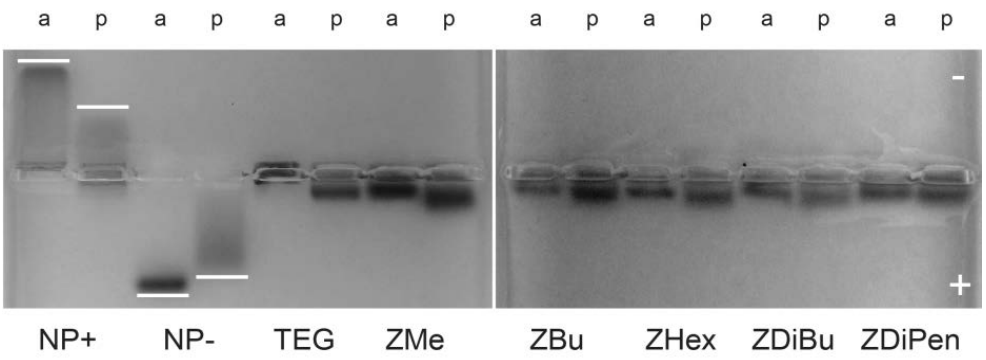

Figure 6.5. Agarose gel electrophoresis showing similar mobilities for NPs ZMe-ZDiPen in the presence and absence of plasma, while NP+ and NP- present a retarded band due to conjugation with proteins (a = NPs alone, p = mixture of plasma and NPs). NP concentration is 1 μM.

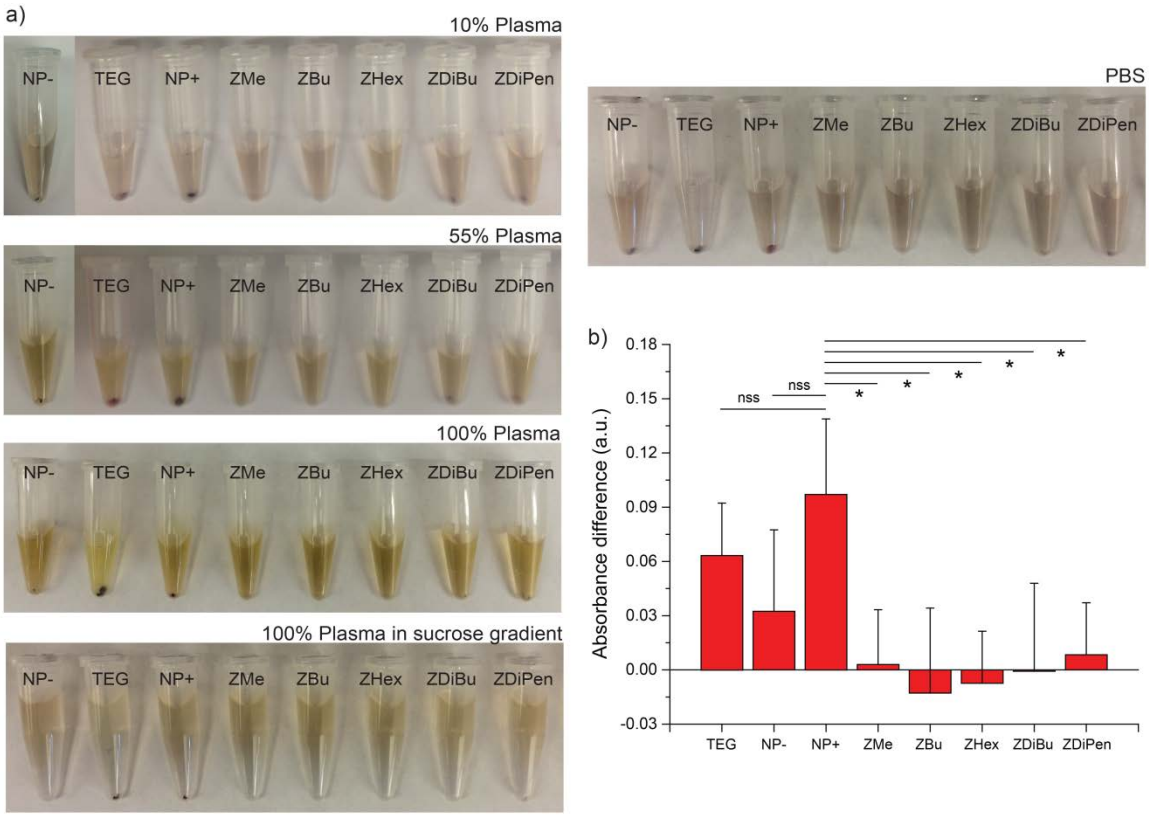

Figure 6.6. (a) Sedimentation experiments at 10% and 55% plasma concentration. (b) UV differences (λ=506nm) of the supernatants before and after centrifugation in 10% serum evidencing the significant difference in sedimentation between TEG, NP+, NP- and ZMe to ZDiPen (*p*-values < 0.05). The sediment observed in the case of ZDiBu and ZDiPen were removed after washing with PBS 1-2 times indicating a reversible binding, while the positive control retained the pellet.

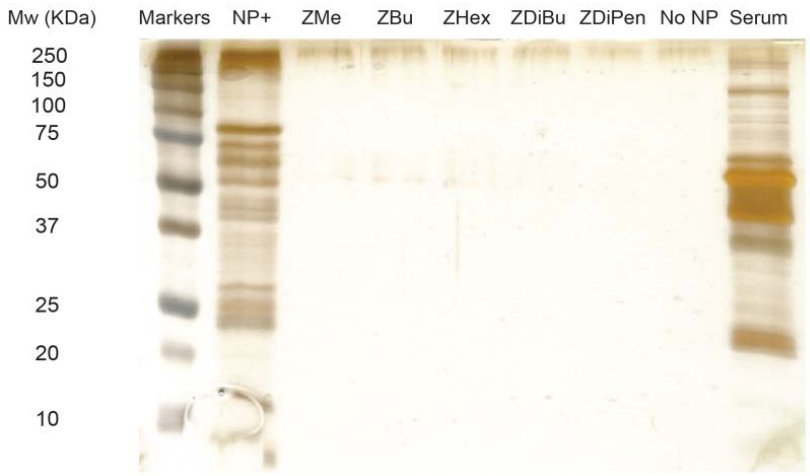

Figure 6.7. Gel electrophoresis of the samples obtained by the 24% sucrose sedimentation, evidencing very low level of proteins in the samples of the zwitterionic NPs (ZMe – ZDiPen, similar to control with no NP), while NP+ presented protein bands indicating corona formation. Serum lane indicates a sample with 0.1% serum directly loaded into the gel.

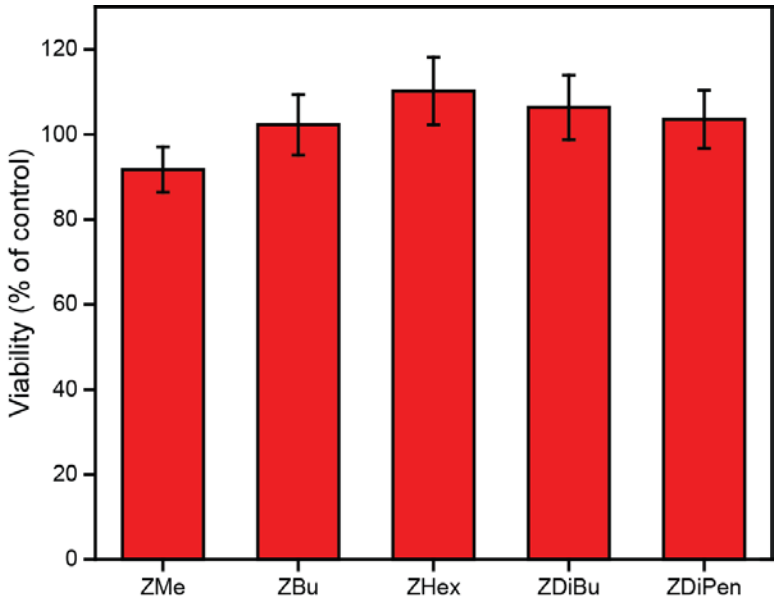

Figure 6.8. %Viability of MCF7 cells at 24h for the different NPs.

6.6. References

1. Sapsford, K. E.; Algar, W. R.; Berti, L.; Gemmill, K. B.; Casey, B. J.; Oh, E.; Stewart, M. H.; Medintz, I. L. *Chem. Rev.* **2013**, *113*, 1904.

2. Mout, R.; Moyano, D. F.; Rana, S.; Rotello, V. M. *Chem. Soc. Rev.* **2012**, *41*, 2539.

3. Khlebtsov, N.; Dykman, L. *Chem. Soc. Rev.* **2011**, *40*, 1647.

4. Kim, S. T.; Saha, K.; Kim, C.; Rotello, V. M. *Acc. Chem. Res.* **2013**, *46*, 681.

5. He, X. X.; Nie, H. L.; Wang, K. M.; Tan, W. H.; Wu, X.; Zhang, P. F. *Anal. Chem.* **2008**, *80*, 9597.

6. Alexis, F.; Pridgen, E.; Molnar, L. K.; Farokhzad, O. C. *Mol. Pharmaceutics.* **2008**, *5*, 505.

7. Walkey, C. D.; Chan, W. C. W. *Chem. Soc. Rev.* **2012**, *41*, 2780.

8. Monopoli, M. P.; Aberg, C.; Salvati, A.; Dawson, K. A. *Nat. Nanotechnol.* **2012**, *7*, 779.

9. Maiorano, G.; Sabella, S.; Sorce, B.; Brunetti, V.; Malvindi, M. A.; Cingolani, R.; Pompa, P. P. *Acs Nano* **2010**, *4*, 7481.

10. Pelaz, B.; Charron, G.; Pfeiffer, C.; Zhao, Y.; de la Fuente, J. M.; Liang, X.-J.; Parak, W. J.; Del Pino, P. *Small*, **2013**, *9*, 1573.

11. Mahmoudi, M.; Lynch, I.; Ejtehadi, M. R.; Monopoli, M.P.; Bombelli, F. B.; Laurent, S. *Chem. Rev.* **2011**, *111*, 5610.

12. Lundqvist, M.; Stigler, J.; Elia, G.; Lynch, I.; Cedervall, T.; Dawson, K. A. *Proc. Natl. Acad. Sci. U.S.A.* **2008**, *105*, 14265.

13. Aggarwal, P.; Hall, J. B.; McLeland, C. B.; Dobrovolskaia, M. A.; McNeil, S. E. *Adv. Drug Deliv. Rev.* **2009**, *61*, 428.

14. Tenzer, S.; Docter, D.; Kuharev, J.; Musyanovych, A.; Fetz, V.; Hecht, R.; Schlenk, F.; Fischer, D.; Kiouptsi, K.; Reinhardt, C.; Landfester, K.; Schild, H.; Maskos, M.; Knauer, S. K.; Stauber, R. H. *Nat. Nanotechnol.* **2013**, *8*, 772.

15. Mirshafiee, V.; Mahmoudi, M.; Lou, K. Y.; Cheng, J. J.; Kraft, M. L. *Chem. Commun.* **2013**, *49*, 2557.

16. Salvati, A.; Pitek, A. S.; Monopoli, M. P.; Prapainop, K.; Bombelli, F. B.; Hristov, D. R.; Kelly, P. M.; Aberg, C.; Mahon, E.; Dawson, K. A. *Nat. Nanotechnol.* **2013**, *8*, 137.

17. Lesniak, A.; Fenaroli, F.; Monopoli, M. R.; Aberg, C.; Dawson, K. A.; Salvati, A. *ACS Nano* **2012**, *6*, 5845.

18. Zhu, Z. J.; Posati, T.; Moyano, D. F.; Tang, R.; Yan, B.; Vachet, R. W.; Rotello, V. M. *Small* **2012**, *8*, 2659.

19. Jokerst, J. V.; Lobovkina, T.; Zare, R. N.; Gambhir, S. S. *Nanomedicine* **2011**, *6*, 715.

20. Karakoti, A. S.; Das, S.; Thevuthasan, S.; Seal, S. *Angew. Chem. Int. Ed.* **2011**, *50*, 1980.

21. Hamad, I.; Al-Hanbali, O.; Hunter, A. C.; Rutt, K. J.; Andresen, T. L.; Moghimi, S. M. *ACS Nano* **2010**, *4*, 6629.

22. Sekiguchi, S.; Niikura, K.; Matsuo, Y.; Ijiro, K. *Langmuir* **2012**, *28*, 5503.

23. Rosen, J. E.; Gu, F. X. *Langmuir* **2011**, *27*, 10507.

24. Yang, W.; Zhang, L.; Wang, S.; White, A. D.; Jiang, S. Y. *Biomaterials* **2009**, *30*, 5617.

25. Cao, Z. Q.; Jiang, S. Y. *Nano Today* **2012**, *7*, 404.

26. Murthy, A. K.; Stover, R. J.; Hardin, W. G.; Schramm, R.; Nie, G. D.; Gourisankar, S.; Truskett, T. M.; Sokolov, K. V.; Johnston, K. P. *J. Am. Chem. Soc.* **2013**, *135*, 7799.

27. McCormick, C. L.; Lowe, A. B. *Acc. Chem. Res.* **2004**, *37*, 312.

28. Matyjaszewski, K. *Macromolecules* **2012**, *45*, 4015.

29. Arvizo, R. R.; Miranda, O. R.; Moyano, D. F.; Walden, C. A.; Giri, K.; Bhattacharya, R.; Robertson, J. D.; Rotello, V. M.; Reid, J. M.; Mukherjee, P. *Plos One* **2011**, *6*, e24374.

30. Maiti, S.; Das, K.; Dutta, S.; Das, P. K. *Chem. Eur. J.* **2012**, *18*, 15021.

31. Zuo, G.; Huang, Q.; Wei, G.; Zhou, R.; Fang, H. *ACS Nano* **2010**, *4*, 7508.

32. Fubini, B.; Ghiazza, M.; Fenoglio, I. *Nanotoxicology* **2010**, *4*, 347.

33. Chompoosor, A.; Saha, K.; Ghosh, P. S.; Macarthy, D. J.; Miranda, O. R.; Zhu, Z. J.; Arcaro, K. F.; Rotello, V. M. *Small* **2010**, *6*, 2246.

34. Moyano, D. F.; Goldsmith, M.; Solfiell, D. J.; Landesman-Milo, D.; Miranda, O. R.; Peer, D.; Rotello, V. M. *J. Am. Chem. Soc.* **2012**, *134*, 3965.

35. Kreuter, J.; Liehl, E.; Berg, U.; Soliva, M.; Speiser, P. P. *Vaccine* **1988**, *6*, 253.

36. Zhang, G.; Yang, Z.; Lu, W.; Zhang, R.; Huang, Q.; Tian, M.; Li, L.; Liang, D.; Li, C. *Biomaterials* **2009**, *30*, 1928.

37. Rana, S.; Yu, X.; Patra, D.; Moyano, D. F.; Miranda, O. R.; Hussain, I.; Rotello, V. M. *Langmuir* **2012**, *28*, 2023.

38. Xiao, Y.; Wiesner, M. R. *J. Hazard. Mater.* **2012**, *215*, 146.

39. Zhang, C.; Macfarlane, R. J.; Young, K. L.; Choi, C. H. J.; Hao, L.; Auyeung, E.; Liu, G.; Zhou, X.; Mirkin, C. A. *Nat. Mater.* **2013**, *12*, 741.

40. Milani, S.; Bombelli, F. B.; Pitek, A. S.; Dawson, K. A.; Rädler, J. *ACS Nano* **2012**, *6*, 2532.

41. Casals, E.; Puntes, V. F. *Nanomedicine* **2012**, *7*, 1917.

42. Monopoli, M. P.; Pitek, A. S.; Lynch, I.; Dawson, K. A. *Methods Mol. Biol.* 2013, 1025, 137.

43. Zhu, Z.-J.; Ghosh, P.; Miranda, O. R.; Vachet, R. W.; Rotello, V. M. *J. Am. Chem. Soc.* **2008**, *130*, 14139.

44. Mortimer, G. M.; Butcher, N. J.; Musumeci, A. W.; Deng, Z. J.; Martin, D. J.; Minchin, R. F. *ACS Nano*, **2014**, *8*, 3357.

45. Walkey, C. D.; Olsen, J. B.; Song, F.; Liu, R.; Guo, H.; Olsen, D. W. H.; Cohen, Y.; Emili, A.; Chan, W. C. W. *ACS Nano* **2014**, *8*, 2439.

46. Walkey, C.D.; Olsen, J.B.; Guo, H.; Emili, A.; Chan, W.C. *J. Am. Chem. Soc.* **2012**, *134*, 2139.

47. Gessner, A.; Waicz, R.; Lieske, A.; Paulke, B. R.; Mader, K.; Muller, R. H. *Int. J. Pharm.* **2000**, *196*, 245.

48. Baier, G.; Costa, C.; Zeller, A.; Baumann, D.; Sayer, C.; Araujo, P. H. H.; Mailander, V.; Musyanovych, A.; Landfester, K. *Macromol. Biosci.* **2011**, *11*, 628.

49. Patil, S.; Sandberg, A.; Heckert, E.; Self, W.; Seal, S. *Biomaterials* **2007**, *28*, 4600.

50. Kim, C. K.; Ghosh, P.; Pagliuca, C.; Zhu, Z.-J.; Menichetti, S.; Rotello, V. M. *J. Am. Chem. Soc.* **2009**, *131*, 1360.

51. Hühn, D.; Kantner, K.; Geidel, C.; Brandholt, S.; Cock, I. D.; Soenen, S. J. H.; Rivera_Gil, P.; Montenegro, J.-M.; Braeckmans, K.; Müllen, K. *et al. ACS Nano* **2013**, *7*, 3253.

52. Fleischer, C. C.; Kumar, U.; Payne, C. K. *Biomater. Sci.* **2013**, *1*, 975.

53. Xiao, W. C.; Lin, J.; Li, M. L.; Ma, Y. J.; Chen, Y. X.; Zhang, C. F.; Li, D.; Gu, H. C. *Contrast Media Mol. Imaging* **2012**, *7*, 320.

54. Lin, Y. S.; Haynes, C. L. *J. Am. Chem. Soc.* **2010**, *132*, 4834.

55. Lin, Y. S.; Haynes, C. L. *Chem. Mater.* **2009**, *21*, 3979.

56. Saha, K.; Moyano, D. F.; Rotello, V. M. *Mater. Horiz.* **2014**, *1*, 102.

57. Brust, M.; Walker, M.; Bethell, D.; Schiffrin, D. J.; Whyman, R. *J. Chem. Soc. Chem. Commun.* **1994**, *7*, 801.

58. Moyano, D. F.; Duncan, B.; Rotello, V. M. *Methods Mol. Biol.* **2013**, *1025*, 3.

59. Hostetler, M. J.; Green, S. J.; Stokes, J. J.; Murray, R. W. *J. Am. Chem. Soc.* **1996**, *118*, 4212.

60. Liu, X.; Atwater, M.; Wang, J.; Huo,Q. *Colloids Surf. B* **2007**, *58*, 3.

61. Chevallet, M.; Luche, S.; Rabilloud, T. *Nat Protoc.* **2006**, *1*, 1852.

CHAPTER 7

ACYLSULFONAMIDE-FUNCTIONALIZED ZWITTERIONIC GOLD NANOPARTICLES FOR ENHANCED CELLULAR UPTAKE AT TUMOR PH

7.1. Introduction

The pH difference between normal tissue (pH 7.2-7.4) and tumor tissue (pH 6.0-6.8)[1] provides an attractive strategy for selective accumulation of nanoparticles (NPs) into tumor tissues for cancer treatment and/or imaging. To supply high tumor selectivity, a pH-responsive bio-interactive surface must be generated with appropriate responses at normal and tumor pH.[2] The most common strategy is the use of a non-interactive functional group bearing an acid-cleavable unit; however, difficulty in controlling the acid sensitivity can result in the cleavage reaction taking place even at neutral pH,[3] or requiring quite low pH (≈ 5.0) for activation.[4] The use of reversible protonation/deprotonation systems provides an alternate strategy that features high tunablity.[5] Recent reports employing polymers such as poly-histidine and poly-amine as a pH-responsive moiety provided high tumor pH sensitivity,[6] demonstrating their utilities for tumor targeting. Solubility can be a challenge, however, with these neutral-to-cationic systems, requiring the use of additional functional group such as poly(ethylene)glycol chains to provide non-interactive surfaces at neutral pH.

Zwitterionic surfaces have recently received considerable attention as non-interacting chemical surfaces.[7] NPs with zwitterionic surfaces exhibit a long circulatory half-life,[8] low cytotoxicity,[9] and high biocompatibility. Integration of these properties with a pH dependent zwitterionic-to-cationic charge conversion system would make them attractive scaffolds for therapeutics. The low cellular uptake of zwitterionic particles[10] makes them excellent candidates for pH-controlled tumor uptake upon protonation to the resulting cationic particle. Moreover,

concomitant cytotoxicity resulting from these cationic NPs[11] would occur only in the tumor environment, leading to the possibility of tumor-selective therapy.

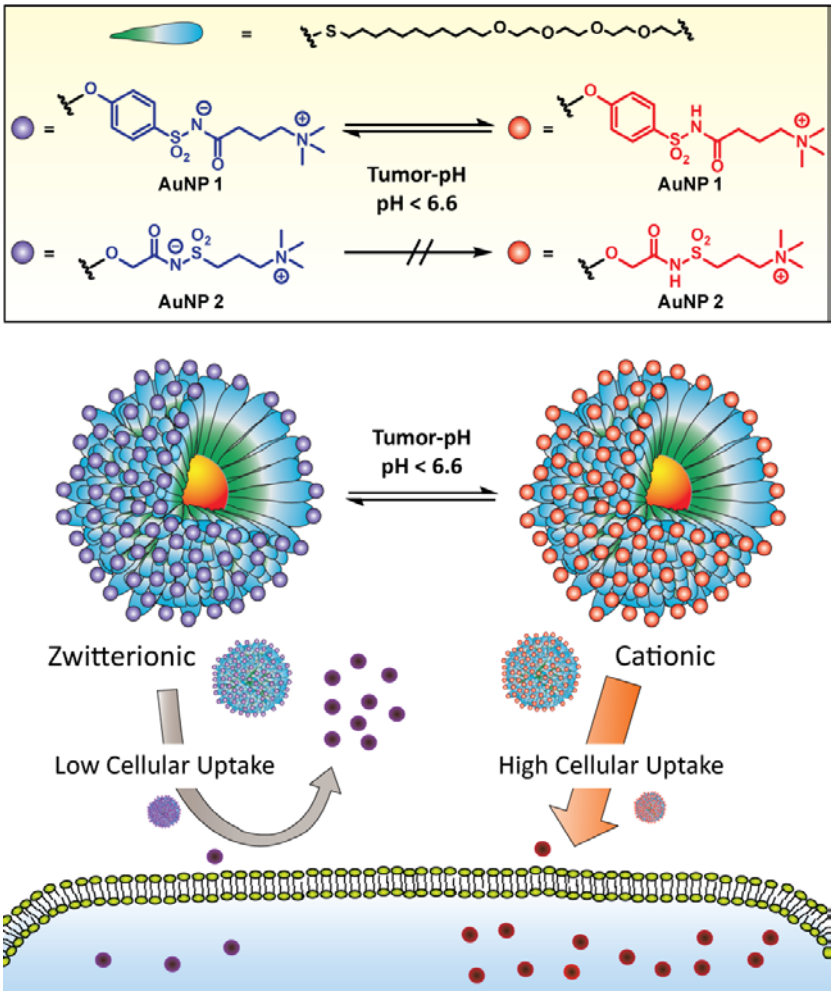

Figure 7.1. Chemical structure of the monolayer-protected gold nanoparticles (AuNPs) and our strategy for a pH-responsive delivery system into tumors.

A few examples of pH-responsive zwitterionic chemical surfaces such as carboxybetaine[12] and phosphorylcholine have been reported.[13] However, the pH-switching abilities of these structures are not sensitive enough to respond to stimuli such as weakly acidic tumor pH, with carboxybetaines protonated at pH <2 and phosphorylcholine at pH <5. The pK_a value of the negatively and charged group is the key for precise pH-responsiveness, but has only been reported using mixed-monolayer particles featuring anionic and cationic ligands.[14] Here, we

report a new pH-responsive zwitterionic surface structure engineered by derivatization of acylsulfonamide group. Due to its precise pK_a value, this designed zwitterionic group becomes cationic at tumor pH (< 6.5), resulting in dramatically enhanced cellular uptake and cytotoxicity. Significantly, these particles show no hemolytic activity at physiological pH (7.4).

7.2. Results and Discussion

The acylsulfonamide group features pH behavior similar to that of carboxylic acid groups and has good metabolic stability.[15] We chose this group as the negatively charged part of the zwitterionic ligand, with pH-responsiveness controlled by the functional group attached to the sulfonyl group. AuNP **1** features an aryl acylsulfonamide while AuNP **2** provides an alkyl analog (Figure 7.1). The ligands have trimethylammonium termini, and a tetra(ethylene glycol) spacer between the negative group and the hydrophobic chain was used as a passivating group to avoid irreversible adsorption and denaturation of serum proteins.[16] These particles were synthesized from pentanethiol-capped AuNPs (ca. 2 nm core) by means of place-exchange reactions.[17]

We initially measured zeta potential at several pH values to examine the pH dependence of the AuNP surface charges (Figure 7.2). The surface charge of both AuNP **1** and **2** were close to neutral at physiological pH (7.4), consistent with the zwitterionic structure of these NPs. AuNP **1** features a sharp transition from neutral to cationic centered at pH 6.5. However, AuNP **2** displayed a zwitterionic surface even at acidic pH, consistent with the reported pK_a value of the acylsulfonamide group ($pK_a \approx 4.5$)[18] and providing a permantly zwitterionic control particle for our studies. Recent reports on a pH-responsive zwitterionic AuNP with a mixed monolayer of carboxylic acid and quaternary ammonium ligands showed that the neutralization of surface charge during the charge alteration process results in the formation of precipitates.[14,19] Therefore, we investigated if similar aggregates formed in our case. Dynamic light scattering data revealed

that no aggregation of these NPs was observed in the pH range from 7.4 to 6.0, preventing potential complications arising from particle aggregation.

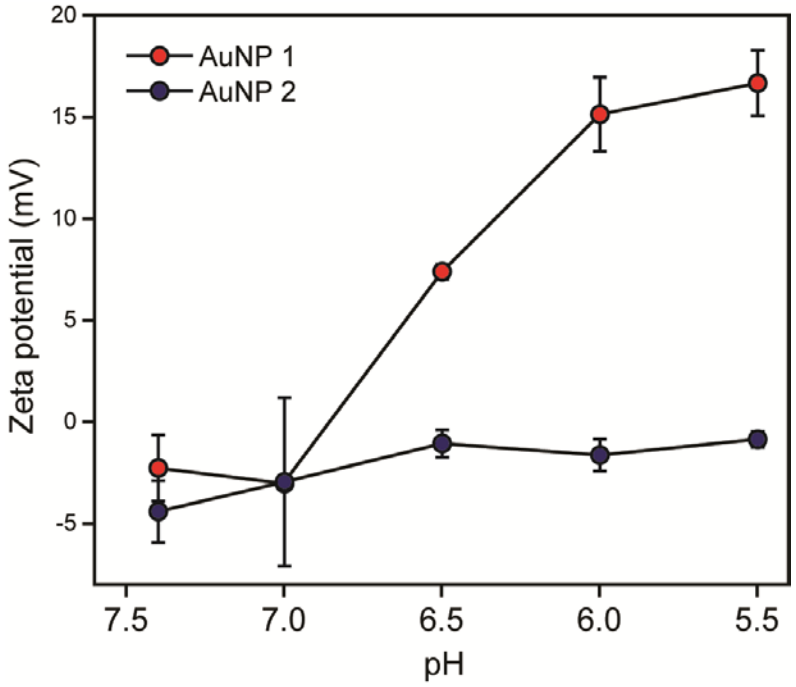

Figure 7.2. Zeta potential *vs.* pH curves obtained for AuNPs **1** and **2** (both 1 µM). Zeta-potentials were measured in 5 mM phosphate buffer at different pH values. Error bars represent standard deviations based on three independent measurements per pH value.

The change of AuNP **1** from zwitterionic to positively charged surface at weakly acidic pH should enhance cellular uptake of AuNP. Both AuNPs **1** (switchable) and **2** (non-switchable) were incubated with HeLa cells for 3 h at three different pH values, with the resulting intracellular amount of gold measured using inductively coupled plasma mass spectrometry (ICP-MS) (Figure 7.3). At pH 7.4, very low uptake (~10 ng/cell) was observed for both AuNPs **1** and **2**, similar to the cellular uptake of recently reported highly nonfouling sulfabetaine-functionalized AuNPs.[7e] Uptake of AuNP **1** increased with decreasing pH value, reaching a four-fold increase at pH 6.0. In contrast, no significant change in uptake was observed with control AuNP **2** over the pH range studied. Taken together, these studies establish the role of acylsulfonamide protonation in determining cellular uptake.

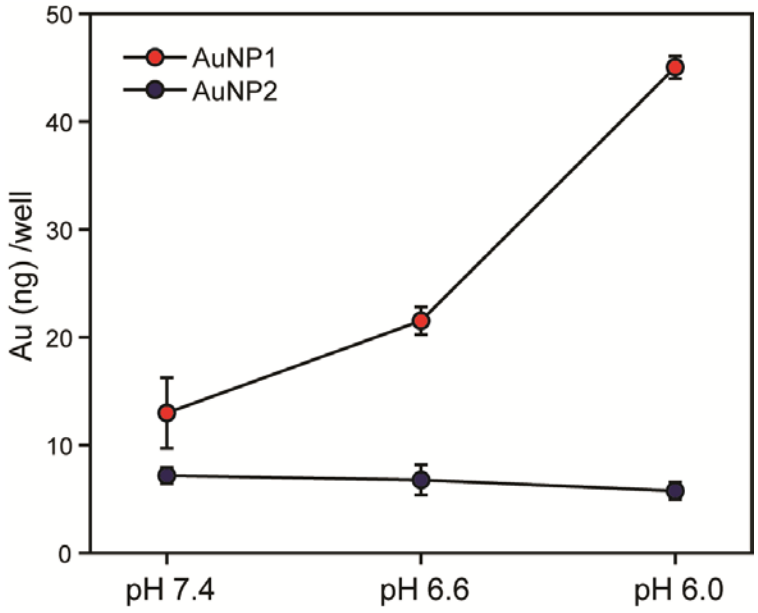

Figure 7.3. Cellular uptake of AuNPs **1** and **2** (both 1 μM) after 3 h incubation with HeLa cells in the presence of 10% serum. All experiments were performed in triplicate, and error bars represent standard error of the mean.

We next evaluated the cytotoxicity of AuNPs **1** and **2** at varying pH values using the Alamar blue viability assay (Figure 7.4). At pH 7.4, no cytotoxicity of AuNPs **1** and **2** was observed due to their non-interactive zwitterionic properties. Enhanced cytotoxicity of AuNP **1** was observed at pH 6.6 and 6.0, as expected due to the conversion of the particle from zwitterionic to cationic.[11] In contrast AuNP **2** did not show any significant toxicity at low pH values. While only a modest toxicity increase was observed at lower pH, these studies demonstrate the potential for this ligand in pH-regulated self-therapeutic.

Hemolysis is an important issue for therapeutic nanomaterials.[20] Therefore, we performed a hemolytic assay to investigate the blood compatibility of our NPs[21] (Figure 7.5). AuNP-mediated cell lysis events were not observed on either AuNP **1** or AuNP**2**.

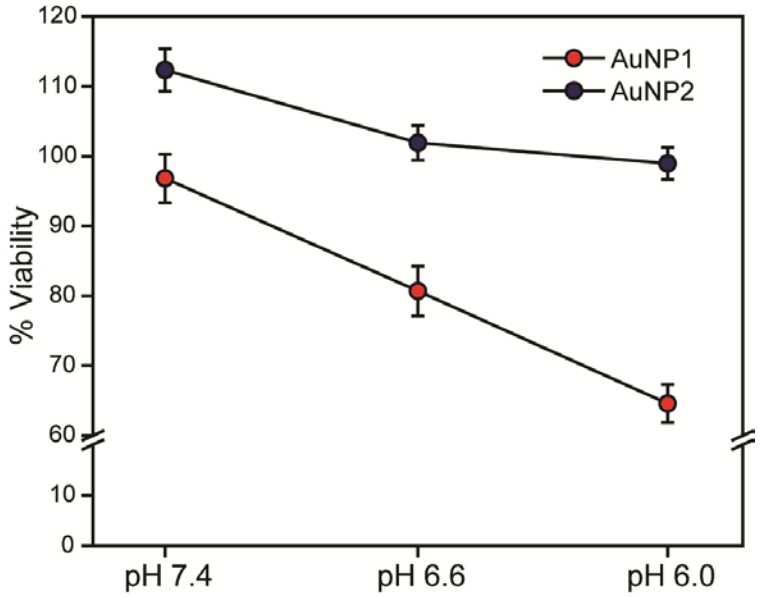

Figure 7.4. Cell viability of HeLa cells after 72 h incubation with AuNPs **1** and **2** (both 1 μM) in the presence of 10% serum at different pH values. All experiments were performed in six replicates. Error bars represent standard error of the mean.

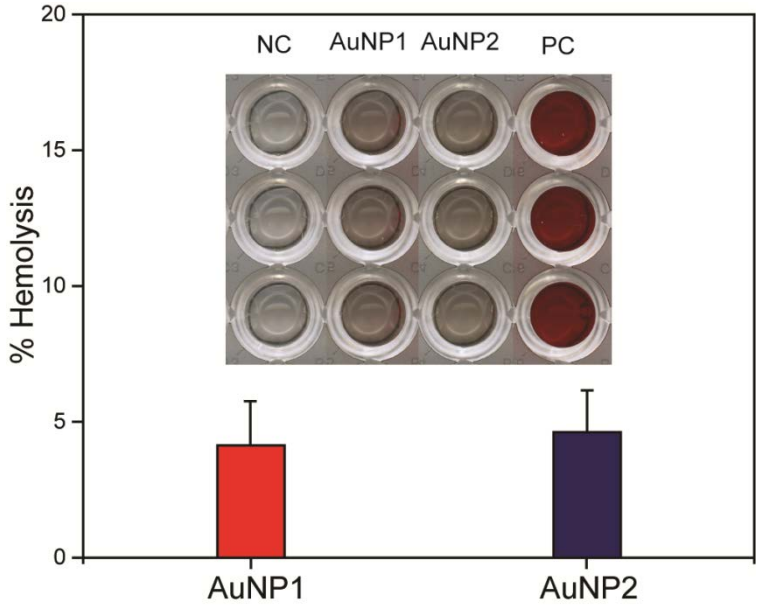

Figure 7.5. Hemolytic activities of AuNP **1** and **2** (1 μM each) after 30 min of incubation with purified RBCs at 37 °C. % Hemolysis was calculated using water as positive control. All experiments were performed in triplicate. Error bars represent standard deviation.; NC = negative control (PBS); PC = positive control (water)

7.3. Conclusions

We have developed a new pH-responsive zwitterionic ligand based on the alkoxyphenyl acylsulfonamide group. Due to its precisely designed surface structure, zwitterionic AuNPs functionalized with this ligand reversibly becomes cationic at tumor pH, with concomitant enhancement of cellular uptake and cytotoxicity. This combination of pH-regulated cellular uptake and cytotoxicity makes this ligand design promising for imaging, delivery, and self-therapeutic applications.

7.4. Experimental Section

General: All the chemicals were purchased from Sigma-Aldrich or Fischer Scientific, unless otherwise specified. The chemicals were used as received. Dichloromethane (DCM) and tetrahydrofuran (THF) used as a solvent for chemical synthesis and dried according to standard procedures. The yields of the compounds reported here refer to the yields of spectroscopically pure compounds after purification. ^{1}H NMR spectra were recorded at 400 MHz on a Bruker AVANCE 400 machine.

Syntheses of Ligands:

Ligand 1:

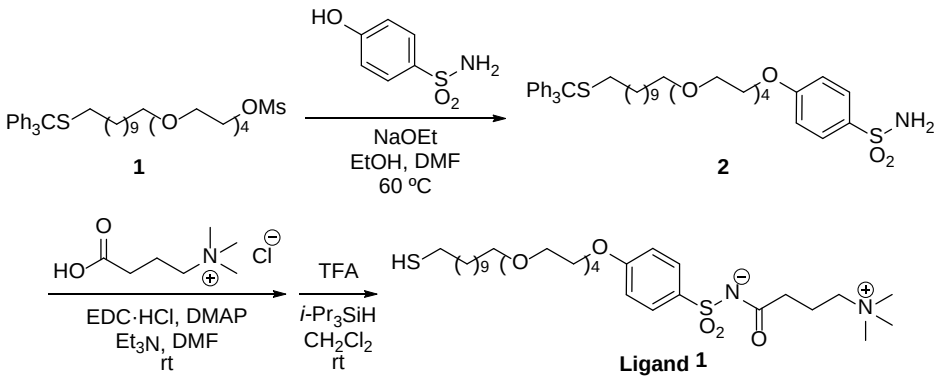

4-((1,1,1-Triphenyl-14,17,20,23-tetraoxa-2-thiapentacosan-25-yl)oxy)benzenesulfonamide (2). To a solution of 4-hydroxybenzenesulfonamide (332 mg, 1.92 mmol) and NaOEt (560 μL, 1.73 mmol, 21 % EtOH solution) in EtOH (3.0 mL) and DMF (1.5 mL) was added the solution of compound 1[22] (400 mg, 0.64 mmol) in DMF (1.5 mL) at rt. After being stirred at 60 °C for 18 h, EtOAc was added. The mixture was washed with sat. $NaHCO_3$ (× 3), H_2O and brine, and dried over $MgSO_4$. After concentration, the residue was purified by flash chromatography over silica gel with *n*-hexane–EtOAc (1:1 to 0:1) to give the desired compound 2 as yellow oil (443 mg, 89%). ^{1}H-NMR (400 MHz, $CDCl_3$) 1.19-1.44 (16H, m, -CH_2-), 1.55-1.61 (2H, m, -CH_2-), 2.15 (2H, t, *J* = 7.3 Hz, -SCH_2-),3.45 (2H, t, *J* = 6.9 Hz, -OCH_2-), 3.57-3.75 (12H, m, -OCH_2-), 3.89 (2H, t, *J* = 4.8 Hz, -OCH_2-), 4.19 (2H, s, *J* = 4.6 Hz -OCH_2-), 5.05 (2H, br s, -NH_2), 6.98 (2H, d, *J* = 8.9 Hz, Ar), 7.20-7.31 (9H, m, Ar), 7.41-7.44 (6H, m, Ar), 7.85 (2H, d, *J* = 8.9Hz,Ar). MALDI-MS: *m/z* calculated for $C_{44}H_{59}NNaO_7S_2$ $[M + Na]^+$ 800.363; found: 800.459.

({4-[(23-Mercapto-3,6,9,12-tetraoxatricosyl)oxy]phenyl}sulfonyl)[4-(trimethylammonio)butanoyl]amide (Ligand 1). To a solution of compound 2 (1.0 g, 1.3 mmol), (3-carboxypropyl)-trimethylammonium chloride (519 mg, 2.86 mmol), DMAP (32 mg, 0.26 mmol) and triethylamine (751 μL, 5.2 mmol) in DMF (6.5 mL) was added EDC·HCl (997 mg, 5.2 mmol). After being stirred at rt for 1 days, EtOAc was added. The mixture was washed with the mixture of 0.1 M HCl and brine (1:1, × 2), and dried over $MgSO_4$. After concentration, the residue was suspended in the mixture of *n*-hexane and Et_2O (1:1), and sonicated. After centrifugation, the supernatant was removed. This *n*-hexane–Et_2O-washing step was repeated three times. And residue was washed with Et_2O for more three times. To a solution of residue in CH_2Cl_2 (6.0 mL) were added trifluoroacetic acid (2.0 mL) and triisopropylsilane (0.5 mL). After being stirred at rt for 10 min, the mixture was concentrated *in vacuo*. The residue was suspended in *n*-hexane, and sonicated. After centrifugation, the supernatant was removed. This *n*-hexane-washing step was repeated five times to give the desired Ligand 1 as pale yellow oil (266 mg,

31%). ^{1}H-NMR (400 MHz, $CDCl_3$) 1.19-1.38 (14H, m, -CH_2-), 1.53-1.63 (4H, m, -CH_2-), 1.97 (2H, br s, -CH_2-), 2.49-2.54 (4H, m, -SCH_2-, -$COCH_2$-), 3.10 (9H, s, CH_3), 3.31 (2H, br s, -CH_2-N^+), 3.44 (2H, t, *J* = 6.9 Hz, -OCH_2-), 3.56-3.71 (12H, m, -OCH_2-), 3.86 (2H, br t, *J* = 4.0 Hz, -OCH_2-), 4.11 (2H, br t, *J* = 4.0 Hz, -OCH_2-), 6.99 (2H, d, *J* = 8.7 Hz, Ar), 7.91 (2H, d, *J* = 8.7Hz, Ar). MALDI-MS: *m/z* calculated for $C_{32}H_{59}N_2O_8S_2$ $[M + H]^+$ 663.371; found: 663.398.

Ligand 2:

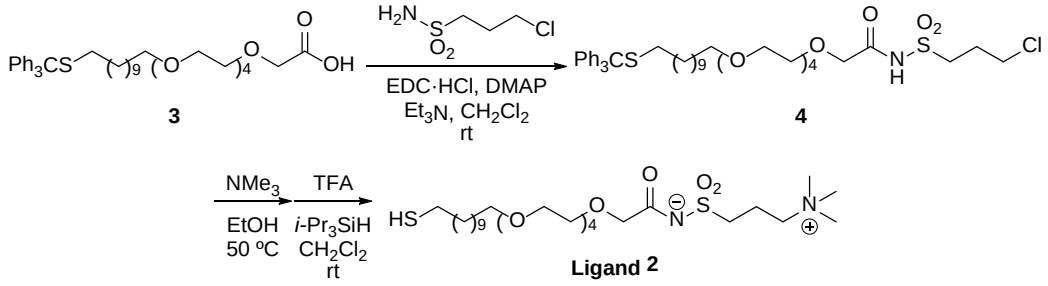

N-[(3-Chloropropyl)sulfonyl]-1,1,1-triphenyl-14,17,20,23,26-pentaoxa-2-thiaoctacosan-28-amide (4). To a solution of compound 3[23] (500 mg, 0.73mmol), 3-chloropropanesulfonamide[24] (230 mg, 1.5 mmol), *N*,*N*-dimethyl-4-aminopyridine (DMAP) (17.9 mg, 0.14 mmol) and triethylamine (211 μL, 1.5 mmol) in CH_2Cl_2 (7.3 mL) was added 1-(3-dimethylaminopropyl)-3-ethylcarbodiimide hydrochloride (EDC·HCl) (280 mg, 1.46 mmol). After being stirred at rt for 2.5 h, EtOAc was added. The mixture was washed with 0.1 M HCl and brine, and dried over $MgSO_4$. After concentration, the residue was purified by flash chromatography over silica gel with *n*-hexane–EtOAc–AcOH (50:49:1 to 0:99:1) to give the desired compound 4 as colorless oil (399 mg, 66%). ^{1}H-NMR (400 MHz, $CDCl_3$) 1.13-1.44 (14H, m, -CH_2-), 1.55-1.62 (4H, m, -CH_2-), 2.15 (2H, t, *J* = 7.3 Hz, -SCH_2-), 2.31-2.37 (2H, m, -CH_2-), 3.46 (2H, t, *J* = 6.9 Hz, -OCH_2-), 3.58-3.77 (20H, m, -OCH_2-), 4.14 (2H, s, -OCH_2-), 7.18-7.32 (9H, m, Ar), 7.41-7.44 (6H, m, Ar), 10.36 (1H, br s, NH). MALDI-MS: *m/z* calculated for $C_{43}H_{62}ClNNaO_8S_2$ $[M + Na]^+$ 842.350; found: 842.544.

26-Mercapto-N-{[3-(trimethylamino)propyl]sulfonyl}-3,6,9,12,15-pentaoxahexacosan-1-amide (Ligand 2) The compound 4 (200 mg, 0.12 mmol) was dissolved in trimethylamine-EtOH

(33 wt%, 1.16 mL). After being stirred at 50 °C for 3 days, CH_2Cl_2 and EtOAc were added to the reaction mixture. The mixture was washed with the mixture of 1M HCl and brine (1:1), and dried over $MgSO_4$. After concentration, the residue was suspended in *n*-hexane, and sonicated. After centrifugation, the supernatant was removed. This *n*-hexane-washing step was repeated five times. To a solution of residue in CH_2Cl_2 (3.0 mL) were added trifluoroacetic acid (1.0 mL) and triisopropylsilane (0.25 mL). After being stirred at rt for 10 min, the mixture was concentrated *in vacuo*. The residue was suspended in *n*-hexane, and sonicated. After centrifugation, the supernatant was removed. This *n*-hexane-washing step was repeated five times to give the desired compound Ligand 2 as pale yellow oil (43.5 mg, 30%). ^{1}H-NMR (400 MHz, $CDCl_3$) 1.28-1.41 (14H, m, -CH_2-), 1.54-1.66 (4H, m, -CH_2-), 2.38 (2H, br s, -CH_2-), 2.54 (2H, q, J = 7.5 Hz, -SCH_2-), 3.22 (9H, s, CH_3), 3.45 (2H, t, J = 6.9 Hz, -OCH_2-), 3.56-3.74 (20H, m, -OCH_2-), 4.20 (2H, s, -OCH_2-). MALDI-MS: *m/z* calculated for $C_{27}H_{57}N_2O_8S_2$ $[M + H]^+$ 601.356; found: 601.304.

Synthesis of Gold Nanoparticles and Characterization:

AuNP **1**:

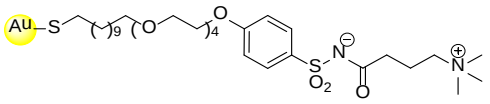

AuNP **1** was prepared through place-exchange reaction of 1-pentanethiolprotected 2 nm gold nanoparticle (Au-C5) according to previously reported procedure.[25] Briefly, to the solution of Au-C5 (10 mg) in CH_2Cl_2 (1 mL) was added the solution of ligand 1 (30 mg) in CH_2Cl_2:MeOH (4:1, 3 mL). After being stirred at rt for 24 h, the solvent was evaporated *in vacuo*. After nanoparticle residue was washed with EtOAc (10 mL × 3), the nanoparticle was immediately dissolved in MilliQ water and the aqueous solution of the nanoparticle was purified by dialysis with distilled water using SnakeSkin™ Dialysis Tubing (Thermo Scientific, 10,000 MWCO).;

MALDI-MS: *m/z* calculated for $C_{32}H_{59}N_2O_8S_2$ $[M + H]^+$ 663.371; found: 663.612., *m/z* calculated for $C_{37}H_{69}N_2O_8S_3$ $[M + S\text{-}C_5H_{11}]^+$ 765.421; found: 765.718.

AuNP **2**:

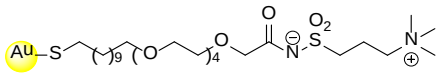

AuNP **2** was prepared by following the similar procedure with AuNP **1**.; MALDI-MS: *m/z* calculated for $C_{27}H_{57}N_2O_8S_2$ $[M + H]^+$ 601.355; found: 601.443., *m/z* calculated for $C_{32}H_{67}N_2O_8S_3$ $[M + S\text{-}C_5H_{11}]^+$ 703.405; found: 703.659.

Cell Culture: HeLa cells were cultured in low glucose Dulbecco's Modified Eagle's Medium (Life technologies, 10567-022) supplemented with 10% fetal bovine serum (Atlanta Biologicals, S11550) and 1% antibiotics (Cellgro, 30-004-CI). Cells were maintained at 37 °C under a humidified atmosphere with 5% CO_2 and subcultured once every four days.

Cellular uptake: 30,000 cells/well were plated in a 24-well plate prior to the experiment. On the following day, cells were washed one time with phosphate buffered saline (PBS) and incubated with AuNP **1** and AuNP **2** (1 μM each) in 10% serum containing media (pH 7.4, 6.6, and 6.0) for 3 h at 37 °C. After incubation, cells were washed three times with PBS and lysis buffer was added to each well. All lysed cell samples were then further processed for ICP-MS analysis (*vide infra*) to determine the intracellular amount of gold. Uptake experiments were performed independently at least two times and each experiment was comprised of three replicates.

Sample preparation for ICP-MS and ICP-MS instrumentation: After cellular uptake, the lysed cells were transferred to 15 mL centrifuge tubes. 0.5 mL of fresh *aqua regia* (highly corrosive and must be used with extreme caution!) were added to each sample. Each sample was then diluted to 10 mL with de-ionized water. A series of gold standard solutions (0, 0.2, 0.5, 1, 2, 5, 10, and 20 ppb) were prepared before the ICP-MS measurements. Each gold standard solution

also contained 5% *aqua regia*. The gold standard solutions and cellular uptake sample solutions were measured on a Perkin-Elmer NexION 300X ICP mass spectrometer. ^{197}Au was measured under standard mode. Operating conditions are listed as below: nebulizer flow rate: 0.95-1 L/min; rf power: 1600 W; plasma Ar flow rate: 18 L/min; dwell time: 50 ms.

Cell proliferation assay: The cell proliferation was determined by alamar blue assay according to manufacturer protocol (Life Technologies, DAL1100). HeLa cells (5000 cells/well) were seeded in a 96-well plate 24 hours prior to the experiment. On the following day, the old media was aspirated and the cells were washed with PBS for one time. AuNP **1** and AuNP **2** (1 μM each) were then incubated with the cells in 10% serum containing media (pH 7.4, 6.6, and 6.0) for 72 h at 37 °C. After the incubation period, the cells were washed three times with PBS and 220 μL of 10 % alamar blue solution in serum containing media was added to each well and cells were further incubated at 37 ˚C for 4 hours. After 4 hours, 200 μL of solution from each well were taken out and loaded in a 96- well black microplate. Red fluorescence, resulting from the reduction of the alamar blue solution by viable cells was measured (Ex: 560 nm, Em: 590 nm) on a SpectroMax M2 microplate reader (Molecular Device). Viability (%) of NP-treated cells was calculated taking untreated cells as 100 % viable. All proliferation experiments were performed independently at least three times and each experiment was comprised of six replicates.

Hemolysis: Citrate-stabilized human whole blood (pooled, mixed gender) was purchased from Bioreclamation LLC, NY and processed as soon as received. 10 mL of phosphate buffered saline (PBS) was added to the blood and centrifuged at 5000 r.pm. for 5 minutes. The supernant was carefully discarded and the red blood cells (RBCs) were dispersed in 10 mL of PBS. This step was repeated at least five times. The purified RBCs were diluted in 10 mL of PBS and kept on ice during the sample preparation. 0.1 mL of RBC solution was added to 0.4 mL of nanoparticle (NP) solution in PBS in 1.5 mL centrifuge tube (Fisher) and mixed gently by pipetting. RBCs incubated with PBS and water were used as negative and positive control, respectively. All NP samples as well as controls were prepared in triplicate. The mixture was

incubated at 37 ˚C for 30 minutes while shaking at 150 r.p.m. After incubation period, the solution was centrifuged at 4000 r.p.m. for 5 minutes and 100 μL of supernatant was transferred to a 96-well plate. The absorbance value of the supernatant was measured at 570 nm using a microplate reader (SpectraMax M2, Molecular devices) with absorbance at 655 nm as a reference. The percent hemolysis was calculated using the following formula:

% Hemolysis = ((sample absorbance-negative control absorbance)) / ((positive control absorbance-negative control absorbance)) × 100.

7.5. References

1. (a) Gatenby, R. A.; Gillies, R. J. *Nat. Rev. Cancer* **2004**, *4*, 891. (b) Cardone, R. A.; Casavola, V.; Reshkin, S. J. *Nat. Rev. Cancer* **2005**, *5*, 786.

2. (a) Tannock, I. F.; Rotin, D. *Cancer Res.* **1989**, *49*, 4373. (b) Storrie, H.; Mooney, D. J. *Adv. Drug Delivery Rev.* **2006**, *58*, 500. (c) Randolph, L. M.; Chien, M. P.; Gianneschi, N. C. *Chem. Sci.* **2012**, *3*, 1363. (d) Mura, S.; Nicolas, J.; Couvreur, P. *Nat. Mater.* **2013**, *12*, 991.

3. (a) Du, J. Z.; Sun, T. M.; Song, W. J.; Wu, J.; Wang, J. *Angew. Chem. Int. Ed.* **2010**, *49*, 3621. (b) Du, J. Z.; Du, X. J.; Mao, C. Q.; Wang, J. *J. Am. Chem. Soc.* **2011**, *133*, 17560.

4. (a) Koren, E.; Apte, A.; Jani, A.; Torchilin, V. P. *J. Control. Release* **2012**, *160*, 264. (b) Nam, J.; Won, N.; Jin, H.; Chung, H.; Kim, S. *J. Am. Chem. Soc.* **2009**, *131*, 13639.

5. Zhou, K. J.; Wang, Y. G.; Huang, X. N.; Luby-Phelps, K.; Sumer, B. D.; Gao, J. M. *Angew. Chem. Int. Ed.* **2011**, *50*, 6109.

6. (a) Lee, E. S.; Na, K.; Bae, Y. H. *Nano Lett.* **2005**, *5*, 325. (b) Lee, E. S.; Gao, Z. G.; Kim, D.; Park, K.; Kwon, I. C.; Bae, Y. H. *J. Control. Release* **2008**, *129*, 228. (c) Wang, Y.; Zhou, K.; Huang, G.; Hensley, C.; Huang, X.; Ma, X.; Zhao, T.; Sumer, B. D.; DeBerardinis, R. J.; Gao, J. *Nat Mater* **2014**, *13*, 204.

7. (a) Holmlin, R. E.; Chen, X. X.; Chapman, R. G.; Takayama, S.; Whitesides, G. M. *Langmuir* **2001**, *17*, 2841. (b) Aldeek, F.; Muhammed, M. A. H.; Palui, G.; Zhan, N.; Mattoussi, H. *ACS Nano* **2013**, *7*, 2509–2521. (c) Zhan, N.; Palui, G.; Safi, M.; Ji, X.; Mattoussi, H. *J. Am. Chem. Soc.* **2013**, *135*, 13786–13795. (d) Bogart, L. K.; Pourroy, G.; Murphy, C. J.; Puntes, V.; Pellegrino, T.; Rosenblum, D.; Peer, D.; Levy, R. *Acs Nano* **2014**, *8*, 3107. (e) Moyano, D. F.; Saha, K.; Prakash, G.; Yan, B.; Kong, H.; Yazdani, M.; Rotello, V. M. *ACS Nano* **2014**, *8*, 6748.

8. Arvizo, R. R.; Miranda, O. R.; Moyano, D. F.; Walden, C. A.; Giri, K.; Bhattacharya, R.; Robertson, J. D.; Rotello, V. M.; Reid, J. M.; Mukherjee, P. *Plos One* **2011**, *6*, e24374.

9. Kim, C. K.; Ghosh, P.; Pagliuca, C.; Zhu, Z.-J.; Menichetti, S.; Rotello, V. M. *J. Am. Chem. Soc.* **2009**, *131*, 1360–1361.

10. Arvizo, R. R.; Miranda, O. R.; Thompson, M. A.; Pabelick, C. M.; Bhattacharya, R.; Robertson, J. D.; Rotello, V. M.; Prakash, Y. S.; Mukherjee, P. *Nano Lett.* **2010**, *10*, 2543.

11. Chompoosor, A.; Saha, K.; Ghosh, P. S.; Macarthy, D. J.; Miranda, O. R.; Zhu, Z. J.; Arcaro, K. F.; Rotello, V. M. *Small* **2010**, *6*, 2246.

12. Sundaram, H. S.; Ella-Menye, J. R.; Brault, N. D.; Shao, Q.; Jiang, S. Y. *Chem. Sci.* **2014**, *5*, 200

13. Jin, Q.; Xu, J. P.; Ji, J.; Shen, J. C. *Chem. Commun.* **2008**, 3058.

14. Pillai, P. P.; Huda, S.; Kowalczyk, B.; Grzybowski, B. A. *J. Am. Chem. Soc.* **2013**, *135*, 6392.

15. Chakravarty, P. K.; Naylor, E. M.; Chen, A.; Chang, R. S. L.; Chen, T. B.; Faust, K. A.; Lotti, V. J.; Kivlighn, S. D.; Gable, R. A.; Zingaro, G. J.; Schorn, T. W.; Schaffer, L. W.; Broten, T. P.; Siegl, P. K. S.; Patchett, A. A.; Greenlee, W. J. *J. Med. Chem.* **1994**, *37*, 4068.

16. Hong, R.; Fischer, N. O.; Verma, A.; Goodman, C. M.; Emrick, T.; Rotello, V. M. *J. Am. Chem. Soc.* **2004**, *126*, 739.

17. Hostetler, M. J.; Wingate, J. E.; Zhong, C. J.; Harris, J. E.; Vachet, R. W.; Clark, M. R.; Londono, J. D.; Green, S. J.; Stokes, J. J.; Wignall, G. D.; Glish, G. L.; Porter, M. D.; Evans, N. D.; Murray, R. W. *Langmuir* **1998**, *14*, 17.

18. Jiang, Y. T.; Andrews, S. W.; Condroski, K. R.; Buckman, B.; Serebryany, V.; Wenglowsky, S.; Kennedy, A. L.; Madduru, M. R.; Wang, B.; Lyon, M.; Doherty, G. A.; Woodard, B. T.; Lemieux, C.; Do, M. G.; Zhang, H. L.; Ballard, J.; Vigers, G.; Brandhuber, B. J.; Stengel, P.; Josey, J. A.; Beigelman, L.; Blatt, L.; Seiwert, S. D. *J. Med. Chem.* **2014**, *57*, 1753.

19. Liu, X. S.; Chen, Y. J.; Li, H.; Huang, N.; Jin, Q.; Ren, K. F.; Ji, J. *Acs Nano* **2013**, *7*, 6244.

20. Rother, R. P.; Bell, L.; Hillmen, P.; Gladwin, M. T. *JAMA* **2005**, *293*, 1653.

21. Saha, K.; Moyano, D. F.; Rotello, V. M. *Mater Horiz* **2014**, *1*, 102.

22. Miranda, O. R.; Chen, H. T.; You, C. C.; Mortenson, D. E.; Yang, X. C.; Bunz, U. H. F.; Rotello, V. M. *J. Am. Chem. Soc.* **2010**, *132*, 5285.

23. Orner, B. P.; Derda, R.; Lewis, R. L.; Thomson, J. A.; Kiessling, L. L. *J. Am. Chem. Soc.* **2004**, *126*, 10808.

24. Li, J. Q.; Smith, D.; Wong, H. S.; Campbell, J. A.; Meanwell, N. A.; Scola, P. M. *Synlett* **2006**, 725.

25. Moyano, D. F.; Duncan, B.; Rotello, V. M. *Methods Mol. Biol.* **2013**, *1025*, 3.

BIBLIOGRAPHY

Agasti, S. S.; Chompoosor, A.; You, C. C.; Ghosh, P.; Kim, C. K.; Rotello, V. M. *J. Am. Chem. Soc.* **2009**, *131*, 5728.

Agasti, S. S.; Rana, S.; Park, M. H.; Kim, C. K.; You, C. C.; Rotello, V. M. *Adv. Drug Delivery Rev.* **2010**, *62*, 316.

Aggarwal, P.; Hall, J. B.; McLeland, C. B.; Dobrovolskaia, M. A.; McNeil, S. E. *Adv. Drug Delivery Rev.* **2009**, *61*, 428.

Aguirre, J. D.; Angeles-Boza, A. M.; Chouai, A.; Pellois, J. P.; Turro, C.; Dunbar, K. R. *J. Am. Chem. Soc.* **2009**, *131*, 11353.

Aldeek, F.; Muhammed, M. A. H.; Palui, G.; Zhan, N. Q.; Mattoussi, H. *Acs Nano* **2013**, *7*, 2509.

Alexis, F.; Pridgen, E.; Molnar, L. K.; Farokhzad, O. C. *Mol. Pharm.* **2008**, *5*, 505.

Al-Hajaj, N. A.; Moquin, A.; Neibert, K. D.; Soliman, G. M.; Winnik, F. M.; Maysinger, D. *Acs Nano* **2011**, *5*, 4909.

Al-Jamal, W. T.; Kostarelos, K. *Acc. Chem. Res.* **2011**, *44*, 1094.

Alkilany, A. M.; Nagaria, P. K.; Hexel, C. R.; Shaw, T. J.; Murphy, C. J.; Wyatt, M. D. *Small* **2009**, *5*, 701.

Allen, T. M.; Cullis, P. R. *Science* **2004**, *303*, 1818.

Allen, T. M.; Cullis, P. R. *Adv. Drug Delivery Rev.* **2013**, *65*, 36.

Andreeva, Z. I.; Nesterenko, V. F.; Fomkina, M. G.; Ternovsky, V. I.; Suzina, N. E.; Bakulina, A. Y.; Solonin, A. S.; Sineva, E. V. *BBA-Biomembranes* **2007**, *1768*, 253.

Araki, N.; Johnson, M. T.; Swanson, J. A. *J. Cell. Biol.* **1996**, *135*, 1249.

Arnida; Malugin, A.; Ghandehari, H. *J. Appl. Toxicol.* **2010**, *30*, 212.

Arvizo, R. R.; Giri, K.; Moyano, D.; Miranda, O. R.; Madden, B.; McCormick, D. J.; Bhattacharya, R.; Rotello, V. M.; Kocher, J. P.; Mukherjee, P. *Plos One* **2012**, *7*.

Arvizo, R. R.; Miranda, O. R.; Moyano, D. F.; Walden, C. A.; Giri, K.; Bhattacharya, R.; Robertson, J. D.; Rotello, V. M.; Reid, J. M.; Mukherjee, P. *Plos One* **2011**, *6*, e24374.

Arvizo, R. R.; Miranda, O. R.; Thompson, M. A.; Pabelick, C. M.; Bhattacharya, R.; Robertson, J. D.; Rotello, V. M.; Prakash, Y. S.; Mukherjee, P. *Nano Lett.* **2010**, *10*, 2543.

Asefa, T.; Duncan, C. T.; Sharma, K. K. *Analyst* **2009**, *134*, 1980.

Aslam, M.; Fu, L.; Su, M.; Vijayamohanan, K.; Dravid, V. P. *J. Mater. Chem.* **2004**, *14*, 1795.

Baier, G.; Costa, C.; Zeller, A.; Baumann, D.; Sayer, C.; Araujo, P. H. H.; Mailander, V.; Musyanovych, A.; Landfester, K. *Macromol. Biosci.* **2011**, *11*, 628.

Bajaj, A.; Rana, S.; Miranda, O. R.; Yawe, J. C.; Jerry, D. J.; Bunz, U. H. F.; Rotello, V. M. *Chem. Sci.* **2010**, *1*, 134.

Banquy, X.; Suarez, F.; Argaw, A.; Rabanel, J. M.; Grutter, P.; Bouchard, J. F.; Hildgen, P.; Giasson, S. *Soft Matter* **2009**, *5*, 3984.

Bareford, L. A.; Swaan, P. W. *Adv. Drug Delivery Rev.* **2007**, *59*, 748.

Bar-Ilan, O.; Albrecht, R. M.; Fako, V. E.; Furgeson, D. Y. *Small* **2009**, *5*, 1897.

Barran-Berdon, A. L.; Pozzi, D.; Caracciolo, G.; Capriotti, A. L.; Caruso, G.; Cavaliere, C.; Riccioli, A.; Palchetti, S.; Lagana, A. *Langmuir* **2013**, *29*, 6485.

Bhargava, S. K.; Booth, J. M.; Agrawal, S.; Coloe, P.; Kar, G. *Langmuir* **2005**, *21*, 5949.

Bhattacharyya, S.; Singh, R. D.; Pagano, R.; Robertson, J. D.; Bhattacharya, R.; Mukherjee, P. *Angew. Chem. Int. Ed.* **2012**, *51*, 1563.

Bogart, L. K.; Pourroy, G.; Murphy, C. J.; Puntes, V.; Pellegrino, T.; Rosenblum, D.; Peer, D.; Levy, R. *Acs Nano* **2014**, *8*, 3107.

Brandenberger, C.; Muhlfeld, C.; Ali, Z.; Lenz, A. G.; Schmid, O.; Parak, W. J.; Gehr, P.; Rothen-Rutishauser, B. *Small* **2010**, *6*, 1669.

Brannon-Peppas, L.; Blanchette, J. O. *Adv. Drug Delivery Rev.* **2012**, *64*, 206.

Brust, M.; Fink, J.; Bethell, D.; Schiffrin, D. J.; Kiely, C. *J. Chem. Soc., Chem. Commun.* **1995**, 1655.

Cao, Z. Q.; Jiang, S. Y. *Nano Today* **2012**, *7*, 404.

Cardone, R. A.; Casavola, V.; Reshkin, S. J. *Nat. Rev. Cancer* **2005**, *5*, 786.

Casals, E.; Puntes, V. F. *Nanomedicine* **2012**, *7*, 1917.

Cedervall, T.; Lynch, I.; Foy, M.; Berggad, T.; Donnelly, S. C.; Cagney, G.; Linse, S.; Dawson, K. A. *Angew. Chem. Int. Ed.* **2007**, *46*, 5754.

Cedervall, T.; Lynch, I.; Lindman, S.; Berggard, T.; Thulin, E.; Nilsson, H.; Dawson, K. A.; Linse, S. *Proc. Natl. Acad. Sci. U.S.A.* **2007**, *104*, 2050.

Chakravarty, P. K.; Naylor, E. M.; Chen, A.; Chang, R. S. L.; Chen, T. B.; Faust, K. A.; Lotti, V. J.; Kivlighn, S. D.; Gable, R. A.; Zingaro, G. J.; Schorn, T. W.; Schaffer, L. W.; Broten, T. P.; Siegl, P. K. S.; Patchett, A. A.; Greenlee, W. J. *J. Med. Chem.* **1994**, *37*, 4068.

Chang, C. *J. Autoimmun.* **2010**, *34*, J234.

Chauhan, V. P.; Jain, R. K. *Nat. Mater.* **2013**, *12*, 958.

Chen, J.; Li, G.; Lu, J.; Chen, L.; Huang, Y.; Wu, H. L.; Zhang, J. X.; Lu, D. R. *Biochem. Biophys. Res. Commun.* **2006**, *347*, 931.

Chen, M.; Liu, J. P.; Sun, S. H. *J. Am. Chem. Soc.* **2004**, *126*, 8394.

Chen, S. W.; Templeton, A. C.; Murray, R. W. *Langmuir* **2000**, *16*, 3543.

Chen, Y.; McMillan-Ward, E.; Kong, J.; Israels, S. J.; Gibson, S. B. *Cell Death Differ.* **2008**, *15*, 171.

Chevallet, M.; Luche, S.; Rabilloud, T. *Nat. Protoc.* **2006**, *1*, 1852.

Chithrani, B. D.; Chan, W. C. W. *Nano Lett.* **2007**, *7*, 1542.

Chithrani, B. D.; Ghazani, A. A.; Chan, W. C. W. *Nano Lett.* **2006**, *6*, 662.

Cho, E. C.; Au, L.; Zhang, Q.; Xio, Y. *Small* **2010**, *6*, 517.

Cho, E. C.; Xie, J. W.; Wurm, P. A.; Xia, Y. N. *Nano Lett.* **2009**, *9*, 1080.

Cho, E. C.; Zhang, Q.; Xia, Y. N. *Nat. Nanotechnol.* **2011**, *6*, 385.

Cho, K. J.; Wang, X.; Nie, S. M.; Chen, Z.; Shin, D. M. *Clin. Cancer Res.* **2008**, *14*, 1310.

Cho, W. S.; Cho, M. J.; Jeong, J.; Choi, M.; Cho, H. Y.; Han, B. S.; Kim, S. H.; Kim, H. O.; Lim, Y. T.; Chung, B. H.; Jeong, J. *Toxicol. Appl. Pharmacol.* **2009**, *236*, 16.

Choi, J.; Reipa, V.; Hitchins, V. M.; Goering, P. L.; Malinauskas, R. A. *Toxicol. Sci.* **2011**, *123*, 133.

Chompoosor, A.; Saha, K.; Ghosh, P. S.; Macarthy, D. J.; Miranda, O. R.; Zhu, Z. J.; Arcaro, K. F.; Rotello, V. M. *Small* **2010**, *6*, 2246.

Conner, S. D.; Schmid, S. L. *Nature* **2003**, *422*, 37.

Connor, E. E.; Mwamuka, J.; Gole, A.; Murphy, C. J.; Wyatt, M. D. *Small* **2005**, *1*, 325.

Danhier, F.; Feron, O.; Preat, V. *J. Control. Release* **2010**, *148*, 135.

Dausend, J.; Musyanovych, A.; Dass, M.; Walther, P.; Schrezenmeier, H.; Landfester, K.; Mailander, V. *Macromol. Biosci.* **2008**, *8*, 1135.

Davis, M. E.; Chen, Z.; Shin, D. M. *Nat. Rev. Drug Discov.* **2008**, *7*, 771.

Davis, M. E.; Zuckerman, J. E.; Choi, C. H. J.; Seligson, D.; Tolcher, A.; Alabi, C. A.; Yen, Y.; Heidel, J. D.; Ribas, A. *Nature* **2010**, *464*, 1067.

De, M.; Ghosh, P. S.; Rotello, V. M. *Adv. Mater.* **2008**, *20*, 4225.

Dell'Orco, D.; Lundqvist, M.; Oslakovic, C.; Cedervall, T.; Linse, S. *Plos One* **2010**, *5*.

Ding, Y.; Jiang, Z. W.; Saha, K.; Kim, C. S.; Kim, S. T.; Landis, R. F.; Rotello, V. M. *Mol. Ther.* **2014**, *22*, 1075.

Discher, D. E.; Eisenberg, A. *Science* **2002**, *297*, 967.

Doane, T.; Burda, C. *Adv. Drug Delivery Rev.* **2013**, *65*, 607.

Dobrovolskaia, M. A.; Patri, A. K.; Zheng, J. W.; Clogston, J. D.; Ayub, N.; Aggarwal, P.; Neun, B. W.; Hall, J. B.; McNeil, S. E. *Nanomedicine* **2009**, *5*, 106.

dos Santos, T.; Varela, J.; Lynch, I.; Salvati, A.; Dawson, K. A. *Plos One* **2011**, *6*, e24438.

Du, J. Z.; Du, X. J.; Mao, C. Q.; Wang, J. *J. Am. Chem. Soc.* **2011**, *133*, 17560.

Du, J. Z.; Sun, T. M.; Song, W. J.; Wu, J.; Wang, J. *Angew. Chem. Int. Ed.* **2010**, *49*, 3621.

Duncan, B.; Kim, C.; Rotello, V. M. *J. Control. Release* **2010**, *148*, 122.

Dykman, L.; Khlebtsov, N. *Chem. Soc. Rev.* **2012**, *41*, 2256.

Faraday, M. *Philos. Trans. R. Soc. London,* **1857**, *147*, 145.

Fink, J.; Kiely, C. J.; Bethell, D.; Schiffrin, D. J. *Chem. Mater.* **1998**, *10*, 922.

Fleischer, C. C.; Kumar, U.; Payne, C. K. *Biomater. Sci.* **2013**, *1*, 975.

Franca, A.; Aggarwal, P.; Barsov, E. V.; Kozlov, S. V.; Dobrovolskaia, M. A.; Gonzalez-Fernandez, A. *Nanomedicine* **2011**, *6*, 1175.

Frens, G. *Nature: Phys. Sci.* **1973**, *241*, 20.

Fubini, B.; Ghiazza, M.; Fenoglio, I. *Nanotoxicology* **2010**, *4*, 347.

Fujimoto, L. M.; Roth, R.; Heuser, J. E.; Schmid, S. L. *Traffic* **2000**, *1*, 161.

Gatenby, R. A.; Gillies, R. J. *Nat. Rev. Cancer* **2004**, *4*, 891.

George, S. R.; O'Dowd, B. F.; Lee, S. R. *Nat. Rev. Drug Discov.* **2002**, *1*, 808.

Gessner, A.; Lieske, A.; Paulke, B.; Muller, R. *Eur J Pharm Biopharm* **2002**, *54*, 165.

Gessner, A.; Lieske, A.; Paulke, B. R.; Muller, R. H. *J Biomed Mater Res A* **2003**, *65*, 319.

Gessner, A.; Waicz, R.; Lieske, A.; Paulke, B. R.; Mader, K.; Muller, R. H. *Int. J. Pharm.* **2000**, *196*, 245.

Ghosh, P.; Yang, X. C.; Arvizo, R.; Zhu, Z. J.; Agasti, S. S.; Mo, Z. H.; Rotello, V. M. *J. Am. Chem. Soc.* **2010**, *132*, 2642.

Ghosh, P. S.; Kim, C. K.; Han, G.; Forbes, N. S.; Rotello, V. M. *Acs Nano* **2008**, *2*, 2213.

Gibson, J. D.; Khanal, B. P.; Zubarev, E. R. *J. Am. Chem. Soc.* **2007**, *129*, 11653.

Gindy, M. E.; Prud'homme, R. K. *Expert Opin. Drug Deliv.* **2009**, *6*, 865.

Goenka, S.; Sant, V.; Sant, S. *J. Control. Release* **2014**, *173*, 75.

Goodman, C. M.; McCusker, C. D.; Yilmaz, T.; Rotello, V. M. *Bioconjugate Chem.* **2004**, *15*, 897.

Grabar, K. C.; Freeman, R. G.; Hommer, M. B.; Natan, M. J. *Anal. Chem.* **1995**, *67*, 735.

Gratton, S. E. A.; Ropp, P. A.; Pohlhaus, P. D.; Luft, J. C.; Madden, V. J.; Napier, M. E.; DeSimone, J. M. *Proc. Natl. Acad. Sci. U.S.A.* **2008**, *105*, 11613.

Greish, K. *J. Drug Target.* **2007**, *15*, 457.

Gunther, E. C.; Von Bartheld, C. S.; Goodman, L. J.; Johnson, J. E.; Bothwell, M. *Neuroscience* **2000**, *100*, 569.

Haisma, H. J.; Kamps, J. A. A. M.; Kamps, G. K.; Plantinga, J. A.; Rots, M. G.; Bellu, A. R. *J. Gen. Virol.* **2008**, *89*, 1097.

Hamad, I.; Al-Hanbali, O.; Hunter, A. C.; Rutt, K. J.; Andresen, T. L.; Moghimi, S. M. *Acs Nano* **2010**, *4*, 6629.

Harush-Frenkel, O.; Debotton, N.; Benita, S.; Altschuler, Y. *Biochem. Biophys. Res. Commun.* **2007**, *353*, 26.

Hasegawa, S.; Hirashima, N.; Nakanishi, M. *Gene Ther.* **2001**, *8*, 1669.

Hauck, T. S.; Ghazani, A. A.; Chan, W. C. W. *Small* **2008**, *4*, 153.

He, X. X.; Nie, H. L.; Wang, K. M.; Tan, W. H.; Wu, X.; Zhang, P. F. *Anal. Chem.* **2008**, *80*, 9597.

Hiramatsu, H.; Osterloh, F. E. *Chem. Mater.* **2004**, *16*, 2509.

Holmlin, R. E.; Chen, X. X.; Chapman, R. G.; Takayama, S.; Whitesides, G. M. *Langmuir* **2001**, *17*, 2841.

Hong, R.; Fernandez, J. M.; Nakade, H.; Arvizo, R.; Emrick, T.; Rotello, V. M. *Chem. Commun.* **2006**, 2347.

Hong, R.; Fischer, N. O.; Verma, A.; Goodman, C. M.; Emrick, T.; Rotello, V. M. *J. Am. Chem. Soc.* **2004**, *126*, 739.

Hong, S.; Leroueil, P. R.; Majoros, I. J.; Orr, B. G.; Baker, J. R.; Holl, M. M. B. *Chem. Biol.* **2007**, *14*, 107.

Hoshino, A.; Fujioka, K.; Oku, T.; Suga, M.; Sasaki, Y. F.; Ohta, T.; Yasuhara, M.; Suzuki, K.; Yamamoto, K. *Nano Lett.* **2004**, *4*, 2163.

Hostetler, M. J.; Green, S. J.; Stokes, J. J.; Murray, R. W. *J. Am. Chem. Soc.* **1996**, *118*, 4212.

Hostetler, M. J.; Templeton, A. C.; Murray, R. W. *Langmuir* **1999**, *15*, 3782.

Hostetler, M. J.; Wingate, J. E.; Zhong, C. J.; Harris, J. E.; Vachet, R. W.; Clark, M. R.; Londono, J. D.; Green, S. J.; Stokes, J. J.; Wignall, G. D.; Glish, G. L.; Porter, M. D.; Evans, N. D.; Murray, R. W. *Langmuir* **1998**, *14*, 17.

Howes, M. T.; Mayor, S.; Parton, R. G. *Curr. Opin. Cell Biol.* **2010**, *22*, 519.

Hubbell, J. A.; Langer, R. *Nat. Mater.* **2013**, *12*, 963.

Huhn, D.; Kantner, K.; Geidel, C.; Brandholt, S.; De Cock, I.; Soenen, S. J. H.; Gil, P. R.; Montenegro, J. M.; Braeckmans, K.; Mullen, K.; Nienhaus, G. U.; Klapper, M.; Parak, W. J. *Acs Nano* **2013**, *7*, 3253.

Iyer, A. K.; Khaled, G.; Fang, J.; Maeda, H. *Drug Discovery Today* **2006**, *11*, 812.

Jamieson, E. R.; Lippard, S. J. *Chem. Rev.* **1999**, *99*, 2467.

Jiang, W.; Kim, B. Y. S.; Rutka, J. T.; Chan, W. C. W. *Nat. Nanotechnol.* **2008**, *3*, 145.

Jiang, Y. T.; Andrews, S. W.; Condroski, K. R.; Buckman, B.; Serebryany, V.; Wenglowsky, S.; Kennedy, A. L.; Madduru, M. R.; Wang, B.; Lyon, M.; Doherty, G. A.; Woodard, B. T.; Lemieux, C.; Do, M. G.; Zhang, H. L.; Ballard, J.; Vigers, G.; Brandhuber, B. J.; Stengel, P.; Josey, J. A.; Beigelman, L.; Blatt, L.; Seiwert, S. D. *J. Med. Chem.* **2014**, *57*, 1753.

Jin, Q.; Xu, J. P.; Ji, J.; Shen, J. C. *Chem. Commun.* **2008**, 3058.

Joglekar, M.; Roggers, R. A.; Zhao, Y. N.; Trewyn, B. G. *Rsc Advances* **2013**, *3*, 2454.

Jokerst, J. V.; Lobovkina, T.; Zare, R. N.; Gambhir, S. S. *Nanomedicine* **2011**, *6*, 715.

Kanaras, A. G.; Kamounah, F. S.; Schaumburg, K.; Kiely, C. J.; Brust, M. *Chem. Commun.* **2002**, 2294.

Kanasty, R.; Dorkin, J. R.; Vegas, A.; Anderson, D. *Nat. Mater.* **2013**, *12*, 967.

Kang, B.; Mackey, M. A.; El-Sayed, M. A. *J. Am. Chem. Soc.* **2010**, *132*, 1517.

Karakoti, A. S.; Das, S.; Thevuthasan, S.; Seal, S. *Angew. Chem. Int. Ed.* **2011**, *50*, 1980.

Khandelwal, P.; Ruiz, W. G.; Apodaca, G. *Embo J.* **2010**, *29*, 1961.

Khlebtsov, N.; Dykman, L. *Chem. Soc. Rev.* **2011**, *40*, 1647.

Kim, B.; Han, G.; Toley, B. J.; Kim, C. K.; Rotello, V. M.; Forbes, N. S. *Nat. Nanotechnol.* **2010**, *5*, 465.

Kim, C.; Agasti, S. S.; Zhu, Z. J.; Isaacs, L.; Rotello, V. M. *Nat. Chem.* **2010**, *2*, 962.

Kim, C. K.; Ghosh, P.; Pagliuca, C.; Zhu, Z. J.; Menichetti, S.; Rotello, V. M. *J. Am. Chem. Soc.* **2009**, *131*, 1360.

Kim, K. J.; Malik, A. B. *Am. J. Physiol. Lung Cell Mol. Physiol.* **2003**, *284*, L247.

Kim, S. T.; Saha, K.; Kim, C.; Rotello, V. M. *Acc. Chem. Res.* **2013**, *46*, 681.

Kopecek, J. *Adv. Drug Delivery Rev.* **2013**, *65*, 49.

Koren, E.; Apte, A.; Jani, A.; Torchilin, V. P. *J. Control. Release* **2012**, *160*, 264.

Koynova, R.; Tenchov, B.; Wang, L.; MacDonald, R. C. *Mol. Pharm.* **2009**, *6*, 951.

Kreuter, J.; Liehl, E.; Berg, U.; Soliva, M.; Speiser, P. P. *Vaccine* **1988**, *6*, 253.

Kumari, S.; Swetha, M. G.; Mayor, S. *Cell Res.* **2010**, *20*, 256.

Kwon, T.; Woo, H. J.; Kim, Y. H.; Lee, H. J.; Park, K. H.; Park, S.; Youn, B. *J. Nanosci. Nanotechnol.* **2012**, *12*, 6168.

Langer, R.; Tirrell, D. A. *Nature* **2004**, *428*, 487.

Lanone, S.; Boczkowski, J. *Curr. Mol. Med.* **2006**, *6*, 651.

Lee, E. S.; Gao, Z. G.; Kim, D.; Park, K.; Kwon, I. C.; Bae, Y. H. *J. Control. Release* **2008**, *129*, 228.

Lee, E. S.; Na, K.; Bae, Y. H. *Nano Lett.* **2005**, *5*, 325.

Leff, D. V.; Brandt, L.; Heath, J. R. *Langmuir* **1996**, *12*, 4723.

Leff, D. V.; Ohara, P. C.; Heath, J. R.; Gelbart, W. M. *J. Phys. Chem.* **1995**, *99*, 7036.

Leroueil, P. R.; Berry, S. A.; Duthie, K.; Han, G.; Rotello, V. M.; McNerny, D. Q.; Baker, J. R.; Orr, B. G.; Holl, M. M. B. *Nano Lett.* **2008**, *8*, 420.

Lesniak, A.; Fenaroli, F.; Monopoli, M. R.; Aberg, C.; Dawson, K. A.; Salvati, A. *Acs Nano* **2012**, *6*, 5845.

Li, J. Q.; Smith, D.; Wong, H. S.; Campbell, J. A.; Meanwell, N. A.; Scola, P. M. *Synlett* **2006**, 725.

Li, Y. T.; Liu, J.; Zhong, Y. J.; Zhang, J.; Wang, Z. Y.; Wang, L.; An, Y. L.; Lin, M.; Gao, Z. Q.; Zhang, D. S. *Int. J. Nanomedicine* **2011**, *6*, 2805.

Lin, Y. S.; Haynes, C. L. *Chem. Mater.* **2009**, *21*, 3979.

Lin, Y. S.; Haynes, C. L. *J. Am. Chem. Soc.* **2010**, *132*, 4834.

Lindman, S.; Lynch, I.; Thulin, E.; Nilsson, H.; Dawson, K. A.; Linse, S. *Nano Lett.* **2007**, *7*, 914.

Link, S.; El-Sayed, M. A. *J. Phys. Chem. B* **1999**, *103*, 4212.

Liu, X. O.; Atwater, M.; Wang, J. H.; Huo, Q. *Colloids Surf. B* **2007**, *58*, 3.

Liu, X. S.; Chen, Y. J.; Li, H.; Huang, N.; Jin, Q.; Ren, K. F.; Ji, J. *Acs Nano* **2013**, *7*, 6244.

Liu, Y. P.; Tong, C.; Dispenzieri, A.; Federspiel, M. J.; Russell, S. J.; Peng, K. W. *Cancer Gene Ther.* **2012**, *19*, 202.

Lorenz, S.; Hauser, C. P.; Autenrieth, B.; Weiss, C. K.; Landfester, K.; Mailander, V. *Macromol. Biosci.* **2010**, *10*, 1034.

Love, S. A.; Thompson, J. W.; Haynes, C. L. *Nanomedicine* **2012**, *7*, 1355.

Lu, S. L.; Duffin, R.; Poland, C.; Daly, P.; Murphy, F.; Drost, E.; MacNee, W.; Stone, V.; Donaldson, K. *Environ. Health Perspect.* **2009**, *117*, 241.

Lundqvist, M.; Stigler, J.; Elia, G.; Lynch, I.; Cedervall, T.; Dawson, K. A. *Proc. Natl. Acad. Sci. U.S.A.* **2008**, *105*, 14265.

Lunov, O.; Syrovets, T.; Loos, C.; Beil, J.; Delecher, M.; Tron, K.; Nienhaus, G. U.; Musyanovych, A.; Mailander, V.; Landfester, K.; Simmet, T. *Acs Nano* **2011**, *5*, 1657.

Lynch, I.; Dawson, K. A. *Nano Today* **2008**, *3*, 40.

Macia, E.; Ehrlich, M.; Massol, R.; Boucrot, E.; Brunner, C.; Kirchhausen, T. *Dev. Cell.* **2006**, *10*, 839.

Mahmoudi, M.; Lynch, I.; Ejtehadi, M. R.; Monopoli, M. P.; Bombelli, F. B.; Laurent, S. *Chem. Rev.* **2011**, *111*, 5610.

Maiorano, G.; Sabella, S.; Sorce, B.; Brunetti, V.; Malvindi, M. A.; Cingolani, R.; Pompa, P. P. *Acs Nano* **2010**, *4*, 7481.

Maiti, S.; Das, K.; Dutta, S.; Das, P. K. *Chemistry-a European Journal* **2012**, *18*, 15021.

Matyjaszewski, K. *Macromolecules* **2012**, *45*, 4015.

Matzinger, P. *Annu. rev. Immunol.* **1994**, *12*, 991.

Mayor, S.; Pagano, R. E. *Nat. Rev. Mol. Cell Biol.* **2007**, *8*, 603.

McCormack, C. L.; Lowe, A. B. *Acc. Chem. Res.* **2004**, *37*, 312.

McLendon, P. M.; Fichter, K. M.; Reineke, T. M. *Mol. Pharm.* **2010**, *7*, 738.

Meng, H.; Xia, T.; George, S.; Nel, A. E. *Acs Nano* **2009**, *3*, 1620.

Merchant, B. *Biologicals* **1998**, *26*, 49.

Milani, S.; Bombelli, F. B.; Pitek, A. S.; Dawson, K. A.; Radler, J. *Acs Nano* **2012**, *6*, 2532.

Miranda, O. R.; Chen, H. T.; You, C. C.; Mortenson, D. E.; Yang, X. C.; Bunz, U. H. F.; Rotello, V. M. *J. Am. Chem. Soc.* **2010**, *132*, 5285.

Mirshafiee, V.; Mahmoudi, M.; Lou, K. Y.; Cheng, J. J.; Kraft, M. L. *Chem. Commun.* **2013**, *49*, 2557.

Mogami, H.; Mills, C. L.; Gallagher, D. V. *Biochem. J.* **1997**, *324*, 645.

Monopoli, M. P.; Aberg, C.; Salvati, A.; Dawson, K. A. *Nat. Nanotechnol.* **2012**, *7*, 779.

Monopoli, M. P.; Pitek, A. S.; Lynch, I.; Dawson, K. A. *Methods Mol. Biol.* **2013**, *1025*, 137.

Monopoli, M. P.; Walczyk, D.; Campbell, A.; Elia, G.; Lynch, I.; Bombelli, F. B.; Dawson, K. A. *J. Am. Chem. Soc.* **2011**, *133*, 2525.

Monteith, G. R.; McAndrew, D.; Faddy, H. M.; Roberts-Thomson, S. J. *Nat. Rev. Cancer* **2007**, *7*, 519.

Mortensen, L. J.; Oberdorster, G.; Pentland, A. P.; DeLouise, L. A. *Nano Lett.* **2008**, *8*, 2779.

Mortimer, G. M.; Butcher, N. J.; Musumeci, A. W.; Deng, Z. J.; Martin, D. J.; Minchin, R. F. *Acs Nano* **2014**, *8*, 3357.

Mout, R.; Moyano, D. F.; Rana, S.; Rotello, V. M. *Chem. Soc. Rev.* **2012**, *41*, 2539.

Moyano, D. F.; Duncan, B.; Rotello, V. M. *Methods Mol. Biol.* **2013**, *1025*, 3.

Moyano, D. F.; Goldsmith, M.; Solfiell, D. J.; Landesman-Milo, D.; Miranda, O. R.; Peer, D.; Rotello, V. M. *J. Am. Chem. Soc.* **2012**, *134*, 3965.

Moyano, D. F.; Rotello, V. M. *Langmuir* **2011**, *27*, 10376.

Moyano, D. F.; Saha, K.; Prakash, G.; Yan, B.; Kong, H.; Yazdani, M.; Rotello, V. M. *ACS Nano* **2014**, *8*, 6748.

Mura, S.; Nicolas, J.; Couvreur, P. *Nat. Mater.* **2013**, *12*, 991.

Murphy, J. E.; Tedbury, P. R.; Homer-Vanniasinkam, S.; Walker, J. H.; Ponnambalam, S. *Atherosclerosis* **2005**, *182*, 1.

Murthy, A. K.; Stover, R. J.; Hardin, W. G.; Schramm, R.; Nie, G. D.; Gourisankar, S.; Truskett, T. M.; Sokolov, K. V.; Johnston, K. P. *J. Am. Chem. Soc.* **2013**, *135*, 7799.

Nam, J.; Won, N.; Jin, H.; Chung, H.; Kim, S. *J. Am. Chem. Soc.* **2009**, *131*, 13639.

Nativo, P.; Prior, I. A.; Brust, M. *Acs Nano* **2008**, *2*, 1639.

Nel, A.; Xia, T.; Madler, L.; Li, N. *Science* **2006**, *311*, 622.

Nel, A. E.; Madler, L.; Velegol, D.; Xia, T.; Hoek, E. M. V.; Somasundaran, P.; Klaessig, F.; Castranova, V.; Thompson, M. *Nat. Mater.* **2009**, *8*, 543.

Newman, J. D. S.; Blanchard, G. J. *Langmuir* **2006**, *22*, 5882.

Oh, E.; Delehanty, J. B.; Sapsford, K. E.; Susumu, K.; Goswami, R.; Blanco-Canosa, J. B.; Dawson, P. E.; Granek, J.; Shoff, M.; Zhang, Q.; Goering, P. L.; Huston, A.; Medintz, I. L. *Acs Nano* **2011**, *5*, 6434.

Orner, B. P.; Derda, R.; Lewis, R. L.; Thomson, J. A.; Kiessling, L. L. *J. Am. Chem. Soc.* **2004**, *126*, 10808.

Osaki, F.; Kanamori, T.; Sando, S.; Sera, T.; Aoyama, Y. *J. Am. Chem. Soc.* **2004**, *126*, 6520.

Owens, D. E.; Peppas, N. A. *Int. J. Pharm.* **2006**, *307*, 93.

Pan, Y.; Leifert, A.; Ruau, D.; Neuss, S.; Bornemann, J.; Schmid, G.; Brandau, W.; Simon, U.; Jahnen-Dechent, W. *Small* **2009**, *5*, 2067.

Pan, Y.; Neuss, S.; Leifert, A.; Fischler, M.; Wen, F.; Simon, U.; Schmid, G.; Brandau, W.; Jahnen-Dechent, W. *Small* **2007**, *3*, 1941.

Panyam, J.; Labhasetwar, V. *Pharm. Res.* **2003**, *20*, 212.

Patel, P. C.; Giljohann, D. A.; Daniel, W. L.; Zheng, D.; Prigodich, A. E.; Mirkin, C. A. *Bioconjugate Chem.* **2010**, *21*, 2250.

Patil, S.; Sandberg, A.; Heckert, E.; Self, W.; Seal, S. *Biomaterials* **2007**, *28*, 4600.

Peer, D.; Karp, J. M.; Hong, S.; FaroKHzad, O. C.; Margalit, R.; Langer, R. *Nat. Nanotechnol.* **2007**, *2*, 751.

Peer, D.; Lieberman, J. *Gene Ther.* **2011**, *18*, 1127.

Pelaz, B.; Charron, G.; Pfeiffer, C.; Zhao, Y. L.; de la Fuente, J. M.; Liang, X. J.; Parak, W. J.; del Pino, P. *Small* **2013**, *9*, 1573.

Perkins, J. *Asian J. Tranfus. Sci.* **2008**, *2*, 20.

Pernodet, N.; Fang, X. H.; Sun, Y.; Bakhtina, A.; Ramakrishnan, A.; Sokolov, J.; Ulman, A.; Rafailovich, M. *Small* **2006**, *2*, 766.

Petros, R. A.; DeSimone, J. M. *Nat. Rev. Drug Discov.* **2010**, *9*, 615.

Pillai, P. P.; Huda, S.; Kowalczyk, B.; Grzybowski, B. A. *J. Am. Chem. Soc.* **2013**, *135*, 6392.

Qian, Z. M.; Li, H. Y.; Sun, H. Z.; Ho, K. *Pharmacol. Rev.* **2002**, *54*, 561.

Rana, S.; Yu, X.; Patra, D.; Moyano, D. F.; Miranda, O. R.; Hussain, I.; Rotello, V. M. *Langmuir* **2012**, *28*, 2023.

Randolph, L. M.; Chien, M. P.; Gianneschi, N. C. *Chem. Sci.* **2012**, *3*, 1363.

Raynal, I.; Prigent, P.; Peyramaure, S.; Najid, A.; Rebuzzi, C.; Corot, C. *Invest. Radiol.* **2004**, *39*, 56.

Rejman, J.; Oberle, V.; Zuhorn, I. S.; Hoekstra, D. *Biochem. J.* **2004**, *377*, 159.

Rodal, S. K.; Skretting, G.; Garred, O.; Vilhardt, F.; van Deurs, B.; Sandvig, K. *Mol. Biol. Cell* **1999**, *10*, 961.

Rosen, J. E.; Chan, L.; Shieh, D. B.; Gu, F. X. *Nanomedicine* **2012**, *8*, 275.

Rosen, J. E.; Gu, F. X. *Langmuir* **2011**, *27*, 10507.

Rosi, N. L.; Mirkin, C. A. *Chem. Rev.* **2005**, *105*, 1547.

Rother, R. P.; Bell, L.; Hillmen, P.; Gladwin, M. T. *JAMA* **2005**, *293*, 1653.

Ruan, G.; Agrawal, A.; Marcus, A. I.; Nie, S. *J. Am. Chem. Soc.* **2007**, *129*, 14759.

Saha, K.; Agasti, S. S.; Kim, C.; Li, X. N.; Rotello, V. M. *Chem. Rev.* **2012**, *112*, 2739.

Saha, K.; Bajaj, A.; Duncan, B.; Rotello, V. M. *Small* **2011**, *7*, 1903.

Saha, K.; Moyano, D. F.; Rotello, V. M. *Mater Horiz* **2014**, *1*, 102.

Sahay, G.; Alakhova, D. Y.; Kabanov, A. V. *J. Control. Release* **2010**, *145*, 182.

Saitoh, D.; Kadota, T.; Senoh, A.; Takahara, T.; Okada, Y.; Mimura, K.; Yamashita, H.; Ohno, H.; Inoue, M. *Am. J. Emerg. Med.* **1993**, *11*, 355.

Salvador-Morales, C.; Flahaut, E.; Sim, E.; Sloan, J.; Green, M. L. H.; Sim, R. B. *Mol. Immunol.* **2006**, *43*, 193.

Salvati, A.; Pitek, A. S.; Monopoli, M. P.; Prapainop, K.; Bombelli, F. B.; Hristov, D. R.; Kelly, P. M.; Aberg, C.; Mahon, E.; Dawson, K. A. *Nat. Nanotechnol.* **2013**, *8*, 137.

Sandhu, K. K.; McIntosh, C. M.; Simard, J. M.; Smith, S. W.; Rotello, V. M. *Bioconjugate Chem.* **2002**, *13*, 3.

Sapsford, K. E.; Algar, W. R.; Berti, L.; Gemmill, K. B.; Casey, B. J.; Oh, E.; Stewart, M. H.; Medintz, I. L. *Chem. Rev.* **2013**, *113*, 1904.

Schaeublin, N. M.; Braydich-Stolle, L. K.; Schrand, A. M.; Miller, J. M.; Hutchison, J.; Schlager, J. J.; Hussain, S. M. *Nanoscale* **2011**, *3*, 410.

Schafer, D. A. *Curr. Opin. Cell Biol.* **2002**, *14*, 76.

Scharte, M.; Fink, M. P. *Crit. Care Med.* **2003**, *31*, S651.

Scherz-Shouval, R.; Shvets, E.; Fass, E.; Shorer, H.; Gil, L.; Elazar, Z. *Embo J.* **2007**, *26*, 1749.

Schmid, G. *Chem. Rev.* **1992**, *92*, 1709.

Sekiguchi, S.; Niikura, K.; Matsuo, Y.; Ijiro, K. *Langmuir* **2012**, *28*, 5503.

Shan, J.; Nuopponen, M.; Jiang, H.; Kauppinen, E.; Tenhu, H. *Macromolecules* **2003**, *36*, 4526.

Shi, X. Y.; Thomas, T. P.; Myc, L. A.; Kotlyar, A.; Baker, J. R. *PCCP* **2007**, *9*, 5712.

Shin, S. J.; Beech, J. R.; Kelly, K. A. *Integr. Biol.* **2013**, *5*, 29.

Shukla, R.; Bansal, V.; Chaudhary, M.; Basu, A.; Bhonde, R. R.; Sastry, M. *Langmuir* **2005**, *21*, 10644.

Storrie, H.; Mooney, D. J. *Adv. Drug Delivery Rev.* **2006**, *58*, 500.

Stroncek, D.; Procter, J. L.; Johnson, J. *Am. J. Hematol.* **2000**, *64*, 67.

Stuart, A. D.; Brown, T. D. K. *J. Virol.* **2006**, *80*, 7500.

Sundaram, H. S.; Ella-Menye, J. R.; Brault, N. D.; Shao, Q.; Jiang, S. Y. *Chem. Sci.* **2014**, *5*, 200.

Swanson, J. A.; Watts, C. *Trends Cell. Biol.* **1995**, *5*, 424.

Tannock, I. F.; Rotin, D. *Cancer Res.* **1989**, *49*, 4373.

Templeton, A. C.; Wuelfing, M. P.; Murray, R. W. *Acc. Chem. Res.* **2000**, *33*, 27.

Tenchov, B. G.; Wang, L.; Koynova, R.; MacDonald, R. C. *BBA-Biomembranes* **2008**, *1778*, 2405.

Tenzer, S.; Docter, D.; Kuharev, J.; Musyanovych, A.; Fetz, V.; Hecht, R.; Schlenk, F.; Fischer, D.; Kiouptsi, K.; Reinhardt, C.; Landfester, K.; Schild, H.; Maskos, M.; Knauer, S. K.; Stauber, R. H. *Nat. Nanotechnol.* **2013**, *8*, 772.

Thomas, M.; Klibanov, A. M. *Proc. Natl. Acad. Sci. U.S.A.* **2003**, *100*, 9138.

Tice, R. R.; Agurell, E.; Anderson, D.; Burlinson, B.; Hartmann, A.; Kobayashi, H.; Miyamae, Y.; Rojas, E.; Ryu, J. C.; Sasaki, Y. F. *Environ. Mol. Mutagen.* **2000**, *35*, 206.

Tonga, G. Y.; Saha, K.; Rotello, V. M. *Adv Mater* **2014**, *26*, 359.

Tsujimoto, Y.; Shimizu, S. *Cell Death Differ.* **2005**, *12*, 1528.

Turkevich, J.; Stevenson, P. C.; Hillier, J. *Discuss. Faraday Soc.* **1951**, 55.

Verma, A.; Stellacci, F. *Small* **2010**, *6*, 12.

Verma, A.; Uzun, O.; Hu, Y. H.; Hu, Y.; Han, H. S.; Watson, N.; Chen, S. L.; Irvine, D. J.; Stellacci, F. *Nat. Mater.* **2008**, *7*, 588.

Walkey, C. D.; Chan, W. C. W. *Chem. Soc. Rev.* **2012**, *41*, 2780.

Walkey, C. D.; Olsen, J. B.; Guo, H.; Emili, A.; Chan, W. C. W. *J. Am. Chem. Soc.* **2012**, *134*, 2139.

Walkey, C. D.; Olsen, J. B.; Song, F. Y.; Liu, R.; Guo, H. B.; Olsen, D. W. H.; Cohen, Y.; Emili, A.; Chan, W. C. W. *Acs Nano* **2014**, *8*, 2439.

Wang, E. C.; Wang, A. Z. *Integr. Biol.* **2014**, *6*, 9.

Wang, Y.; Zhou, K.; Huang, G.; Hensley, C.; Huang, X.; Ma, X.; Zhao, T.; Sumer, B. D.; DeBerardinis, R. J.; Gao, J. *Nat Mater* **2014**, *13*, 204.

Weare, W. W.; Reed, S. M.; Warner, M. G.; Hutchison, J. E. *J. Am. Chem. Soc.* **2000**, *122*, 12890.

Xiao, W. C.; Lin, J.; Li, M. L.; Ma, Y. J.; Chen, Y. X.; Zhang, C. F.; Li, D.; Gu, H. C. *Contrast Media Mol. Imaging* **2012**, *7*, 320.

Xiao, Y.; Wiesner, M. R. *J. Hazard. Mater.* **2012**, *215*, 146.

Yan, B.; Kim, S. T.; Kim, C. S.; Saha, K.; Moyano, D. F.; Xing, Y. Q.; Jiang, Y.; Roberts, A. L.; Alfonso, F. S.; Rotello, V. M.; Vachet, R. W. *J. Am. Chem. Soc.* **2013**, *135*, 12564.

Yang, H.; Fung, S. Y.; Liu, M. Y. *Angew. Chem. Int. Ed.* **2011**, *50*, 9643.

Yang, W.; Zhang, L.; Wang, S. L.; White, A. D.; Jiang, S. Y. *Biomaterials* **2009**, *30*, 5617.

Yen, H. J.; Hsu, S. H.; Tsai, C. L. *Small* **2009**, *5*, 1553.

Yonamine, Y.; Yoshimatsu, K.; Lee, S. H.; Hoshino, Y.; Okahata, Y.; Shea, K. J. *ACS Appl. Mater. Interfaces* **2013**, *5*, 374.

You, C. C.; Chompoosor, A.; Rotello, V. M. *Nano Today* **2007**, *2*, 34.

You, C. C.; De, M.; Han, G.; Rotello, V. M. *J. Am. Chem. Soc.* **2005**, *127*, 12873.

You, C. C.; Miranda, O. R.; Gider, B.; Ghosh, P. S.; Kim, I. B.; Erdogan, B.; Krovi, S. A.; Bunz, U. H. F.; Rotello, V. M. *Nat. Nanotechnol.* **2007**, *2*, 318.

You, C. C.; Verma, A.; Rotello, V. M. *Soft Matter* **2006**, *2*, 190.

Yu, T.; Malugin, A.; Ghandehari, H. *Acs Nano* **2011**, *5*, 5717.

Zaki, N. M.; Tirelli, N. *Expert Opin. Drug Deliv.* **2010**, *7*, 895.

Zhan, N. Q.; Palui, G.; Safi, M.; Ji, X.; Mattoussi, H. *J. Am. Chem. Soc.* **2013**, *135*, 13786.

Zhang, C.; Macfarlane, R. J.; Young, K. L.; Choi, C. H. J.; Hao, L. L.; Auyeung, E.; Liu, G. L.; Zhou, X. Z.; Mirkin, C. A. *Nat. Mater.* **2013**, *12*, 741.

Zhang, G. D.; Yang, Z.; Lu, W.; Zhang, R.; Huang, Q.; Tian, M.; Li, L.; Liang, D.; Li, C. *Biomaterials* **2009**, *30*, 1928.

Zhang, L. W.; Monteiro-Riviere, N. A. *Toxicol. Sci.* **2009**, *110*, 138.

Zhang, R.; Niu, Y. J.; Zhou, Y. K. *Toxicol. Lett.* **2010**, *192*, 108.

Zhao, Y. N.; Sun, X. X.; Zhang, G. N.; Trewyn, B. G.; Slowing, I. I.; Lin, V. S. Y. *Acs Nano* **2011**, *5*, 1366.

Zheng, D.; Giljohann, D. A.; Chen, D. L.; Massich, M. D.; Wang, X. Q.; Iordanov, H.; Mirkin, C. A.; Paller, A. S. *Proc. Natl. Acad. Sci. U.S.A.* **2012**, *109*, 11975.

Zheng, M.; Davidson, F.; Huang, X. Y. *J. Am. Chem. Soc.* **2003**, *125*, 7790.

Zhou, K. J.; Wang, Y. G.; Huang, X. N.; Luby-Phelps, K.; Sumer, B. D.; Gao, J. M. *Angew. Chem. Int. Ed.* **2011**, *50*, 6109.

Zhu, M. Q.; Wang, L. Q.; Exarhos, G. J.; Li, A. D. Q. *J. Am. Chem. Soc.* **2004**, *126*, 2656.

Zhu, Z. J.; Ghosh, P. S.; Miranda, O. R.; Vachet, R. W.; Rotello, V. M. *J. Am. Chem. Soc.* **2008**, *130*, 14139.

Zhu, Z. J.; Posati, T.; Moyano, D. F.; Tang, R.; Yan, B.; Vachet, R. W.; Rotello, V. M. *Small* **2012**, *8*, 2659.

Zolnik, B. S.; Gonzalez-Fernandez, A.; Sadrieh, N.; Dobrovolskaia, M. A. *Endocrinology* **2010**, *151*, 458.

Zuo, G. H.; Huang, Q.; Wei, G. H.; Zhou, R. H.; Fang, H. P. *Acs Nano* **2010**, *4*, 7508.